MECHANISTIC STUDIES OF ACTIVE SITE MUTANTS OF MERCURIC REDUCTASE; STEREOCHEMICAL STUDIES OF A FLUOROACETATE HALIDOHYDROLASE

by

Karin G. Au

B.A., Vanderbilt University (1981)

Submitted to the Department of Chemistry
in Partial Fulfillment of the
Requirements for the Degree of

Doctor of Philosophy

at the

Massachusetts Institute of Technology

February, 1986

Signature of Author: Signature redacted
Department of Chemistry
January 29, 1985

Certified by: Signature redacted
Christopher Walsh
Thesis Supervisor

Accepted by: Signature redacted
Glenn A. Berchtold
Chairman
Departmental Committee on Graduate Students

This doctoral thesis has been examined by a Committee of the Department of Chemistry as follows:

Signature redacted

Professor Glenn Berchtold _____ _____

Chairman

Signature redacted

Professor Christopher Walsh _____ _____

Thesis Supervisor

Signature redacted

Professor Daniel Kemp _____ _____

MECHANISTIC STUDIES OF ACTIVE SITE MUTANTS OF MERCURIC REDUCTASE

STEREOCHEMICAL STUDIES OF A FLUOROACETATE HALIDOHYDROLASE

by

Karin G. Au

Submitted to the Department of Chemistry
on January 29, 1986 in partial fulfillment of the
requirements for the Degree of Doctor of Philosophy

Abstract

Mercuric ion reductase, a flavoenzyme with an active site redox-active cystine, cys_{135}-cys_{140}, is an unusual enzyme which reduces Hg(II) to Hg(0) with stoichiometric NADPH oxidation. As an approach toward studying the catalytic mechanism, we have constructed active site cys to ser (ser_{135}, cys_{140} and cys_{135}, ser_{140}) and cys to ala (ala_{135}, cys_{140} and cys_{135}, ala_{140}) mutations by oligonucleotide-directed mutagenesis and characterized the physical and catalytic properties of the resulting mutant proteins.

The native and mutant enzymes are expressed on an overproducing plasmid and purified to homogeneity by a one-step procedure in high yield. The optical spectra of the mutant proteins are distinct, with the ser_{135}, cys_{140} and ala_{135}, cys_{140} mutants displaying a thiolate-flavin charge transfer band (cys_{140} pK_a = 5.1 in the ser_{135}, cys_{140} mutant; cys_{140} pK_a = 6.3 in the ala_{135}, cys_{140} mutant), confirming that cys_{140}, not cys_{135}, is in charge transfer distance both in these mutants and in two electron-reduced native enzyme. Thiol titrations with DTNB indicate that all four mutants contain three kinetically accessible thiols in both the presence and absence of NADPH. The native enzyme has two titratable thiols when oxidized and four in the two electron-reduced state.

The native and mutant enzymes show differentiable NADPH-dependent catalytic behavior with $Hg(SR)_2$ (R = CH_2CH_2OH), $Hg(CN)_2$, DTNB, thioNADP$^+$, and O_2. Only native enzyme reduces $Hg(SR)_2$. The ser_{135}, cys_{140} mutant enzyme, when compared to the native and other mutant enzymes, shows extremely low rates toward O_2 and thioNADP$^+$, which may reflect its particularly low redox potential. In general, O_2 and thioNADP$^+$ rates correlate to some extent with estimates of bound flavin redox potentials. Although it occurs at low rates, DTNB reduction catalyzed under anaerobic conditions by the mutant enzymes as well as by the native enzyme suggests that monodentate chelation to a given enzyme-SH may be sufficient for this activity and that reduction can occur by direct electron transfer from $FADH_2$. The ser_{135}, cys_{140} mutant enzyme catalyzes NADPH oxidation in the presence of $Hg(CN)_2$. This activity was shown to be dependent on the presence of O_2 and is attributed to an increase in the O_2 reductase activity of the ser_{135}, cys_{140} mutant upon binding of $Hg(CN)_2$ to the enzyme.

In a separate study, the stereochemical course of action of haloacetate halidohydrolase H-1 from Pseudomonas sp., strain A, which catalyzes the dehalogenation of fluoroacetate to glycolate, has been determined by enzymatic analysis of products from incubations with both enantiomers of

2-fluoropropionate and by ^{1}H-NMR analysis of the ester of (-)-α-methoxy-α-(trifluoromethyl)-phenylacetic acid with phenacyl [2-^{2}H$_{1}$]-glycolate derived from the product of incubation with (S)-monodeuterofluoroacetate. The results support a direct displacement mechanism for this enzyme, since they indicate that the reaction is catalyzed with inversion of configuration.

Thesis supervisor: Dr. Christopher Walsh

Title: Professor of Chemistry and Biology

Little Willie from his mirror
   Licked the mercury right off,
Thinking, in his childish error,
   It would cure the whooping cough.

At the funeral his mother
   Smartly said to Mrs. Brown:
"'Twas a chilly day for Willie
When the mercury went down."

Anonymous

from What Cheer; an Anthology of American and British Humorous and Witty Verse (David McCord, Ed.) Coward-McCann, New York, c. 1945.

Acknowledgments

I thank Dr. Christopher Walsh for advice and support. Chris has been an outstanding research director in many ways. In particular, I would like to note his encouragement of scientific independence in his laboratory, his versatility in pursuing a wide variety of research problems, and the consideration he shows on a personal level toward members of his laboratory.

I also thank Dr. Peter Schultz, who introduced me and many others in the lab to mutagenesis and recombinant DNA work. As the first person to work on directed mutagenesis of merA, Pete was responsible for much of the early work on the cys to ser mutations described in this thesis.

In addition I express my thanks to Barbara Fox, whose studies of native enzyme laid the groundwork for many of the studies carried out on the mutant enzymes, Mark Distefano, who has been extremely helpful in such varied capacities as coworker on active site merA mutagenesis, photographer, and proofreader, and Drs. Susan Miller, Vincent Massey, David Ballou, and Charles Williams at the University of Michigan, who have generously provided us with advice, experimental data, and enzymes.

I thank John Latham for all the personal and scientific benefits of sharing a lab with him for four years. Dr. Hung-Wen (Ben) Liu was particularly helpful as my coworker on the quinolinate synthetase project and for providing advice on the fluoroacetate project and running high field NMR spectra. In addition, many other past and present members of the Walsh group deserve thanks for providing advice and materials.

I first heard the "Little Willie" poem during a lecture by Professor David Tuleen at Vanderbilt University, and I thank him for providing me with a copy of this poem.

I also thank the National Science Foundation and W. R. Grace and Co.

for financial support.

Finally, I express my appreciation for support and encouragement from Bob Foglesong and from my family.

In consideration of the support received from the National Science Foundation, the author hereby grants to the United States Government an irrevocable, non-exclusive, royalty-free license to reproduce, translate, publish, use and dispose of copies of this work for Government purposes.

Table of Contents

List of Figures

List of Tables

Abbreviations used

ATP.....adenosine 5'-triphosphate

bp.....base pair

BV_{ox}, BV_{red}.....oxidized and reduced benzyl viologen

dNTP.....deoxynucleoside triphosphate

DMT.....4,4'-dimethoxytrityl.

DTNB.....5,5'-dithiobis-(2-nitrobenzoate)

E.....oxidized enzyme

EDTA.....ethylenediamine tetraacetic acid

EH_2.....two electron reduced enzyme

EH_4.....four electron reduced enzyme

EHR.....monoalkylated enzyme

FAD, $FADH_2$.....oxidized and two electron reduced flavin adenine dinucleotide

HPLC.....high performance liquid chromatography

IPTG.....isopropyl β-D-thiogalactopyranoside

kb.....kilobase

$NADP^+$, NADPH.....oxidized and reduced nicotinamide adenine dinucleotide phosphate

PAGE.....polyacrylamide gel electrophoresis

SDS.....sodium dodecyl sulfate

$thioNADP^+$.....thio-nicotinamide adenine dinucleotide phosphate

TLCK.....Nα-p-tosyl-L-lysine chloromethyl ketone

TPCK.....L-1-tosylamide-2-phenylethyl chloromethyl ketone

Xgal.....5-bromo-4-chloro-3-indolyl-β-D-galactopyranoside

YT.....yeast tryptone medium

CHAPTER ONE

INTRODUCTION

Microorganisms play an important role in the biological cycling of mercury. Methylation of mercury, decomposition of organomercurials, and reduction of Hg(II) are all processes which have been observed in microorganisms. A key reaction in the detoxification of mercurials by mercury resistant microbes is the reduction of Hg(II) to a volatile form, Hg(0). This thesis describes the use of site specific mutagenesis to study the enzyme which catalyzes this reduction, the flavoenzyme mercuric reductase.

The toxicity of mercurials

Mercury and compounds containing it are toxic to many organisms, ranging from mammals to microbes. Exposure to mercury is an occupational hazard which has been or is presently associated with various industries and workplaces, such as the paper industry, fertilizer production, paint manufacturing, mining, sewage treatment facilities (Robinson and Tuovinen, 1984), the silvering of mirrors (Farrar and Williams, 1977) and chemical research laboratories. Hundreds of people and untold numbers of birds, fish, and microorganisms have been dispatched by the pollution of the environment with mercurials or by the use of mercury-containing disinfectants and fungicidal agents.

The toxicity of mercurials is generally ascribed to their extremely high affinity for thiols, which results in complexation of essential sulfhydryls and damage to proteins in the cell. In addition, Hg(II) can bind to polynucleotides and may activate RNase (Foster, 1983).

Such factors as oxidation state and solubility influence the degree of toxicity of a given mercurial. Hg(II) poses the greatest risk to the cell in terms of thiol complexation, as estimates of stability constants for

$Hg(SR)_2$ complexes range from 10^{35} to 10^{44} (Casas and Jones, 1980). On the other hand, membrane barriers are often impermeable to the relatively polar inorganic Hg(II) salts. Hg(0), being uncharged, diffuses more easily across membranes than Hg(II) salts; however, unless oxidized in vivo, Hg(0) displays a much lower affinity for thiols than Hg(II), and it furthermore has a low solubility in water and a high vapor pressure, which facilitates diffusion of the Hg(0) out of the cell and out of the microbial growth medium (Foster, 1983). Organomercurials, which contain divalent mercury and have lipophilic character, are generally the most toxic of mercury-containing compounds.

Microbial resistance to mercurials

A number of microorganisms display inducible resistance to mercurials. Such resistance was first identified in strains isolated from organomercury-polluted soils in Japan and in clinical isolates in Great Britain (Summers and Silver, 1978). In clinical isolates, antibiotic resistance usually accompanies mercury resistance (Brown, 1985).

The enrichment of mercury-resistant bacteria in these sources is readily attributed to selective pressures resulting from human activity in their environment, such as the presence of mercurial pollutants in soil or the use of mercury-containing disinfectants in hospitals (Robinson and Tuovinen, 1984). However, among other factors, the known complexity of the mercury resistance systems makes extremely unlikely the possibility that these resistance mechanisms evolved only under such recent selective pressures. Comparison of the abundance of mercurials from natural and from human derived sources indicates that human activity has produced only about 1%, (10^6 tons) of the total amount of mercury that is found in the biosphere

(10^8 tons) (Summers and Silver, 1978). Although areas of local high concentration of mercurials are often associated with industrial pollution, high levels of toxic heavy metals have existed in such natural environments as volcanic soils and deep sea vents long before humans began to pollute the environment (Williams and Silver, 1984). The wide distribution of mercury in rocks, soil, air, and water is due to its volatility, adsorption to surfaces, and ability to form complexes (Robinson and Tuovinen, 1984).

Resistance to mercurials has been found in a wide variety of bacteria and appears in all known cases to be plasmid-encoded (Brown, 1985; Foster, 1983; Robinson and Tuovinen, 1984). In several cases, the resistance determinants have been identified on transposons, some of which carry antibiotic resistance in addition to heavy metal resistance (Brown, 1985).

Two major classes of mercury resistance phenotypes have been described for Gram negative bacteria (Foster, 1983). The first is termed narrow spectrum resistance. This involves resistance to Hg(II) and a few organomercurials, such as merbromin (mercurochrome) and fluorescein mercuric acetate. The second, which is observed only 5-10% as often as the first, is called broad spectrum resistance. Broad spectrum resistance extends narrow spectrum resistance to include several more organomercurials, such as phenyl mercuric acetate, methyl mercuric chloride, thimerosal (merthiolate), and p-chloromercuribenzoate. Some differences within each class of resistance are observed with different types of bacteria.

Several different mechanisms of mercury resistance have been proposed. Cells may block transport of mercurials into the cell (Pan-Hou et al., 1981) or sequester the mercurial in an unreactive form (Pan-Hou and Imura, 1981; Pan-Hou et al., 1980). Methylation of mercury has also been suggested as a detoxification mechanism, since methyl mercury is more volatile, although

also more toxic, than inorganic Hg(II) (Robinson and Tuovinen, 1984). The most prevalent mechanism of resistance appears to involve transport of the mercurial into the cell, conversion of the mercurial to Hg(0), and finally volatilization of the Hg(0) from the medium.

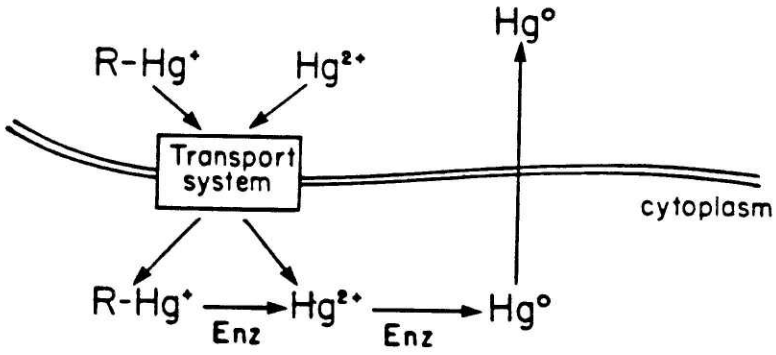

(from Fox, 1983)

In narrow spectrum resistance, this conversion is accomplished by mercuric reductase, the subject of this thesis, which catalyzes the two electron reduction of Hg(II) to Hg(0). Narrow spectrum resistance to the organomercurials mentioned above is probably due to permeability barriers, but the gene responsible has not been identified (Foster, 1983). Broad spectrum resistance requires a second conversion step, cleavage of the Hg-C bond of the organomercurial (RHgX) to produce Hg(II) and the corresponding RH. This reaction is carried out by a different enzyme, organomercury lyase. Broad spectrum resistance also requires the presence of mercuric reductase to convert the lyase product Hg(II) to Hg(0).

The mer system

The mercury resistance (mer) operons from several sources have been described. Three have been sequenced. The best characterized sources at present are transposon Tn501, originally from the Pseudomonas aeruginosa

plasmid pVS1 (Stanisch et al., 1977; Bennett et al., 1978) and plasmid R100 (also known as plasmid NR1), originally from a clinical Shigella flexnerii strain (Watanabe, 1966). A Gram positive system, in the S. aureus plasmid pI258, has also recently been sequenced (S. Silver, unpublished). The Tn501 and R100 systems show many similarities but also some major differences, which are discussed below. A map of the resistance genes in these sources is shown in Figure 1-1.

Our current understanding of the organization of the mercury resistance operon is described below. Expression of the mer operon is regulated by the merR protein, which is transcribed separately from the rest of the operon, in the opposite direction (Foster and Brown, 1985). A variety of evidence suggests that this protein acts both as a positive and a negative regulatory element (Foster, 1983). O'Halloran and Walsh (1986) have recently placed the merR gene under the control of the tac promoter for overexpression and have partially purified the merR protein. By DNA binding experiments, they have observed Hg(II)-dependent preferential binding of the merR protein to small restriction fragments containing the 5' flanking control region of the mer operon. In the absence of Hg(II), the protein binds to a fragment containing the promoter elements. In the presence of Hg(II), its affinity switches to a fragment containing an upstream portion of the 5' flanking DNA. These results support the following model. The merR protein functions as a repressor in the absence of Hg(II) by binding to the RNA polymerase binding site and thereby preventing transcription. Binding of Hg(II) to the merR protein is proposed to induce a conformational change that results in a decrease in its affinity for the RNA polymerase binding site and an increase in its affinity for a second sequence upstream of the first site, where by protein-protein interaction it may facilitate the binding of RNA polymerase

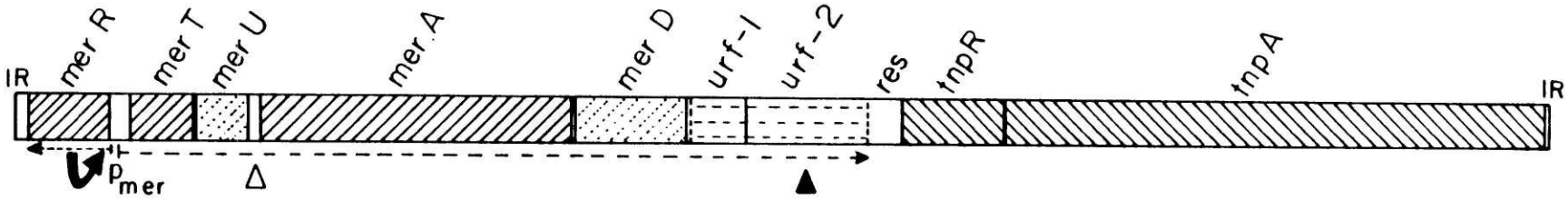

Figure 1-1. Map of transposon Tn501 (adapted from Brown, 1985) showing the locations of the mercury resistance genes, discussed in the text, and directions of their transcription. P_{mer} is the promoter regulated by the merR protein. The black triangle marks the location of the 11.2 kb insert found in urf-2 of R100, but not in urf-2 of Tn501. The open triangle marks the location of merC in R100. Res, tnpR, and tnpA are genes involved in transposition.

to its entry site.

Following the operator-promoter region in the mer operon is a polycistronic region, which appears to form a single transcriptional unit. This region starts with merT, which codes for a transport protein, and includes merA, which codes for the reductase, and a number of other small genes which are not necessarily present in both Tn501 and R100, and for which the nomenclature has been confusing. It is not yet clear how far the mercury resistance determinants extend in each of these systems (Brown et al., 1985). In this discussion, the nomenclature of Brown et al., (1985) will be used.

The Tn501 DNA sequence predicts that the merT protein is a highly hydrophobic 12,500 dalton protein with three potential trans-membrane regions and one pair of cysteine residues at or near each face of the membrane (Brown, 1985). The merT product is a transport protein which resistant cells use to transport Hg(II) in from the medium. Although such a transport mechanism might appear to result in higher intracellular levels of Hg(II) and therefore a much greater risk to the cell, it has been proposed that this protein, and possibly others encoded on the mer operon, might prevent the Hg(II) from binding to sensitive sulfhydryls as it passes through the membrane and eventually to the reductase (Foster, 1983; Brown, 1985). Mutations in merA, which prevent completion of the detoxification process, lead to hypersensitivity to Hg(II) in cells expressing a functional merT (Foster, 1983). Such cells are seven-fold more sensitive to Hg(II) than plasmid-free cells. The product of merT has yet to be isolated.

The DNA sequence of merU (U for uptake; also called merP (P for periplasmic) or merC) suggests that merU codes for a periplasmic protein, since the predicted N-terminal sequence is homologous to the leader

sequences of several periplasmic proteins (Brown, 1985). Mutations in merU were previously mapped in merT (Brown et al., 1985). The amino acid sequence predicted from the sequence downstream of the proposed leader sequence aligns rather well with the N-terminal sequence of mercuric reductase, with amino acid identities of 25-26% and with 40% conservative substitutions (Misra et al., 1985; Brown and Goddette, 1984). A proposed function of the merU protein is to scavenge Hg(II) in the periplasmic space for delivery to the merT protein. Subcloning experiments indicate that the merT and merU proteins are sufficient for transport of Hg(II) into the cell (Brown, 1985).

The R100 sequence shows a reading frame after merU that is not observed in the Tn501 sequence. The precise function of this gene, named merC (previously merX), has yet to be determined (Brown et al., 1985).

The gene following merC in R100 and following merU in Tn501 is merA, which codes for mercuric reductase, a soluble enzyme. Although tentative evidence for some membrane association of the reductase has been presented (Jackson and Summers, 1982), recent attempts to demonstrated membrane association have failed (Brown et al., 1985). A detailed discussion of mercuric reductase is presented in the following section.

Following merA in both Tn501 and R100 is the merD gene. Again, the function of this gene has not yet been determined. Mutants in merD show Hg(II) sensitivity only on high copy number plasmids (Brown, 1985). Brown and Goddette (1984) have proposed that this protein may facilitate removal of Hg(0) from the cell. Brown (1985) suggests that the presence of the mer operon on high copy number plasmids in merD mutants exposed to Hg(II) leads to product inhibition of mercuric reductase and therefore an increase in intracellular Hg(II) levels. Presumably, passive diffusion of Hg(0) out of

the cell would be sufficient for viability of merD mutants carrying the mer genes on low copy number plasmids.

The Tn501 and R100 DNA sequences both indicate the presence of a reading frame after merD. This reading frame, previously called urf-1 (unidentified reading frame 1), is tentatively assigned the name merE. The function of merE is unknown (Brown et al., 1985).

Tn501 contains an additional reading frame past merE which is disrupted by 11.2 kb of DNA in R100 (Brown et al., 1985). This unidentified reading frame (urf-2) has not to date been shown to be involved in mercury resistance. The extra reading frame (merC) in R100 shows no homology to urf-2 in Tn501 at either the DNA or protein level.

Mapping by transposon mutagenesis (Ogawa et al., 1984) indicates that the merB gene, which encodes organomercury lyase, lies 13.5 kb apart from the mer operon, and that it is apparently under the control of a separate promoter. The merB genes from E. coli plasmid R831 (A. Summers, unpublished) and from S. aureus plasmid pI258 (S. Silver, unpublished) are being sequenced. Begley et al., (1986a) have recently overexpressed the R831 merB gene with the T7 polymerase/T7 promoter system of Tabor and Richardson (1985) and have purified the enzyme to homogeneity. This enzyme has a very broad substrate specificity, which has proved to be useful in mechanistic studies of the enzyme (Begley et al., 1986b).

Figure 1-2 summarizes a current model of the mer proteins and their known or proposed functions.

Mercuric reductase

Mercuric reductase, the product of the merA gene, is a flavoenzyme which carries out the two electron reduction of Hg(II) to Hg(0) according

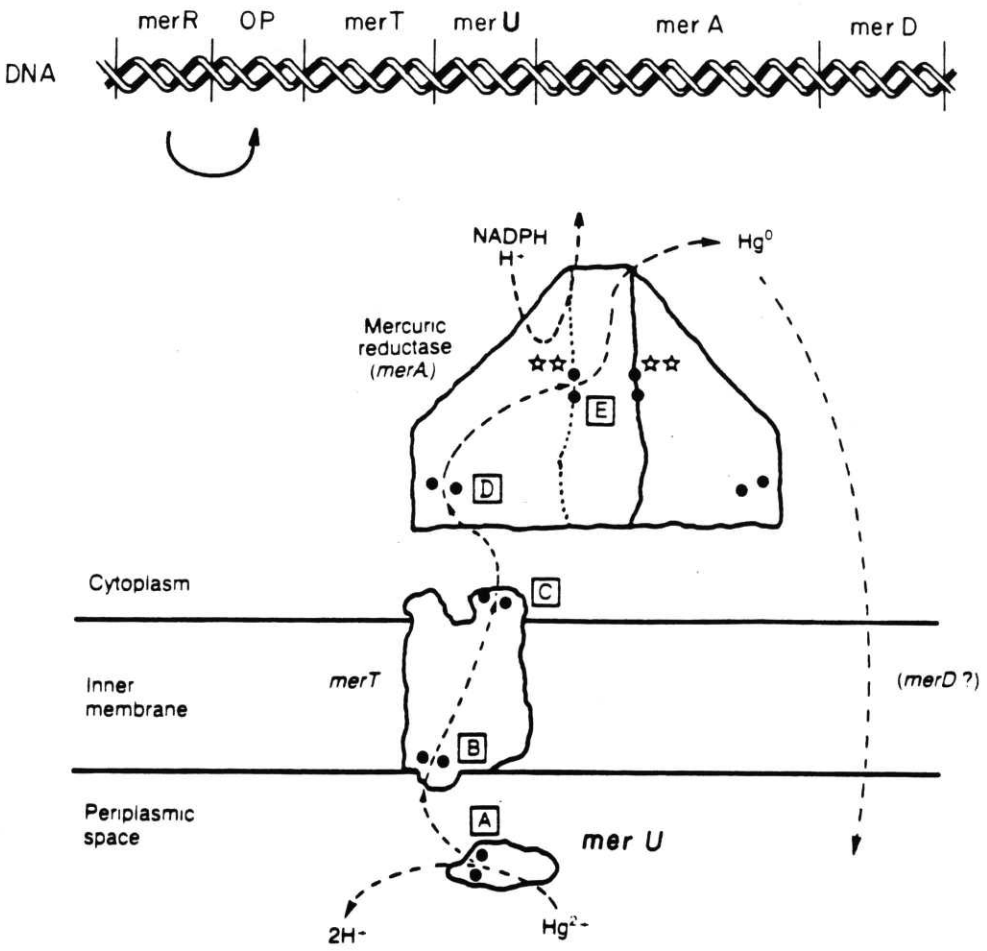

Figure 1-2. Current model of the mer proteins and their known or proposed functions (adapted from Brown, 1985). This model is largely based on predicted primary sequences of the various mer gene products and should be regarded as speculation. Solid circles represent paired cysteine residues to which Hg(II) is suggested to bind. According to the model, the merR protein regulates transcription at the operator promoter region. In the periplasmic space, the merU protein scavenges Hg(II), which binds to cysteine pair [A], then is transferred to cysteine pair [B] of the membrane-bound merT protein. The merT protein transports the Hg(II) through the inner membrane from cysteine pair [B] to cysteine pair [C] on the inner face of the merT protein. From cysteine pair [C], the Hg(II) is passed to a cysteine pair (possibly N-terminal pair [D]) of mercuric reductase, which may transiently associate with the merT protein. Then, the Hg(II) may be transferred to the C-terminal cysteine pair [E] on the same or other subunit, then to the active site redox active cysteine pair, represented by stars, where it is reduced to Hg(0). The Hg(0) is released to the cytoplasm and then leaves the cell be simple diffusion or by diffusion facilitated by some additional mer gene product, possibly merD.

to the following reaction in vitro:

$$Hg(SR)_2 + H^+ + NADPH \longrightarrow Hg(0) + 2RSH + NADP^+ \quad \text{(Equation 1-1)}$$

Izaki (1981) reports a mercuric reductase which reduces Hg(I) as well as Hg(II). It is unclear whether this enzyme reduces Hg(I) directly or reduces Hg(II) which results from disproportionation of Hg(I) in solution, especially since thiols, which promote disproportionation of Hg(I) to Hg(II) plus Hg(0) (Cotton and Wilkinson, 1980) were added to the enzyme incubation mixtures.

MerA has been sequenced in Tn501 (Brown et al., 1983), in R100 (Misra et al., 1985), and in S. aureus plasmid pI258 (S. Silver, unpublished). Figure 1-3 shows the predicted amino acid sequence of mercuric reductase from Tn501 and from R100. The two sequences show 86% identity when optimally aligned, with the remainder of the sequence consisting predominantly of conservative changes clustered in specific regions (Misra et al., 1985).

The two sequences show strong homology to those of the FAD-containing pyridine nucleotide disulfide oxidoreductases glutathione reductase (Krauth-Siegel et al., 1982) (see Figure 1-4) and lipoamide dehydrogenase (Stephens et al., 1983). As will be discussed below, strong similarities among these enzymes were also evident from mechanistic studies and partial amino acid sequencing of the proteins. Comparison of the R100 mercuric reductase sequence with the sequence of glutathione reductase indicates that 26% of the amino acids are identical and that many of the changes are conservative (Misra et al., 1985). All nonconservative substitutions fit on outer positions of the glutathione reductase structure (Brown, 1985), which has

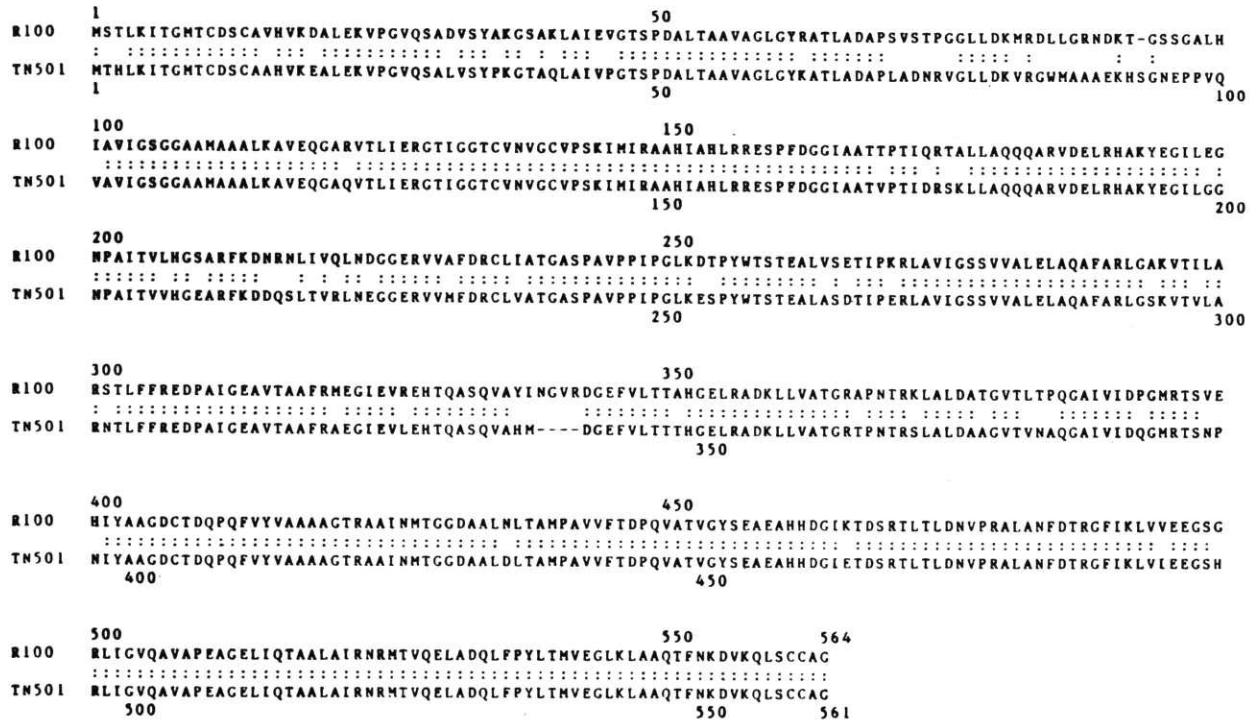

Figure 1-3. Predicted amino acid sequences of mercuric reductase from Tn501 and R100 showing optimal alignment (from Misra et al., 1985).

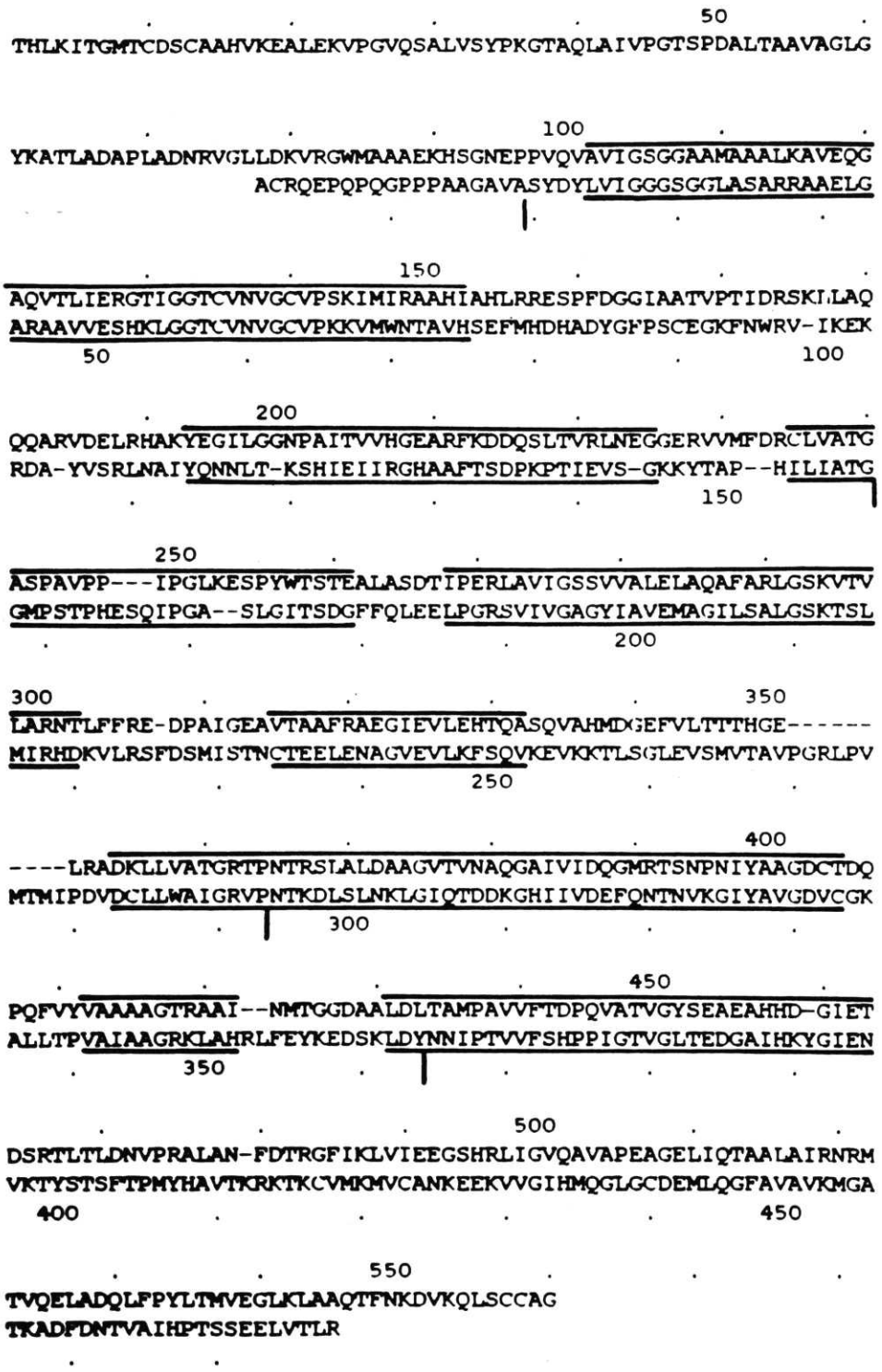

Figure 1-4. Alignment of amino acid sequences of Tn501-encoded mercuric reductase (top line) and human erythrocyte glutathione reductase (bottom line) (from Brown et al., 1983). Horizontal lines indicate regions showing a notably high degree of homology (determined on the basis of natural substitution frequencies of homologous proteins). Hyphens are spacing to align the sequences.

been determined at 2 Å resolution (Thieme et al., 1981). The FAD- and NADPH-binding domains and the active site (see Figure 1-5) are the regions of highest homology between the two enzymes, whereas the N- and C-terminal regions are the most different. The C-terminus of the Tn501 mercuric reductase extends 15 residues further than does that of glutathione reductase (Brown et al., 1983). This C-terminal region, which contains a pair of cysteines (cys_{557} and cys_{558}), has been proposed to be important in subunit interaction and substrate binding (Brown et al., 1983). The N-terminal region of 77 amino acids, which also contains a pair of cysteines (cys_{10} and cys_{13}), has no counterpart in glutathione reductase or in lipoamide dehydrogenase. The next 18 amino acids are flexible in the glutathione reductase structure (Thieme et al., 1981). Proteolytic removal of 85 amino acids of the N-terminal region of mercuric reductase had no apparent effect on the V_{max} or dimeric structure of the enzyme, and clipping in this manner places the active site cysteines at positions 50 and 55, in register with the active site cysteines in glutathione reductase and lipoamide dehydrogenase (see Figure 1-6) (Fox and Walsh, 1983). The homology between this region and merU (see above) suggests that one of the two sequences arose by a gene duplication event and that the selective pressure was for more efficient Hg(II) detoxification (Brown and Goddette, 1984; Misra et al., 1985). Brown et al. (1983) have proposed that this region may have an in vivo role in transient Hg(II) binding, perhaps between binding by the merT protein and binding by the reductase active site. A possible biological advantage of such an arrangement would be protection of the cell from free intracellular Hg(II) in solution. Our laboratory is currently addressing the question of the role of the cysteines in the N- and C-terminal regions by constructing cys to ala mutants (Moore and Walsh,

A

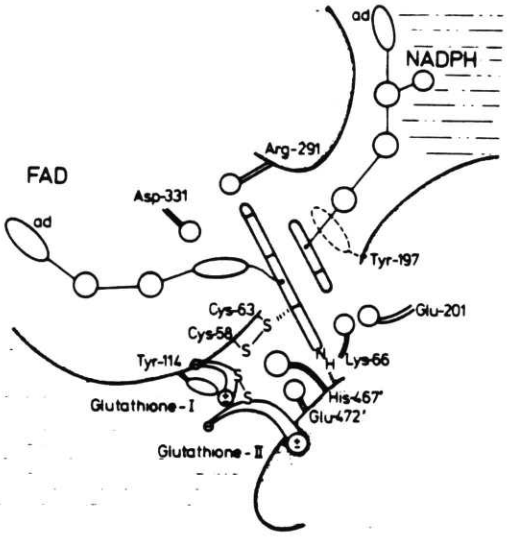

B

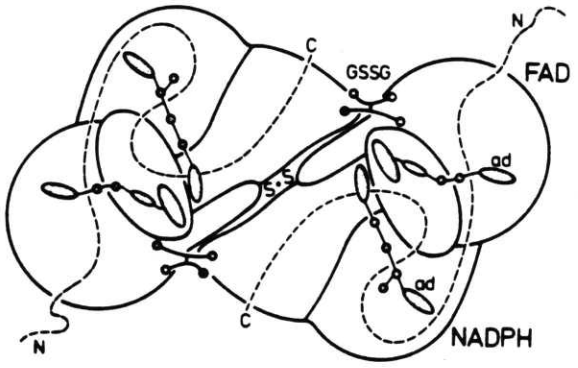

Figure 1-5. Structure of human erythrocyte glutathione reductase (from Pai and Schulz, 1983). A) The catalytic center of glutathione reductase. B) Overall structure of glutathione reductase.

	Location of CysT7 and T12 (from NH_2 terminus)
Mercuric Reductase[1]	135, 140
Glutathione Reductase[2]	58, 63
Lipoamide Dehydrogenase[3]	44, 49
Clipped Mercuric Reductase[1,4]	50, 55

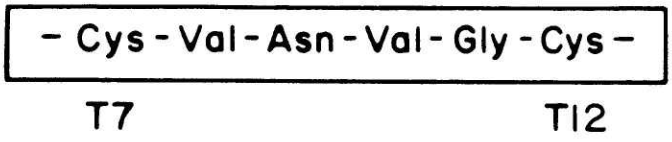

[1]Brown et al., 1983
[2]Untucht-Grau et al., 1982
[3]Rice et al., 1984
[4]Fox and Walsh, 1983

Figure 1-6. Location of active site cysteines in amino acid sequence of mercuric reductase, glutathione reductase, and lipoamide dehydrogenase.

unpublished).

Mercuric reductase has been isolated from a number of sources. The best studied are the Tn501- and R100-encoded enzymes from Pseudomonas aeruginosa plasmid pVS1 and E. coli plasmid pRR130, respectively. The Tn501 enzyme has been reported to be a dimer (Fox and Walsh, 1982), and the R100 enzyme a trimer (Kinscherf and Silver, unpublished observations cited in Foster, 1983) or a dimer (Rinderle et al., 1983). Schottel (1978) reports the R831 enzyme to be a trimer. Tonomura has observed a monomeric enzyme from the soil Pseudomonas sp., strain K62 (Furukawa and Tonomura, 1971) and an enzyme which reversibly forms monomers, dimers, tetramers, and octamers (unpublished observations cited in Williams and Silver, 1984). A difference between the subunit structures of the Tn501 and R100 enzymes would be surprising, considering the high degree of sequence homology between the two enzymes.

In this laboratory, we are studying the Tn501 encoded mercuric reductase. Fox and Walsh (1982) purified the enzyme in 80% yield from merbromin-induced Pseudomonas aeruginosa carrying the plasmid pVS1 by a two step procedure. Spectroscopic studies and thiol titrations first indicated that mercuric reductase was closely related to glutathione reductase and lipoamide dehydrogenase. These enzymes contain two two-electron acceptors (FAD and a redox active disulfide), and therefore can exist as an oxidized (E), a two electron reduced (EH_2), or four electron reduced (EH_4) form as diagrammed in Figure 1-7. Figure 1-8 shows the reactions catalyzed by glutathione reductase, lipoamide dehydrogenase, and thioredoxin reductase.

The presence of the redox active disulfide gives rise to unusual absorbance spectra for these enzymes. In particular, two electron reduction

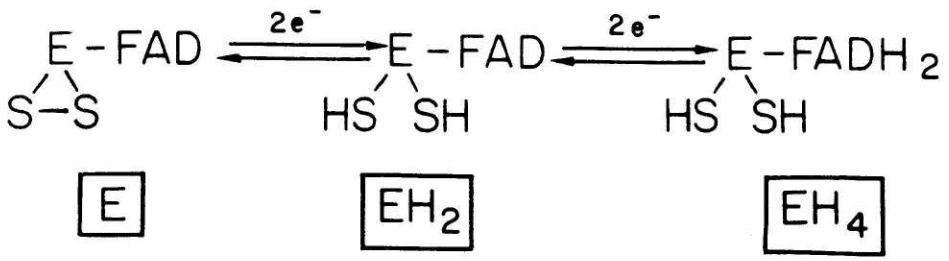

Figure 1-7. Redox states of mercuric reductase.

Glutathione reductase	$NADPH + GSSG \rightleftharpoons NADP + 2GSH$
Lipoamide dehydrogenase	$NADH + lipoamide\text{-}S_2 \rightleftharpoons NAD + lipoamide\text{-}(SH)_2$
Thioredoxin reductase	$NADPH + thioredoxin\text{-}S_2 \rightleftharpoons NADP + thioredoxin\text{-}(SH)_2$
General reaction	$NAD(P)H + RSSR \rightleftharpoons NAD(P) + 2RSH$

Figure 1-8. Reactions catalyzed by glutathione reductase, lipoamide dehydrogenase, and thioredoxin reductase (from Fox, 1983).

of these enzymes results in the formation of a charge transfer complex between an active site cysteine thiolate and the enzyme-bound FAD with an absorbance maximum near 540 nm (for example, see Figure 1-9). Other similarities between mercuric reductase and lipoamide dehydrogenase include dimeric structure, bound flavin redox potential, stereochemistry of nicotinamide oxidation, and fluorescence properties (Fox and Walsh, 1982).

Studies of mercuric reductase alkylated with [^{14}C]-iodoacetamide (Fox and Walsh, 1983) revealed further similarities between mercuric reductase and lipoamide dehydrogenase. Oxidized mercuric reductase was unreactive toward [^{14}C]-iodoacetamide. Two electron reduced enzyme was labeled predominantly at the active site. Sequencing of the major radiolabeled tryptic peptide indicated that alkylation occurred predominantly at the amino proximal cysteine in the active site and that the active site peptide sequence showed a high degree of homology to that of both glutathione reductase and lipoamide dehydrogenase (Fig. 1-10). Alignment of the active site peptide sequence with the amino acid sequence predicted from the DNA sequence indicated that the cysteines of the redox active disulfide were cys_{135} and cys_{140}. Amino acid analysis of a minor labeled peptide containing 20% of the total radioactivity compared favorably with the composition of the carboxy terminal tryptic peptide. Amino terminal sequencing indicated that the N-terminal formylmethionine is removed during post-translational processing.

The mercuric reductase dependent reduction of Hg(II) to Hg(0) can be observed by volatilization assays with ^{203}Hg (Schottel, 1978). Early studies revealed that thiols were required for the enzymatic reaction (Schottel, 1978; Izaki et al., 1974). The substrate is therefore written as $Hg(SR)_2$ in Equation 1-1, where the thiol commonly is 2-mercaptoethanol in in

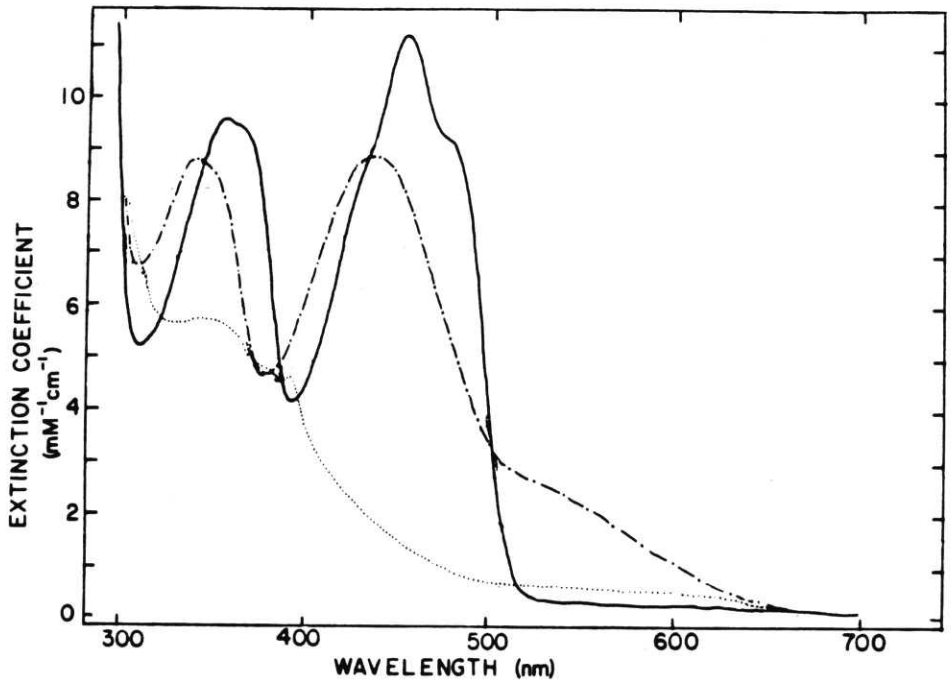

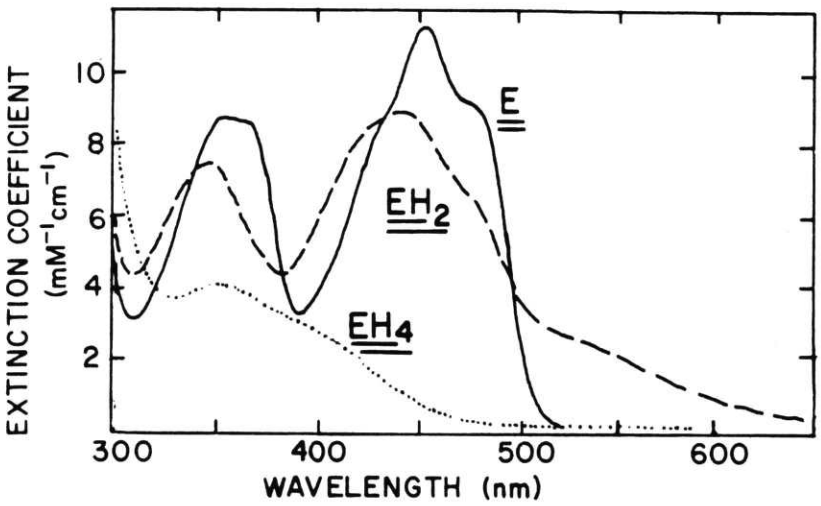

Figure 1-9. Spectral similarities between mercuric reductase and lipoamide dehydrogenase (from Fox and Walsh, 1983).

		T7	T12	[^{14}C]-Iodoacetamide Labeling (T7/T12)
Mercuric Reductase	Gly	Thr Ile Gly Gly Thr Cys Val Asn Val Gly Cys Val Pro Ser Lys		18/1
Glutathione Reductase[1]	His Lys	Leu Gly Gly Thr Cys Val Asn Val Gly Cys Val Pro	Lys Lys	8/1
Lipoamide Dehydrogenase[2]	Asn	Thr Leu Gly Gly Val Cys Leu Asn Val Gly Cys	Ile Pro Ser Lys	13/1

1. Arscott, Thorpe and Williams, 1981
2. Thorpe and Williams, 1976

Figure 1-10. Active site sequence comparison of mercuric reductase, glutathione reductase, and lipoamide dehydrogenase (from Fox and Walsh, 1983).

vitro studies. The effect of thiols on the enzymatic reaction has recently been addressed by Rinderle et al. (1983) and by Miller et al. (1986). Biphasic kinetics have been reported in both aerobic and anaerobic assays (Fox and Walsh, 1982; Rinderle et al., 1983). Rinderle et al. proposed that this observation is due to a hysteretic phenomenon in which mercuric reductase is slowly converted by thiols to a less active form, perhaps via disulfide reduction. Miller et al. (1986) have observed two major effects of thiol on the anaerobic enzymatic reaction at saturating NADPH. First, at high thiol/Hg(II) ratios, thiols show inhibitory K_m and V_{max} effects which can be explained respectively as the result of competition between free thiols and enzyme thiols for Hg(II) and as product inhibition, since free thiol ligand is a product of the reaction (see Equation 1-1). Second, at low thiol/Hg(II) ratios, substrate inhibition by Hg(II) occurs, apparently because under those conditions the Hg(II) binds incorrectly to the enzyme. Improper binding of Hg(II) in the absence of added thiol has also been proposed by Rinderle et al. to account for their observation of turnover followed by inactivation of mercuric reductase when the weaker ligand EDTA, rather than 2-mercaptoethanol, is used as the ligand for Hg(II). They furthermore suggest that recovery of activity, observed upon addition of 2-mercaptoethanol to Hg(EDTA)-inactivated enzyme, is due to a reversal of this improper binding of Hg(II) to the enzyme.

Despite the striking sequence homology between mercuric reductase and the disulfide oxidoreductases, mercuric reductase is a unique member of this class in its ability to catalyze the reduction of mercuric complexes (Fox and Walsh, 1982). Mechanistic properties which can account for this major difference between mercuric reductase and the disulfide oxidoreductases have recently been described through stopped flow studies on mercuric reductase

carried out by Sahlman et al. (1984) and through studies of two electron reduced mercuric reductase carried out by Miller et al. (1986), which will be described further in Chapter 4. Progress toward crystallization of the enzyme has been made (E. Pai, unpublished), and it is hoped that the Xray crystal structure will eventually be determined. Clearly, further studies of native mercuric reductase have been and should continue to be useful in elucidating the mechanism of mercuric ion reduction.

This thesis describes the use of site directed mutagenesis as an alternative approach to the study of mercuric reductase's physical and catalytic properties. In this case we have specifically altered the redox active disulfide (cys_{135}-cys_{140}) by single cys to ser or cys to ala mutations at $residue_{135}$ or $residue_{140}$. Such mutations introduce two major differences from the native enzyme. First, the native enzyme's potential for either monodentate or bidentate complexation of Hg(II) by the active site cysteines is replaced in the mutants by a potential for only monodentate complexation by an active site cysteine (with perhaps weak complexation by serine in the cys to ser mutants). Second, removal of the redox active disulfide results in mutant enzymes which have only a two electron redox capacity rather than the four electron redox capacity of native enzyme. By characterizing the physical and catalytic properties of these mutant proteins, we hope to gain some insight into the influence of the redox active disulfide in the native enzyme which enables it to bind and then reduce Hg(II) and various other substrates. As no previous work on cys to ser or cys to ala mutants of mercuric reductase or the related disulfide oxidoreductases has yet been reported, much of the work on these proteins will also be exploratory in nature.

CHAPTER TWO

GENERATION AND EXPRESSION OF MERCURIC REDUCTASE MUTANTS

Introduction

We have begun to address the mechanism by which mercuric reductase binds and reduces Hg(II) via oligonucleotide directed mutagenesis of the active site cystine disulfide residues. These residues, $cysteine_{135}$ and $cysteine_{140}$, have been shown to play a key role in catalysis (Fox and Walsh, 1982; 1983), serving as one of two two-electron acceptors in the active site (FAD is the second) and, in the reduced form, acting as the Hg(II) ion binding site.

Although no X-ray crystal structure is yet available for mercuric reductase (crystallization attempts are underway), the Tn501 merA gene has been sequenced (Fig. 2-1) (Brown et al., 1983), and the enzyme's primary structure bears strong homology to that of human red cell glutathione reductase. There is an excellent 1.9 Å resolution map available for glutathione reductase alone and in its complex with $NADP^+$ or glutathione (Thieme et al., 1981; Schulz et al., 1982; Pai and Schulz, 1983). The structural similarity between the two enzymes, especially the identity of 12 residues in the active site tryptic peptide, suggested that the glutathione reductase structure would serve as an initial framework against which to plan mutant mercuric reductase species. The glutathione reductase X-ray structure coupled with previous physical studies of mercuric reductase strongly point to the active site cysteines as playing a key role in Hg(II) binding and reduction.

The availability of chemically synthesized oligonucleotides (for a recent review see Itakura et al., 1984), the development of rapid DNA sequencing techniques (Maxam and Gilbert, 1979; Sanger et al., 1981), and the development of M13 cloning vectors (Messing, 1983) have provided a convenient method for performing site-directed mutagenesis (Zoller and

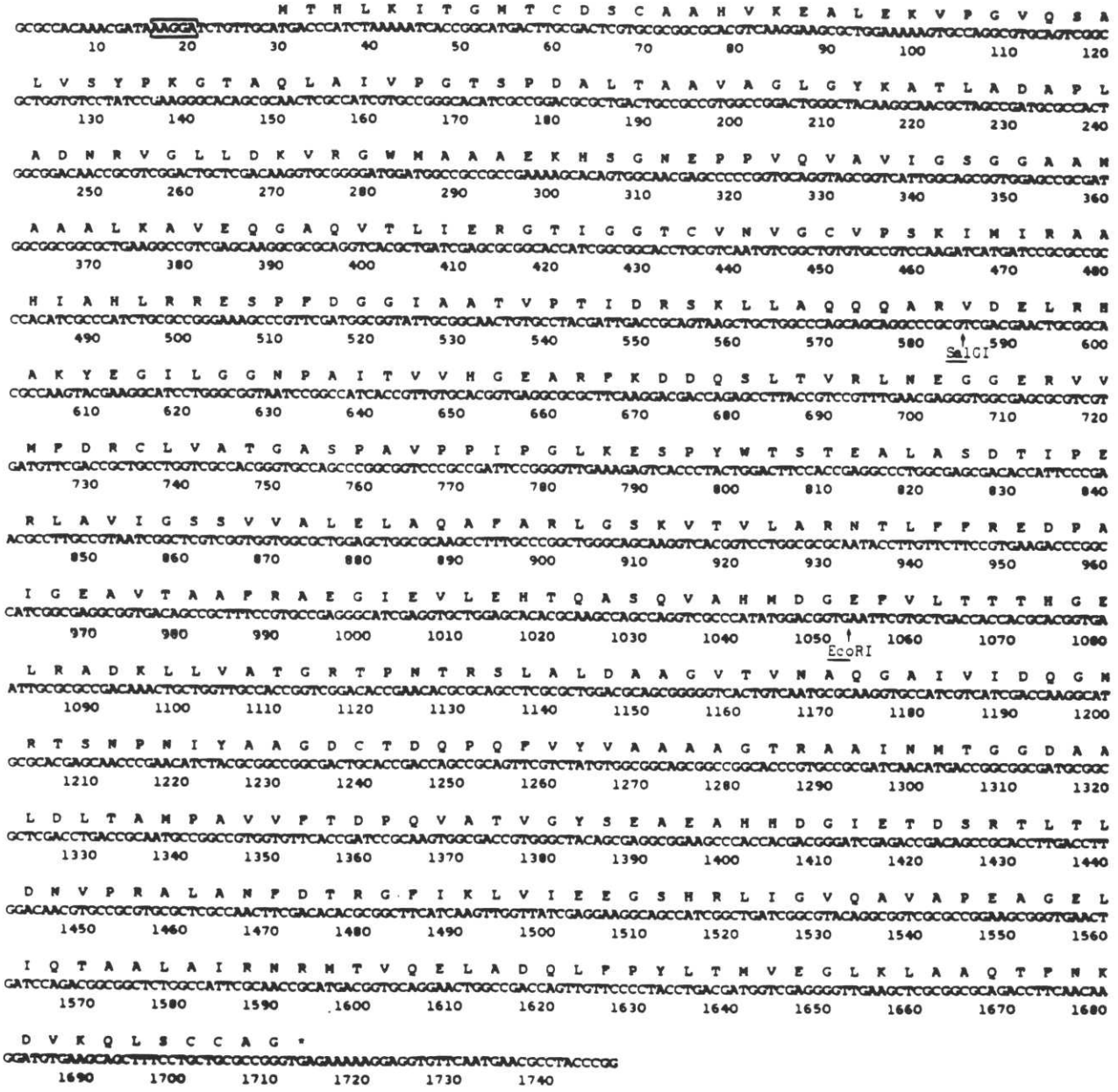

Figure 2-1. DNA sequence and predicted amino acid sequence of 1747 base pairs of Tn501 DNA which contains the merA gene (from Brown et al., 1983). The Shine-Dalgarno sequence is boxed. A NarI cleavage site is located at position 2 in the sequence.

Smith, 1983). Alternatively, mutagenesis may be carried out using double-stranded plasmid DNA as the template (Inouye and Inouye, 1985). The merits and disadvantages of each method have been discussed (see Zoller and Smith, 1983 and Inouye and Inouye, 1985). The availability of convenient cloning sites in or near the Tn501 merA gene influenced our decision to pursue the M13 approach for merA mutagenesis. As will be discussed in this chapter, we in fact encountered some problems as a result of this approach, but are now overcoming these by combining a modification of our cloning strategy with more sophisticated M13 mutagenesis techniques that have recently become available.

The Tn501-encoded native mercuric reductase has previously been purified in our laboratory in high yield from Pseudomonas aeruginosa PA09501 (pVS1) in which mercuric reductase constitutes 6% of the soluble cellular protein upon induction (Fox and Walsh, 1982). The availability of large quantities of native enzyme greatly facilitated a number of experiments reported by Fox and Walsh (1982; 1983) which we planned to repeat with our mutant mercuric reductase proteins for comparison with the native enzyme. This chapter also describes the construction of plasmids placing the merA native or mutant genes behind the tac promoter (de Boer et al., 1982), which enabled us to overexpress native and mutant merA proteins in E. coli at levels comparable to or higher than that observed in the Pseudomonas strain.

Experimental Procedures

Materials

E. coli strain DS714 carrying the plasmid pJOE114 (Brown et al., 1983) was the generous gift of Dr. Nigel Brown of the University of Bristol, Department of Biochemistry, Bristol BS8 1TD, U.K., who also kindly provided us with a detailed restriction map of pJOE114 (Fig. 2-2). *E. coli* strain W3110 *lacI*^{q} and plasmid pSE181 were generously provided by Dr. Graham Walker of the Massachusetts Institute of Technology, Department of Biology, Cambridge, Massachusetts 01239. *E. coli* strain JM101, M13mp8 RF DNA, and M13mp9 RF DNA were obtained from New England Biolabs.

All restriction enzymes, T4 polynucleotide kinase, and T4 ligase were obtained from New England Biolabs. DNA polymerase I (Klenow fragment) was obtained from New England Biolabs or Boehringer-Mannheim. Calf intestinal alkaline phosphatase was obtained from Boehringer-Mannheim. Reagents and enzymes for Sanger sequencing, deoxyadenosine 5'-[α-^{32}P]triphosphate (>400 Ci/mmol), deoxyadenosine 5'-(α-[^{35}S]thio)phosphate (>600 Ci/mmol), and adenosine 5'-[γ-^{32}P]triphosphate (>5000 Ci/mmol) were purchased from Amersham. Deoxyribonucleotide triphosphates were from Boehringer-Mannheim or Pharmacia and riboATP from Sigma. Agarose, low melting point agarose, and nucleic acid grade phenol were from Bethesda Research Laboratories. Polyethylene glycol 6000 was purchased from J. T. Baker.

Protected deoxydinucleotides for oligonucleotide synthesis were obtained from P-L Biochemicals. Substituted aminomethylpolystyrene resins were obtained from Vega. Protected deoxymononucleotides and substituted Fractosil resins for automated oligonucleotide synthesis were purchased from Biosearch. Sep-Pak cartridges were obtained from Waters Associates.

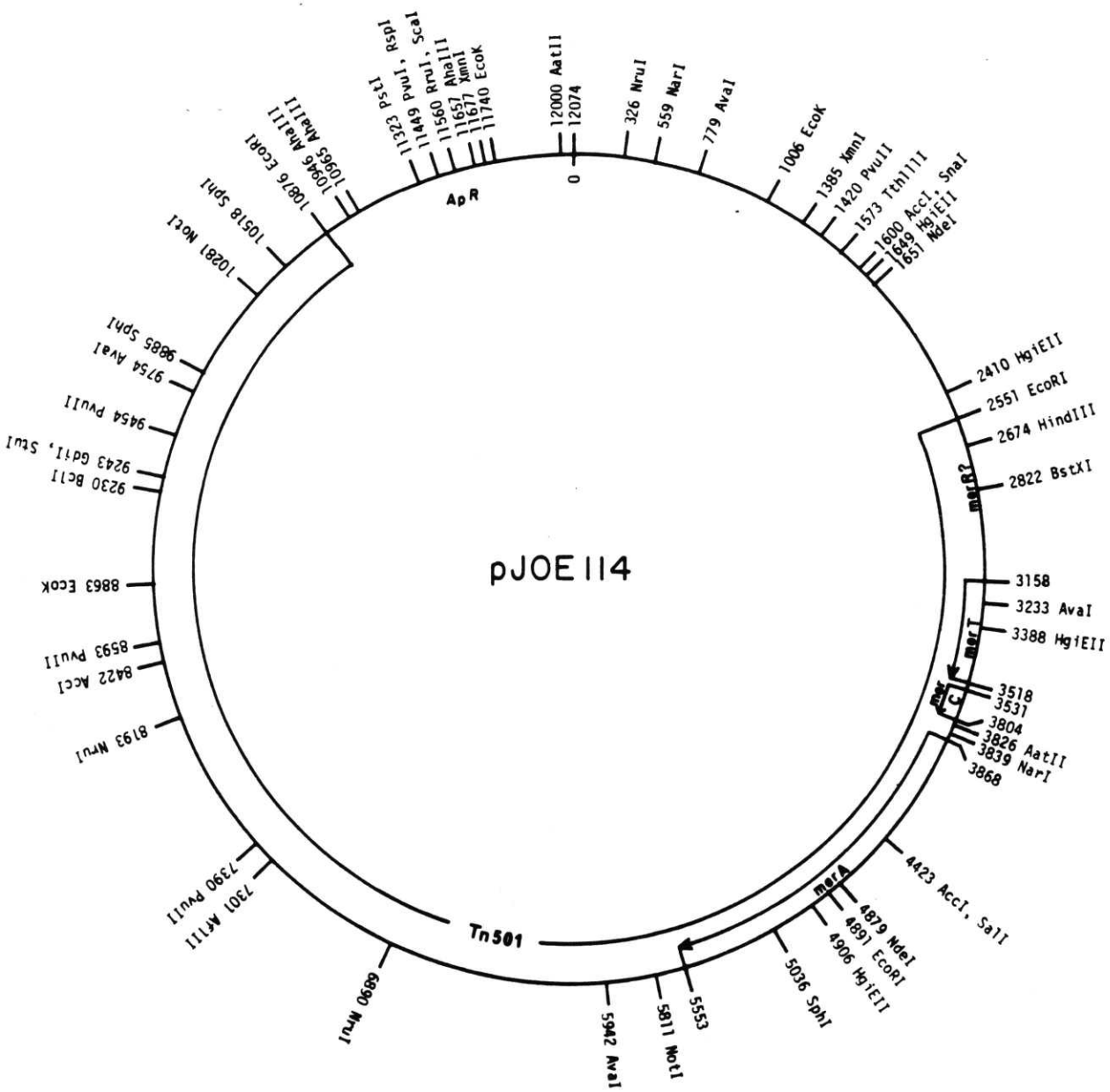

Figure 2-2. Restriction map of plasmid pJOE114, a recombinant made by replacement of the EcoRI fragments of Tn1721 with those of Tn501 in the pBR322 (ΔSalI-EcoRI)::Tn1721 recombinant pJOE105 (Brown et al., 1983).

Sephadex G-50 and Sephacryl S-300 were purchased from Pharmacia.

Ampicillin sodium salt, IPTG, and Xgal were from Sigma.

Methods

Growth of Bacteria

Cells used for work described in this chapter were grown in yeast-tryptone (YT) media (Miller, 1972), supplemented with the appropriate antibiotic or indicator necessary for cell selection.

Quantitation of DNA

Double stranded plasmid DNA, single stranded closed circular DNA and oligonucleotides were quantitated spectrophotometrically as described in Maniatis et al. (1982). In some instances, when insufficient DNA was available for spectrophotometric quantitation, the amount of DNA present was estimated by comparison of the ethidium bromide fluorescence of the sample on an agarose gel with that of known standards. Stock solutions of dNTPs were quantitated spectrophotometrically as described in Maniatis et al. (1982).

Oligonucleotide synthesis

Oligonucleotides for cysteine to serine mutations were synthesized from protected 3'-terminating deoxydinucleotide phosphotriesters by the solid phase phosphotriester method of Itakura (Tan et al., 1983), as diagrammed in Fig. 2-3. After removal of the phosphate and base protecting groups and cleavage from the aminomethylpolystyrene support, the 5'-DMT-oligonucleotides were purified by reverse phase chromatography, carried out

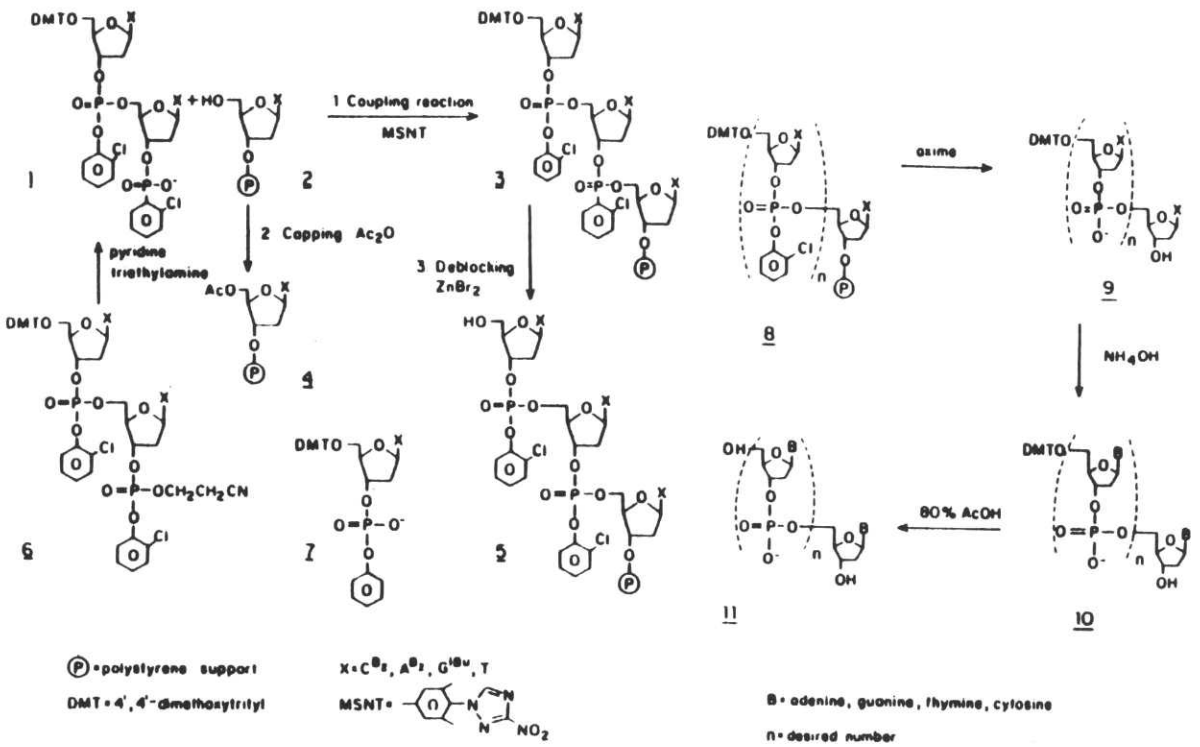

Figure 2-3. Scheme outlining the phosphotriester solid-phase method of oligonucleotide synthesis (from Tan et al., 1983).

on a Waters Associates HPLC equipped with an Automated Gradient Controller or a Model 660 solvent programmer and a Model 440 absorbance detector, using a 2 ml/min 20 min linear gradient from 15 to 30% CH_3CN in 0.1 M triethylammonium acetate buffer (pH 7.2). The trityl group was then removed, and the resulting deoxyoligonucleotide was purified by reverse phase chromatography using a 20 min linear gradient run at 2 ml/min from 5 to 30% CH_3CN in 0.1 M triethylammonium acetate (pH 7.2). The oligonucleotide was then 5'-phosphorylated with 5'-[γ-^{32}P]ATP and T4 polynucleotide kinase and sequenced using a modified Maxam and Gilbert protocol (Zoller and Smith, 1983).

Oligonucleotides for cysteine to alanine mutations were synthesized on a Biosearch SAM I automated DNA synthesizer, using a modified phosphotriester procedure provided by the manufacturer of the instrument. The synthesizer was programmed to leave the remaining trityl group on the oligonucleotide after the final coupling step. After removal of the base and phosphate protecting groups and cleavage of the oligomer from the support, the crude oligonucleotide was partially purified on a Sep-Pak cartridge using the procedure of Khorana (Lo et al., 1984). The trityl group was then removed (Tan et al, 1983), and the oligonucleotide was then further purified by polyacrylamide gel electrophoresis, followed by Sephadex G-50 chromatography, using a procedure provided by Biosearch (SAM I manual).

5' Phosphorylation of Oligonucleotides

5' Phosphorylation of oligonucleotides was carried out on a 400 pmol scale (approximately 2 µg for a 17mer) using the procedure of Zoller and Smith (1983). For experiments requiring radiolabeling of the oligonucleotide, the procedure was carried out on a 100 pmol scale using 100

μCi of [γ-^{32}P]ATP in a total volume of 60 μl. This yields a solution of end-labeled oligonucleotide sufficiently concentrated for hybridization screening and specific priming tests, even after the Sephadex G-50 chromatography is carried out to remove excess [γ-^{32}P]ATP.

Plasmid Preparations

Plasmid DNA was prepared on a large scale (about 500 μg) by a lysozyme-Triton lysis procedure obtained from the laboratory of Professor David Botstein, Department of Biology, Massachusetts Institute of Technology, Cambridge, MA 02139 (Wasserman, 1983).

Miniscale preparations of plasmid DNA (2-5 μg) were prepared by Ish-Horowicz's modification of the procedure of Birnboim and Doly (Maniatis et al., 1982).

M13 Phage and Single Stranded DNA Preparations

M13 phage and single stranded DNA were prepared according to the procedure of Zoller and Smith (1983) with two modifications: first, the culture supernatant containing the phage was centrifuged twice to efficiently remove host cells, a potential source of contaminating RNA or chromosomal DNA, and second, one chloroform extraction rather than two diethyl ether extractions of the single stranded DNA solution was carried out.

Restriction Enzyme Digests

Restriction enzyme digests were carried out under conditions recommended by the supplier of the restriction enzymes used. Buffers, reagents, tubes, and pipette tips used for these digests were sterile.

Sequential digests with two or more incompatible restriction enzymes were carried out either by ethanol precipitation (Maniatis et al., 1982) after the first incubation (which always contained the enzyme requiring the buffer with the lowest salt concentration) or by adjusting the buffer and salt concentrations as needed after the first digest was complete. Digests were terminated either by phenol extraction (Maniatis et al., 1982) or by loading directly onto gels for electrophoresis after addition of loading buffer.

Dephosphorylations

After digestion with the appropriate restriction enzyme(s) followed by ethanol precipitation, DNA fragments were dephosphorylated as needed with calf intestinal alkaline phosphatase (CIP) as described in Maniatis et al. (1982). CIP reaction mixtures were loaded directly onto agarose gels for electrophoresis after addition of loading buffer.

Agarose Gel Electrophoresis

Horizontal agarose gel electrophoresis was carried out in 40 mM Tris-acetate, 1 mM EDTA, pH 8.0 buffer, according to procedures described in Maniatis et al. (1982), using HindIII-digested lambda DNA as standards. Samples were loaded in 5% Ficoll 400 (w/v), 20 mM EDTA, 0.1% SDS, and 0.02% bromphenol blue. DNA fragments were isolated by electrophoresis on low melting point agarose followed by standard phenol extraction procedures (Maniatis et al., 1982).

Ligations

Ligations were carried out at 14°C overnight with a 5:1 molar ratio of insert to vector DNA under conditions recommended by the supplier of the T4

DNA ligase. Some blunt end ligations were carried out at 14°C for 2 hr in the presence of 13% polyethylene glycol 6000 using a procedure from Pharmacia (1984).

Transformations

Competent *E. coli* JM101 or W3110 *lacI*^{q} cells were prepared by $CaCl_2$ treatment according to a procedure from New England Biolabs (1983). 100 µl of competent cells were added to various amounts of ligation mixture (up to approximately 50 ng of DNA) at 0°C and incubated with occasional mixing for 30 min. The transformation reaction mixtures were then heated at 37°C for 2 min, and then plated onto the appropriate medium to select for transformants.

DNA Sequencing

Oligonucleotides were sequenced by a modified Maxam and Gilbert protocol (Zoller and Smith, 1983). The procedure of Maxam and Gilbert (1979), as outlined in Maniatis et al. (1982) was used to sequence the DNA encoding the *merA* active site after reconstruction of the *merA* gene following mutagenesis. The procedure of Sanger et al. (1981) as outlined in the Amersham M13 Cloning and Sequencing Handbook (1983) was used to sequence recombinant M13 DNA. Sanger sequencing was carried out with either deoxyadenosine 5'-[α-^{32}P]triphosphate (>400 Ci/mmol) or deoxyadenosine 5'-(α-[^{35}S]thio)phosphate (>600 Ci/mmol). In the latter case, gels were fixed in an aqueous solution of 10% acetic acid and 10% methanol, then dried on a BioRad Model 1125B slab gel dryer. With [^{35}S]-labeling we typically were able to read 300-350 bases from the priming site.

Mutagenesis

Oligonucleotide-directed mutagenesis was carried out by the method of Zoller and Smith (1983), with the exception of extending the mutagenesis primer in the presence of a universal sequencing primer (Messing, 1983), located 280 bases from the cys_{135} codon, and deleting the alkaline sucrose gradient centrifugation. Primer specificity was assayed by *in vitro* primer extension followed by HaeIII and NciI digestion and denaturing gel electrophoresis. Optimal specificity was obtained by annealing 30 pmol primer to 1 pmol M13ps1 template at 55°C for 10 min, followed by cooling to 0°C for 20 min and extension. For the mutagenesis reactions, extension and ligation were carried out under the above conditions for 18 h at 15°C in the presence of 5 pmol New England Biolab sequencing primer #1211. Mutants were screened by dot-blot hybridization with wash temperatures of 58°C for the ser_{135}, cys_{140} mutant (5'-ACATTGACGCTGGTGCC-3'; T_D = 54°C), 26°C for the cys_{135}, ser_{140} mutant (5'-CAGCCTTCACACGGCAG-3'; T_D = 56°C), 52°C for the ala_{135}, cys_{140} mutant (5'-GACATTGACGGCGGTGCC-3'; T_D = 60°C), and 54°C for the cys_{135}, ala_{140} mutant (5'-GACGGCACAGCGCCGACAT-3'; T_D = 64°C). After plaque purification and a second round of hybridization screening, the presence of the desired mutation was confirmed by Sanger sequencing (Sanger et al., 1981). The resulting mutant plasmids are M13ps2 (ser_{135}, cys_{140}), M13ps3 (cys_{135}, ser_{140}), M13ps4 (ala_{135}, cys_{140}), and M13ps5 (cys_{135}, ala_{140}).

Plasmid Constructions

Figure 2-4 is an enlarged map of the *merA* gene in pJOE114 showing restriction sites relevant to the work described in this section.

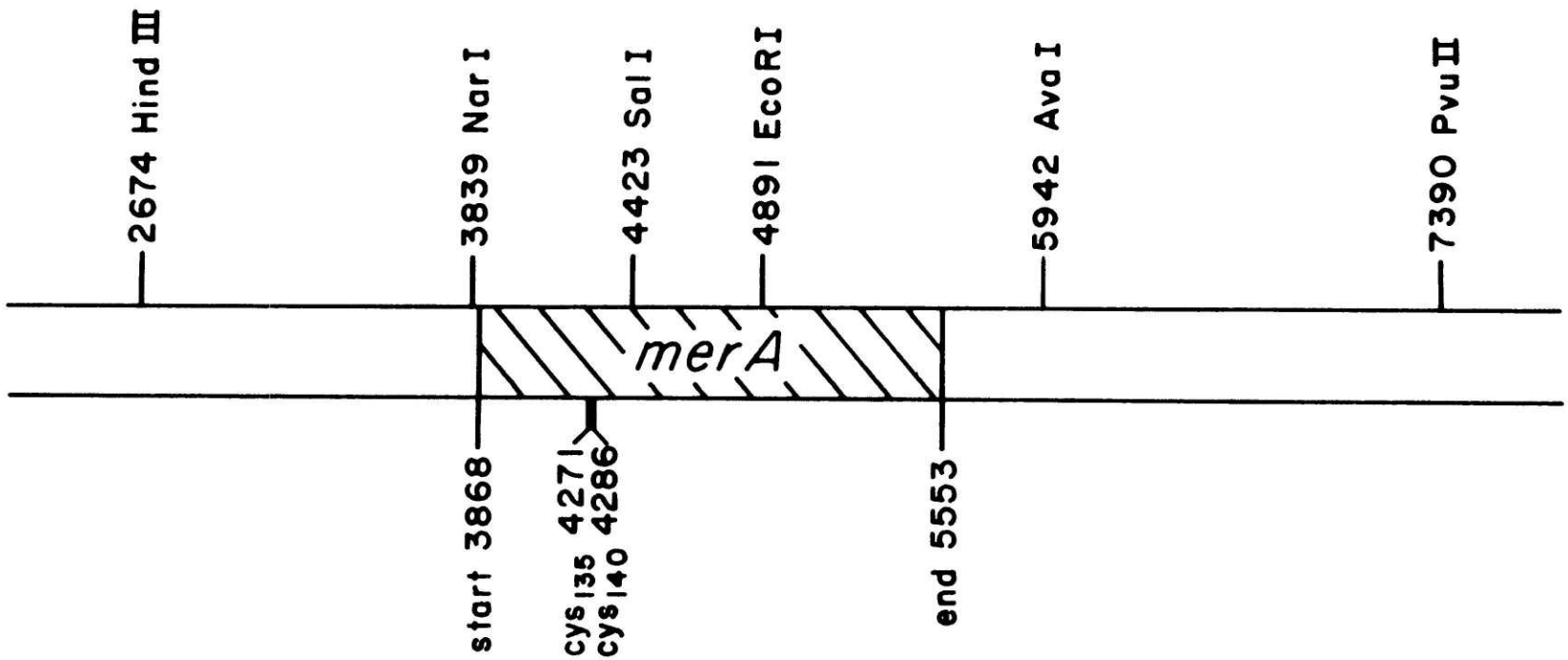

Figure 2-4. Enlarged map of the merA gene in pJOE114. The locations of restriction sites used for subcloning and the positions of the active site cysteines are indicated.

M13ps1

The 1748 base pair HindIII-SalI fragment of pJOE114 was isolated by low melting point agarose gel electrophoresis and ligated in the presence of HindIII-SalI cleaved M13mp9 (RF) DNA pretreated with calf intestinal alkaline phosphatase (Fig. 2-5). The resulting mixture was used to transform competent E. coli JM101. Six colorless plaques were then selected from YT plates containing 3% Xgal and 0.6% IPTG. Single strand and replicative form DNA were isolated and RF DNA was shown to contain the desired insert by analysis with the restriction enzymes HindIII, SalI, and EcoRI.

pPSM2, pPSM3, pKAM1, and pKAM2

The 1748 base pair HindIII-SalI fragment of M13ps2, M13ps3, M13ps4, or M13ps5 replicative form DNA was ligated to the large dephosphorylated HindIII-SalI fragment of pJOE114 and transformed into JM101 or W3110 $lacI^q$ (Fig. 2-6). These procedures yielded the mutant merA-containing plasmids pPSM2 (ser_{135}, cys_{140}), pPSM3 (cys_{135}, ser_{140}), pKAM1 (ala_{135}, cys_{140}), and pKAM2 (cys_{135}, ala_{140}).

The DNA encoding the active site residues (amino acids 130-180) of pPSM2 and pPSM3 was sequenced from the unique SalI site of these plasmids by the method of Maxam and Gilbert (1979) by the following procedure. Contaminating RNA and protein were first removed from 0.5 mg each of pPSM2 and pPSM3 by chromatography on a 2.5 x 30 cm Sephacryl S-300 column run in 0.2 M NaCl, 0.5 mM EDTA, 10 mM Tris, pH 7.6 buffer at a flow rate of 100 ml/hr. Fractions were monitored by A_{260}; DNA eluted as the first peak. After SalI digestion, 15 μg of linear pPSM2 or pPSM3 was treated with calf intestinal alkaline phosphatase and then 5'-phosphorylated with T4

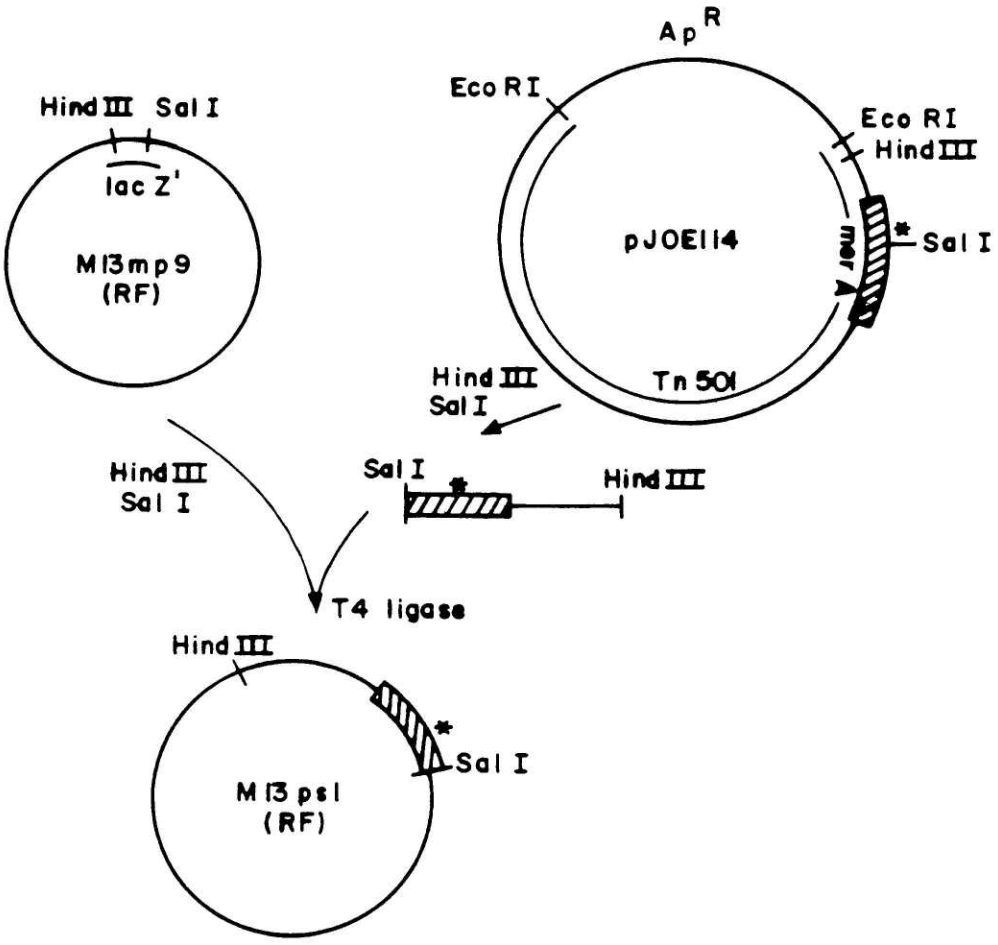

Figure 2-5. Preparation of template M13ps1 for mutagenesis.

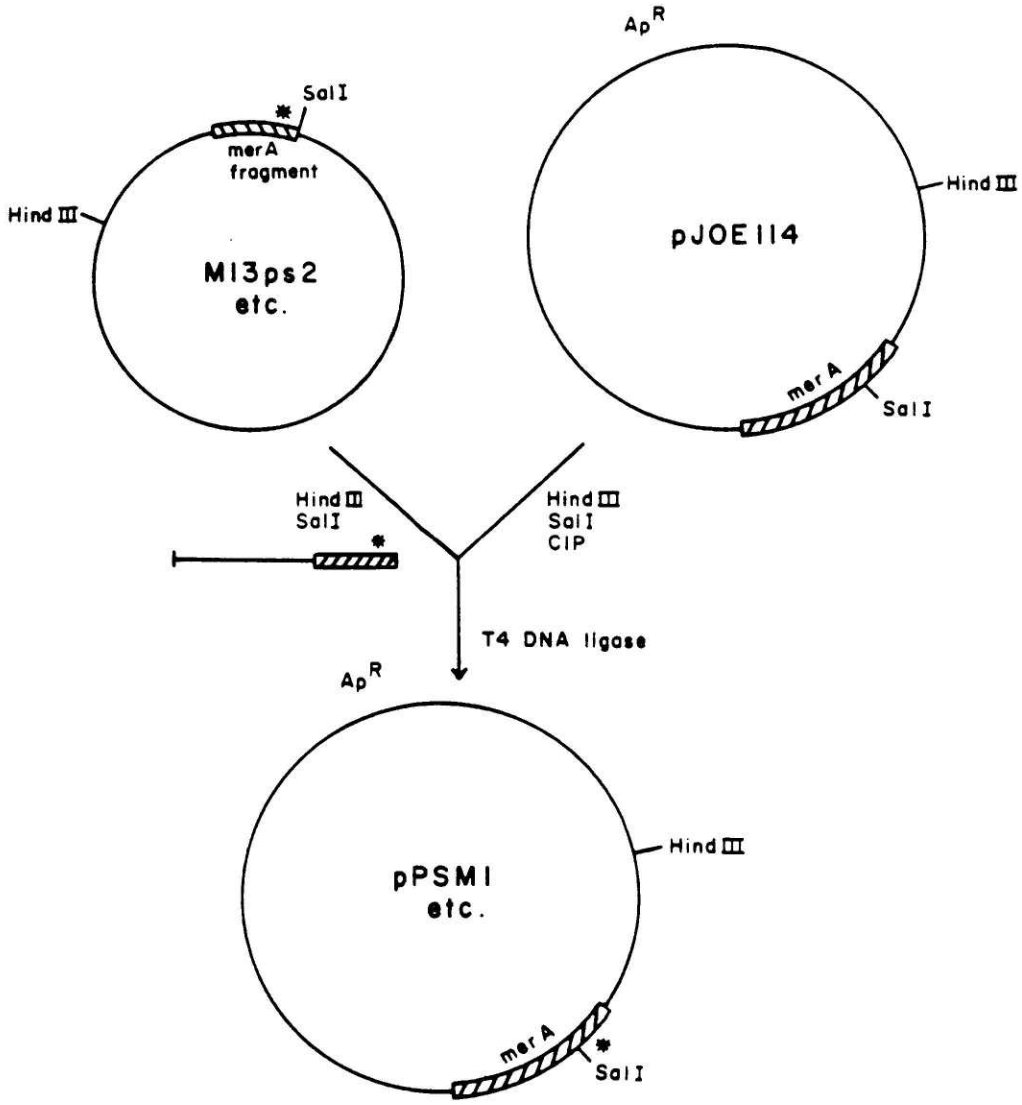

Figure 2-6. Reconstruction of the mutant merA genes after mutagenesis. The resulting plasmids are pPSM2, pPSM3, pKAM1, and pKAM2 from M13ps2, M13ps3, M13ps4, and M13ps5, respectively. Asterisks indicate the presence of an active site mutation.

polynucleotide kinase and 5'-[γ-^{32}P]ATP (50 μCi) using methods described above. The resulting end-labeled DNA was then digested with BglI to yield two end-labeled fragments (231 and 167 base pairs long) which were separated by polyacrylamide gel electrophoresis and visualized by autoradiography for 5 min. The band containing the 231 base pair long fragment, which contains the active site sequence, was cut out and crushed, and the DNA was eluted at 37°C overnight in 1 ml of 0.5 M NH_4OAc, 10 mM $MgCl_2$, 1 mM EDTA, and 0.1% SDS. Particulate matter was removed by gravity filtration through a 0.45 micron syringe filter. After ethanol precipitation, the sample was ready for the Maxam and Gilbert sequencing reactions.

The DNA from the merA start through the unique SalI site in plasmids pKAM1 and pKAM2 was sequenced by the method of Sanger et al. (1981) by subcloning appropriate fragments of these plasmids into M13mp8 and M13mp9 as described below to produce plasmids M13ka1, M13ka2, M13ka3, and M13ka4.

M13ka1, M13ka2, M13ka3, and M13ka4

The 584 bp NarI-SalI fragment of pKAM1 and pKAM2 was ligated to the large dephosphorylated NarI-SalI fragment of M13mp9 to produce plasmids M13ka1 and M13ka2, respectively (Fig. 2-7). The 1052 bp NarI-EcoRI fragment of pKAM1 and pKAM2 was ligated to the large AccI-EcoRI fragment of M13mp8 to produce plasmids M13ka3 and M13ka4, respectively (Fig. 2-8). Transformants were identified as described above for M13ps1, and the presence of the desired insert was confirmed by Sanger sequencing.

pPS01, pPS02, and pPS03

The 3550 base pair NarI-PvuII pJOE114 fragment and large dephosphorylated ClaI-SmaI pSE181 fragment were isolated by low melting

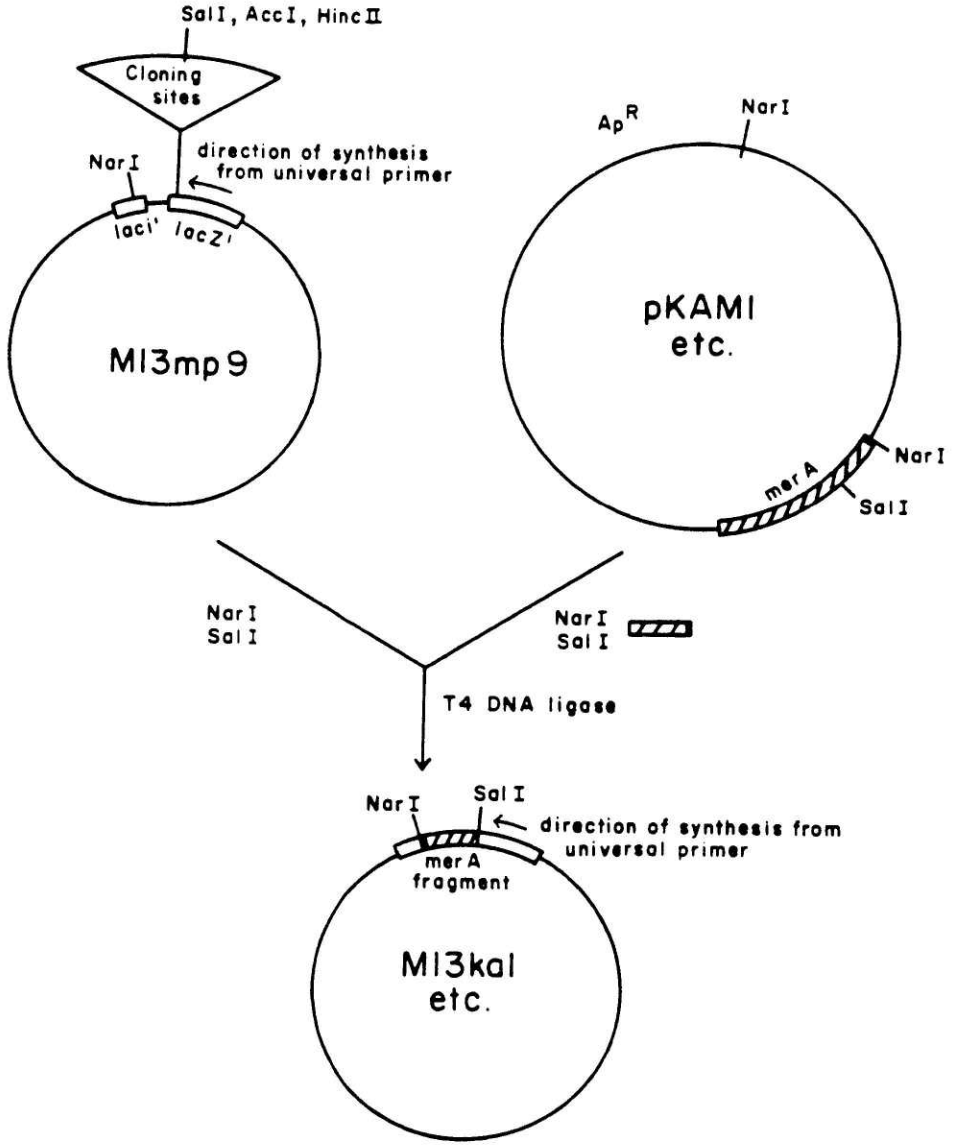

Figure 2-7. Preparation of mutagenesis and sequencing templates M13ka1 and M13ka2 from pKAM1 and pKAM2, respectively.

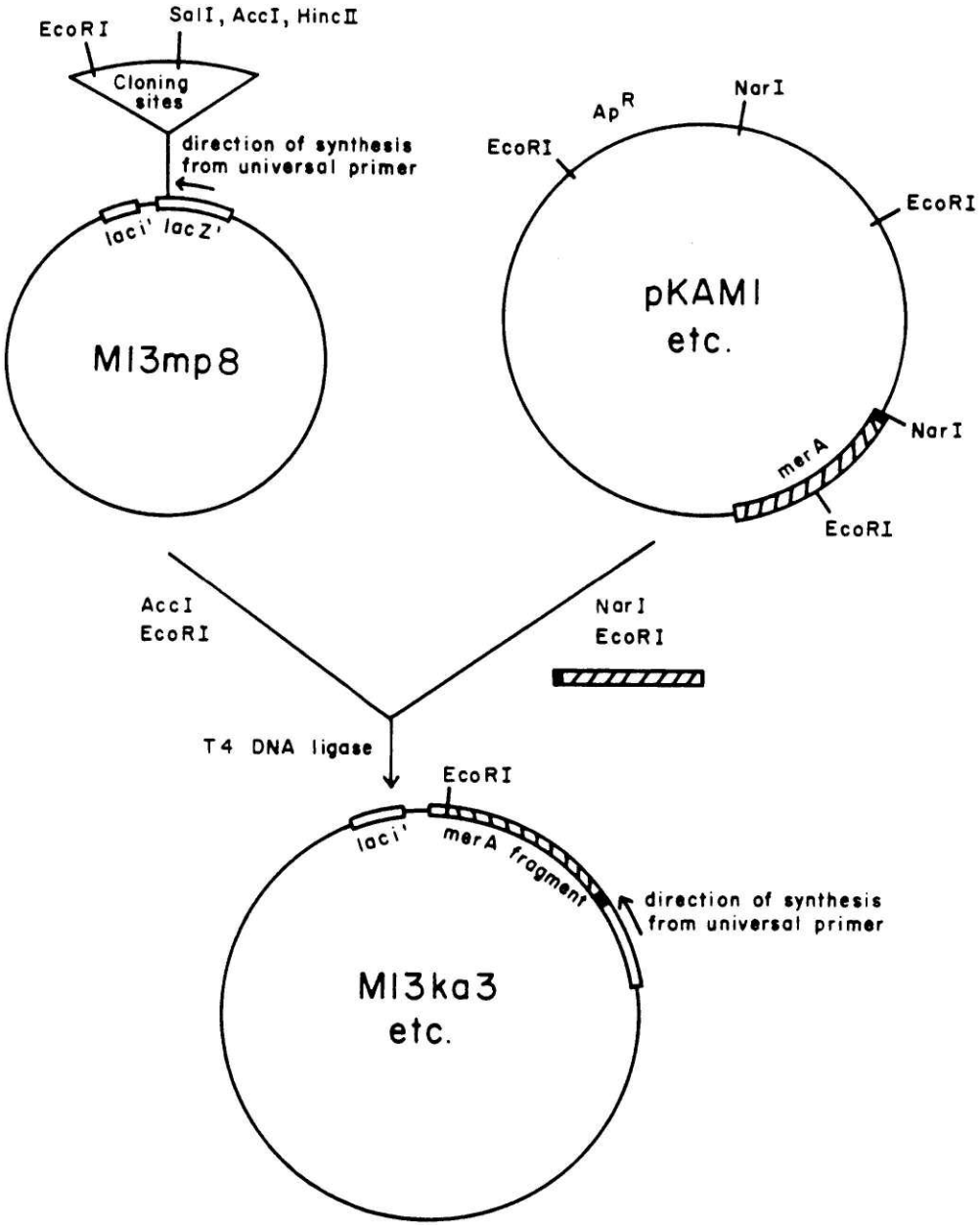

Figure 2-8. Preparation of sequencing templates M13ka3 and M13ka4 from pKAM1 and pKAM2, respectively.

point gel electrophoresis and ligated in the presence of T4 DNA ligase. The resulting mixture was used to transform E. coli W3110 lacI^q, and six Ap^R colonies were selected on YT plates containing 50 μg/ml ampicillin. Plasmid isolated from each colony was in each case shown to contain the desired insert by restriction analysis with the enzyme EcoRI. Overproduction of mercuric reductase by these cells (W3110 lacI^q/pPSO1) was demonstrated by SDS polyacrylamide gel electrophoresis of crude extract after induction with IPTG. Insertion of the 3550 base pair NarI-PvuII fragment of plasmids pPSM2 (ser_{135}, cys_{140}) and pPSM3 (cys_{135}, ser_{140}) into ClaI-SmaI-cleaved pSE181 afforded plasmids pPSO2 and pPSO3, respectively (Fig. 2-9).

pKAO1 and pKAO2

Plasmids pKAM1 and pKAM2 were each digested with AvaI. The AvaI digestions were terminated by phenol extraction. The resulting DNA fragments were then treated with DNA polymerase I (Klenow fragment), dATP, dCTP, dGTP, and dTTP as described by Amersham (1983) to fill in the recessed 3' terminii. The resulting blunt-ended DNA fragments were then separated by agarose gel electrophoresis. The desired 2708 bp fragment was then treated with NarI to give two fragments, which were separated on a second agarose gel. The desired fragment (2102 bp) was then ligated to the large dephosphorylated ClaI-SmaI pSE181 fragment as described above to yield plasmids pKAO1 and pKAO2 from pKAM1 and pKAM2, respectively (Fig. 2-10). The presence of the desired insert was confirmed by restriction analysis with SalI and by SDS gel electrophoresis of crude sonicate after induction with IPTG.

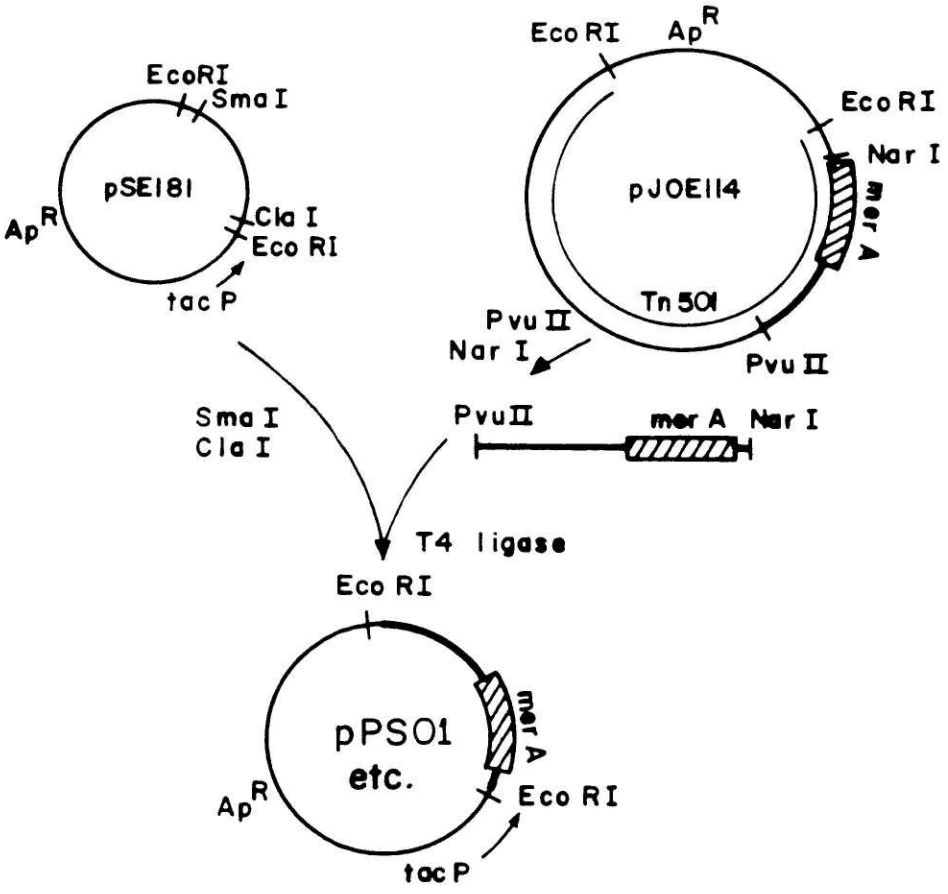

Figure 2-9. Preparation of plasmids pPSO1, pPSO2, and pPSO3 from pJOE114, pPSM2, and pPSM3, respectively, for overproduction of the native and cys to ser mutant merA gene products.

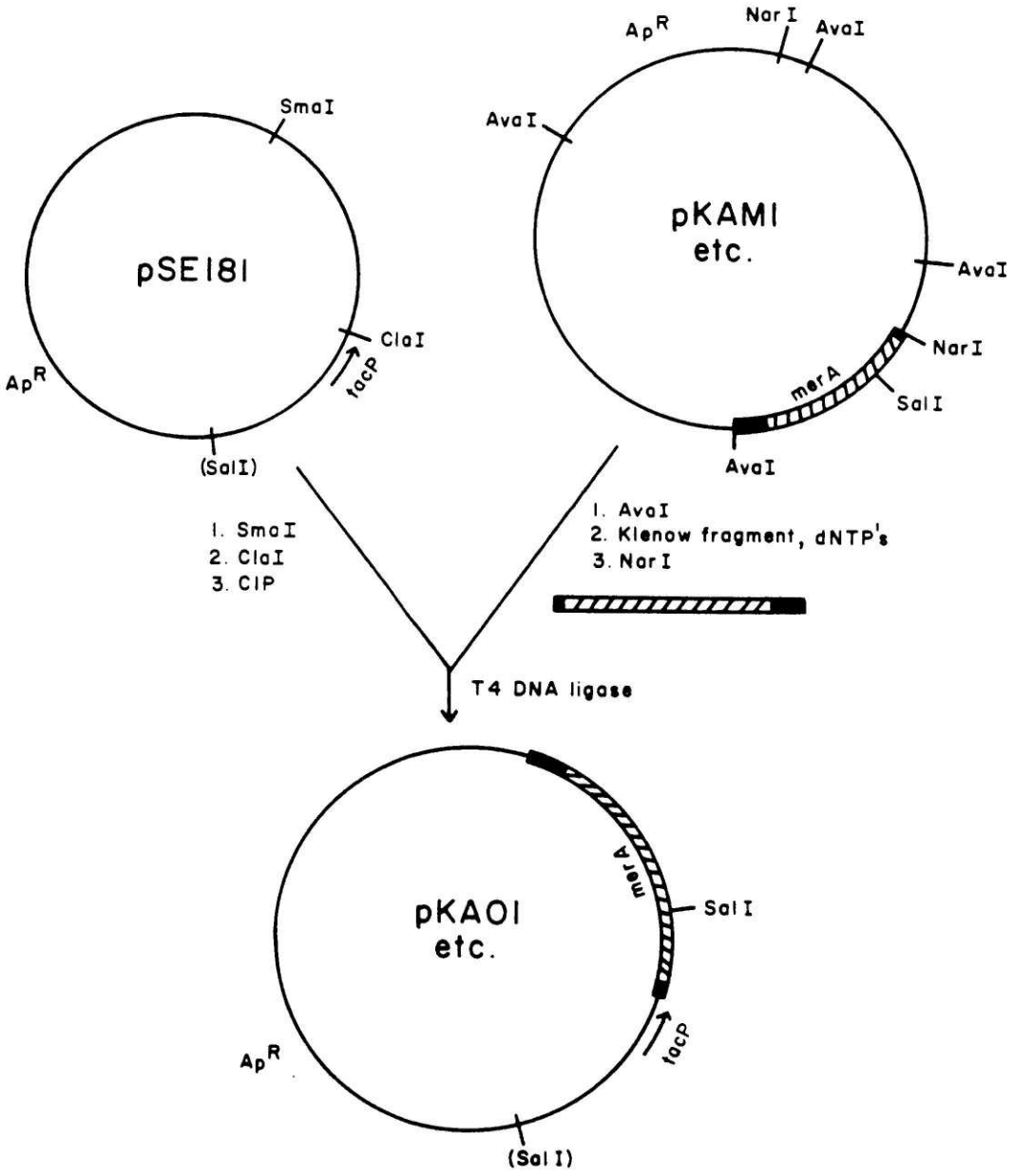

Figure 2-10. Preparation of plasmids pKA01 and pKA02 from pKAM1 and pKAM2, respectively, for overproduction of the cys to ala mutant merA gene products.

Results

For clarity, names and brief description of the plasmids discussed in this chapter are presented in Table 2-I.

Mutagenesis

Mutagenesis was carried out on a 1748 base pair active site-containing merA fragment (encoding amino acids 1-186 of the enzyme) subcloned from the plasmid pJOE114 into the single-stranded phage M13mp9. The method of Zoller and Smith (1983) was used with modifications described in Methods. The mutagenesis primers 5'-ACATTGACGCTGGTGCC-3', 5'GACGGCACACTTCCGAC-3', 5'-GACATTGACGGCGGTGCC-3', and 5'-GACGGCACAGCGCCGACAT-3' contain one mismatch at the eleventh base (cys_{135} (TGC) -> ser (AGC)), two mismatches at the eleventh and twelfth bases (cys_{140} (TGT) -> ser (AGT); gly_{139} (GGC) -> gly (GGA)), two mismatches at the eleventh and twelfth bases (cys_{135} (TGC) -> ala (GCC)), and two mismatches at the tenth and eleventh bases (cys_{140} (TGT) -> ala (GCT)), respectively (Fig. 2-11). For unknown reasons, no mutants were obtained with the primer 5'-ACGGCACACTGCCGACA-3' which contains one mismatch at the tenth base (cys_{140} (TGT) -> ser (AGT)). Possibly the effective concentration of this primer was reduced by self-hybridization, perhaps via a hairpin structure, since this 17mer contains two strings of 5 bases, separated by 3 bases, which are complementary to each other. Overall mutagenesis yields of 3% were obtained for cys to ser mutations. In contrast, for the cys to ala mutations, over 300 phage samples each were screened before a desired mutant could be found. False positives occurred frequently during hybridization screening for the cys to ala mutants, and subsequent Sanger sequencing of these samples indicated that deletions of a portion of the merA insert had occurred (for example, see Fig. 2-12). The

Table 2-I: Plasmids Containing Native or Mutant MerA Active Site Sequence

Plasmid	Source(s)	Description	Purpose
M13ps1	M13mp9, pJOE114	cys_{135}, cys_{140}	mutagenesis template
M13ps2	mutagenized M13ps1	ser_{135}, cys_{140}	mutagenesis product
M13ps3	" "	cys_{135}, ser_{140}	" "
M13ps4	" "	ala_{135}, cys_{140}	" "
M13ps5	" "	cys_{135}, ala_{140}	" "
M13ka1[a]	M13mp9, pKAM1	ala_{135}, cys_{140}	mutagenesis/sequencing template
M13ka2[a]	M13mp9, pKAM2	cys_{135}, ala_{140}	" "
M13ka3	M13mp8, pKAM1	ala_{135}, cys_{140}	sequencing template
M13ka4	M13mp8, pKAM2	cys_{135}, ala_{140}	" "
pJOE114[b]	pJOE105, Tn501	cys_{135}, cys_{140}	source of native merA
pPSM2	pJOE114, M13ps2	ser_{135}, cys_{140}	reconstructed mutant merA
pPSM3	pJOE114, M13ps3	cys_{135}, ser_{140}	" " "
pKAM1	pJOE114, M13ps4	ala_{135}, cys_{140}	" " "
pKAM2	pJOE114, M13ps5	cys_{135}, ala_{140}	" " "
pPSO1	pSE181, pJOE114	cys_{135}, cys_{140}	native merA overproducer
pPSO2	pSE181, pPSM2	ser_{135}, cys_{140}	mutant merA overproducer
pPSO3	pSE181, pPSM3	cys_{135}, ser_{140}	" " "
pKAO1	pSE181, pKAM1	ala_{135}, cys_{140}	" " "
pKAO2	pSE181, pKAM2	cys_{135}, ala_{140}	" " "

[a]Note that M13ka1 and M13ka2 are 1.4 kb smaller than M13ps4 and M13ps5 as shown in Fig. 2-17.

[b]Brown et al., 1983. See Fig. 2-2. Note that there is no pPSM1.

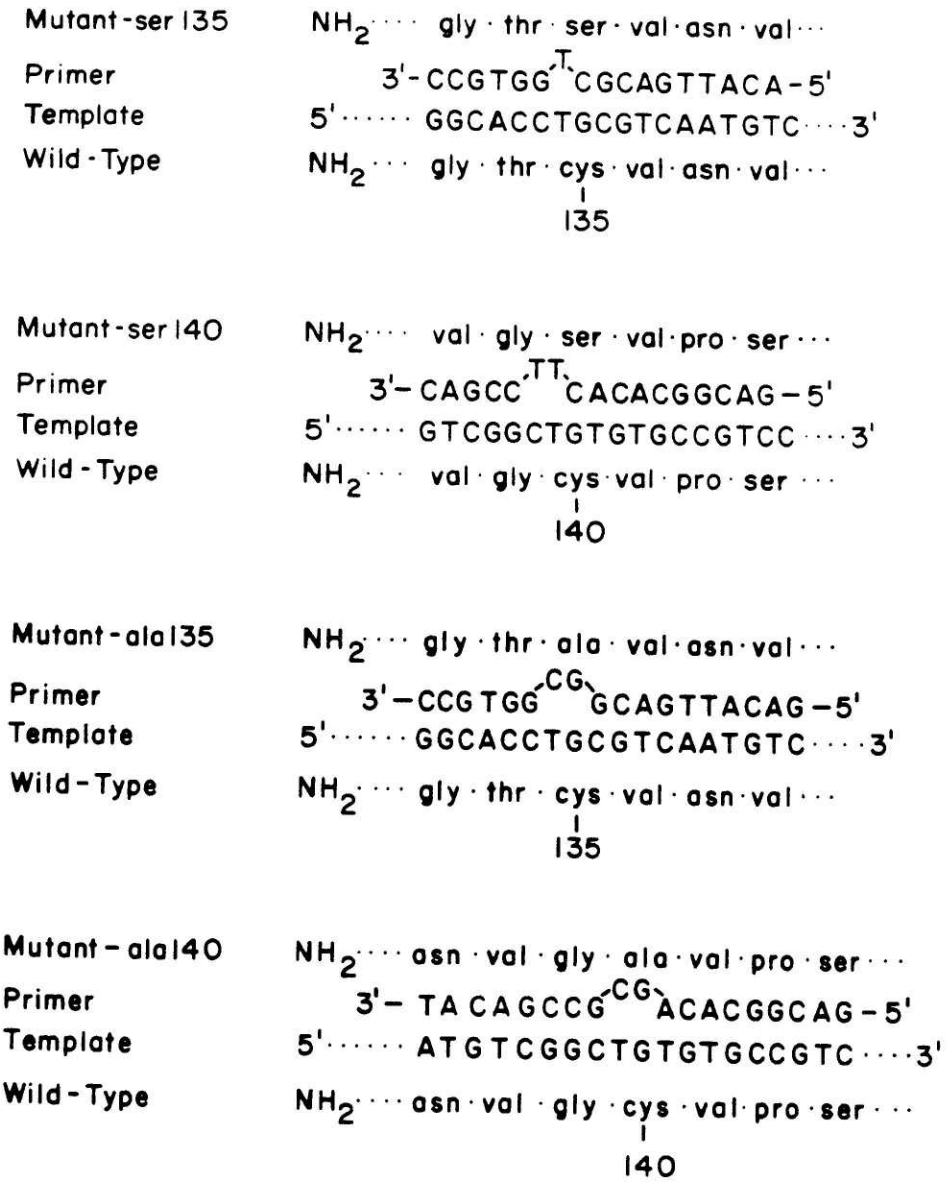

Figure 2-11. Oligonucleotide primers used for merA active site cys to ser and cys to ala mutageneses.

Figure 2-12. Portion of a Sanger sequencing gel demonstrating the occurrence of a 360 base pair deletion during attempted cys to ala merA mutagenesis.

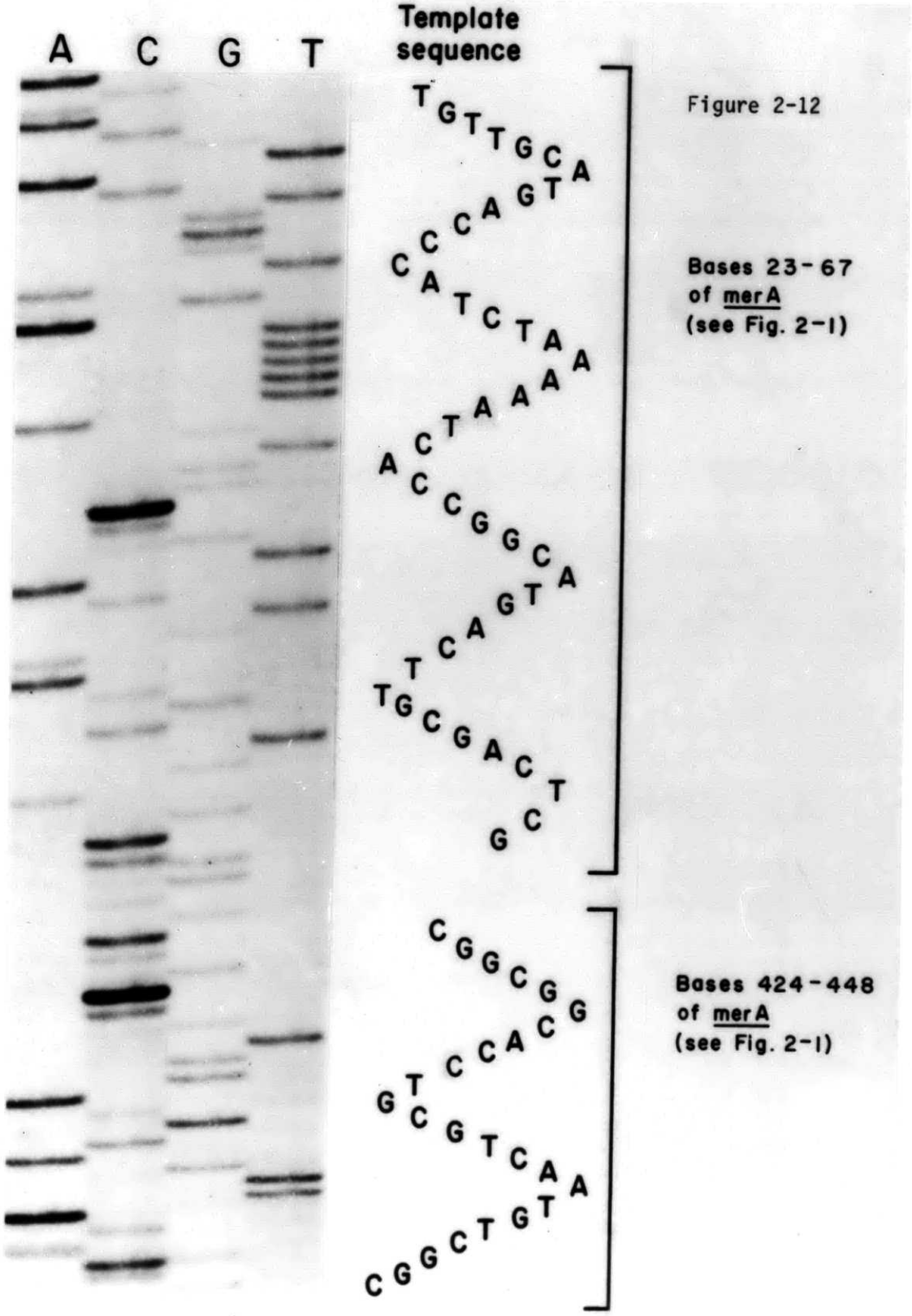

Figure 2-12

Bases 23-67 of merA (see Fig. 2-1)

Bases 424-448 of merA (see Fig. 2-1)

presence of the desired mutation was established by Sanger sequencing with a universal sequencing primer (Messing, 1983).

Reconstruction and Sequencing of the Mutant MerA Genes

The 1748 base pair mutant HindIII-SalI recombinant M13 fragment (encoding residues 1-186) was subcloned into pJOE114 to reconstruct the merA gene (residues 1-561) (Fig. 2-6). The resulting plasmids containing the cys to ser mutations, pPSM2 (cys_{135} -> ser) and pPSM3 (cys_{140} -> ser), were sequenced by the method of Maxam and Gilbert (1979) to verify insertion of the active site-containing mutant sequence. Because of the problems we encountered with deletions, we used a different procedure to sequence the DNA from the merA start through the SalI site of the cys to ala mutant plasmids pKAM1 and pKAM2. These plasmids were Sanger sequenced by subcloning the small NarI-SalI merA active site-containing fragment of pKAM1 or pKAM2 back into M13mp9 and sequencing from the SalI end with the universal sequencing primer or the mutagenesis primers (Fig. 2-7), and by subcloning the 1052 bp NarI-EcoRI fragment of pKAM1 or pKAM2 into M13mp8 and sequencing from the NarI end with the universal sequencing primer (Fig. 2-8). Sequencing gels of the active site region for the cys to ser and the cys to ala mutations are shown in Fig. 2-13 and Fig. 2-14, respectively. Certain GC rich regions were difficult to read because of band compression resulting from the formation of stable secondary structures during electrophoresis. This problem was eliminated by sequencing these regions with deoxyinosine triphosphate replacing dGTP (Mills and Kramer, 1979). In each case, the mutation was first verified in 6 out of 6 transformants by Sanger screening with the A- or T-reactions. By this strategy we were able to verify that no deletions or additional mutations had occurred in merA

Figure 2-13. Portion of a Sanger sequencing gel showing the active site native and mutant cys to ser DNA sequences. The locations of the base changes resulting from mutagenesis are indicated with arrows. The sequencing template corresponds to the coding strand of the merA gene. The universal sequencing primer (Messing, 1983) was used. The direction of primer extension in the sequencing reactions is from the unique SalI site toward the merA start.

Figure 2-13

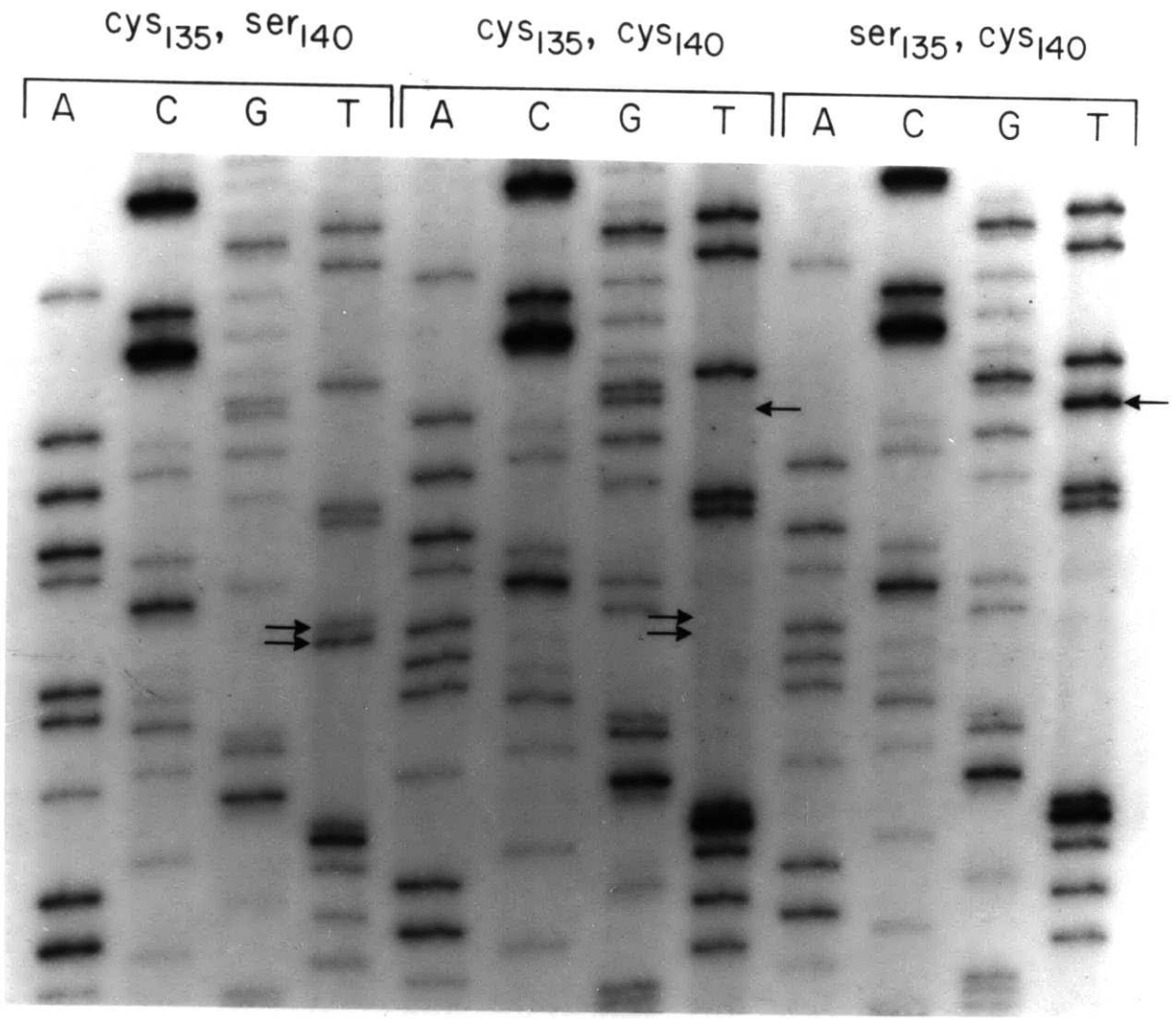

Figure 2-14. Portion of a Sanger sequencing gel showing the active site mutant cys to ala DNA sequences. The locations of the base changes resulting from mutagenesis are indicated with arrows. The sequencing template corresponds to the coding strand of the merA gene. The universal sequencing primer (Messing, 1983) was used. The direction of primer extension in the sequencing reactions is from the merA start toward the unique SalI site. Note the anomalous spacing of some bands in the upper portion of this picture. This was later shown to be due to band compression by sequencing with dITP replacing dGTP (Mills and Kramer, 1979).

Figure 2-14

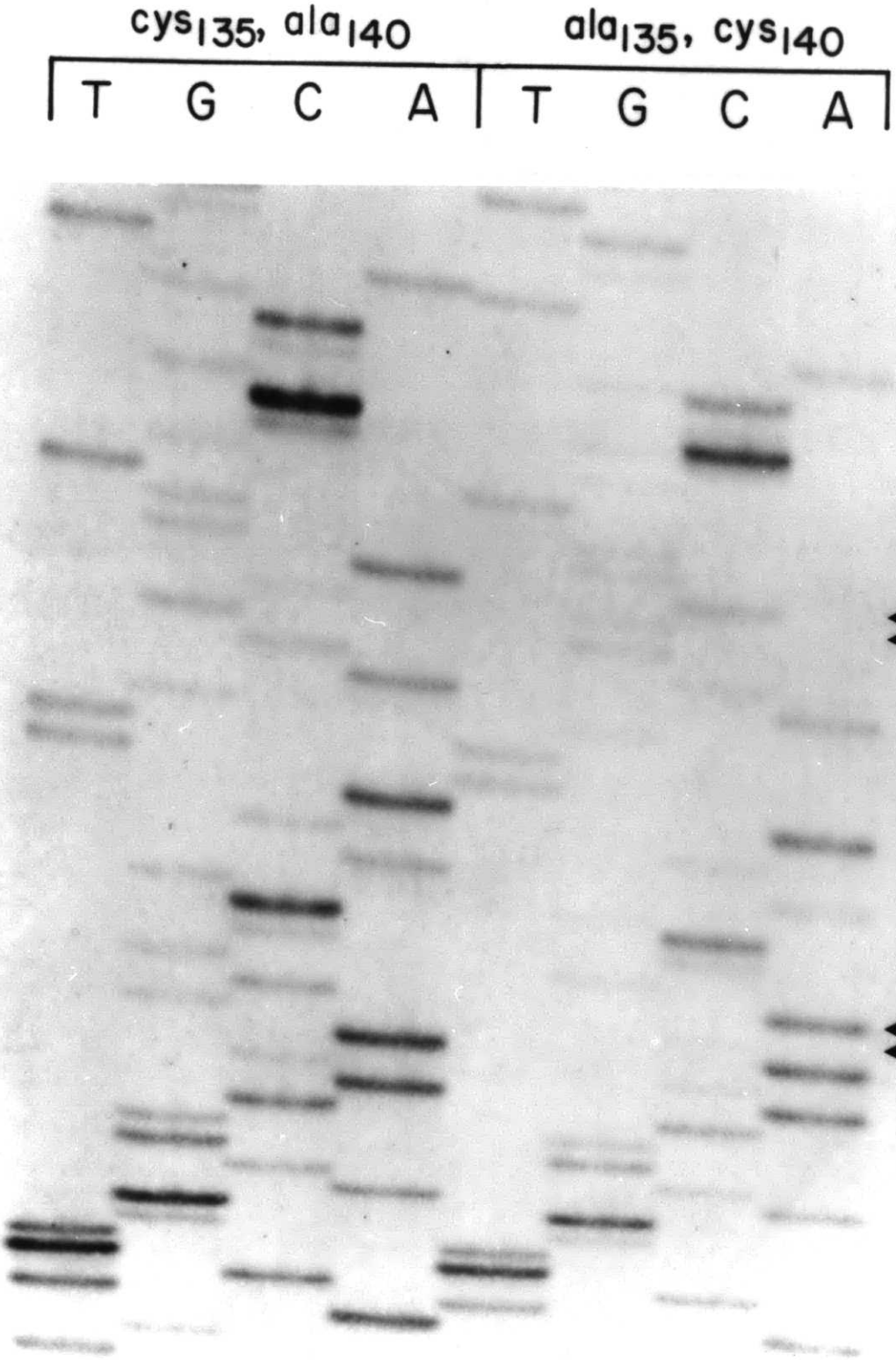

during cys to ala mutagenesis. This method enables us to sequence between the unique SalI site and the NarI site which lies close to the start of merA. The remaining portion of the DNA subcloned from M13ps4 and M13ps5 into pKAM1 and pKAM2, respectively, is not sequenced; however, as described below, the mutant merA gene, all of which is downstream of this NarI site, is then subcloned into another plasmid for expression so that the sequence of the portion preceding the NarI site is not needed for our purposes (see Fig. 2-15).

Overproduction

Plasmid pJOE114 was expressed in the host E. coli JM101 and induced by incubating cells in 10-20 μM merbromin. Purification by methods previously described (Fox and Walsh, 1982) yielded 125 units (25 mg) of enzyme from 40 g of cells. To increase expression and facilitate purification, we placed merA under control of the hybrid tac promoter (de Boer et al., 1982) contained in the plasmid pSE181. The 3550 base pair NarI-PvuII merA-containing fragments of pJOE114, pPSM2, and pPSM3 or the 2102 bp NarI-AvaI (blunt-ended at AvaI end) fragments of pKAM1 and pKAM2 were cloned into ClaI- and SmaI-digested pSE181 (Fig. 2-9 and 2-10). These constructions leave intact the merA Shine-Dalgarno sequence (see Fig. 2-1). The resulting plasmids pPSO1, pPSO2, pPSO3, pKAO1, and pKAO2 were expressed in E. coli W3110 $lacI^q$ and induced with the gratuitous inducer IPTG. Overproduction of native or mutant mercuric reductase was demonstrated by SDS gel electrophoresis of the crude extract (for example, see Fig. 2-16). The crude soluble cellular extract contained 5% mercuric reductase (pPSO1) as determined by Hg(II) reductase activity, an approximate 6-fold enhancement over that of pJOE114.

Figure 2-15. Diagram demonstrating that sequencing of the DNA between the unique HindIII site and the NarI site close to the start of merA is not needed, even though this portion of DNA is present in the original mutagenesis template. Asterisks indicate the presence of an active site mutation. The dotted area represents DNA present in the original mutagenesis template which is not sequenced. The striped area represents the merA gene or a fragment thereof.

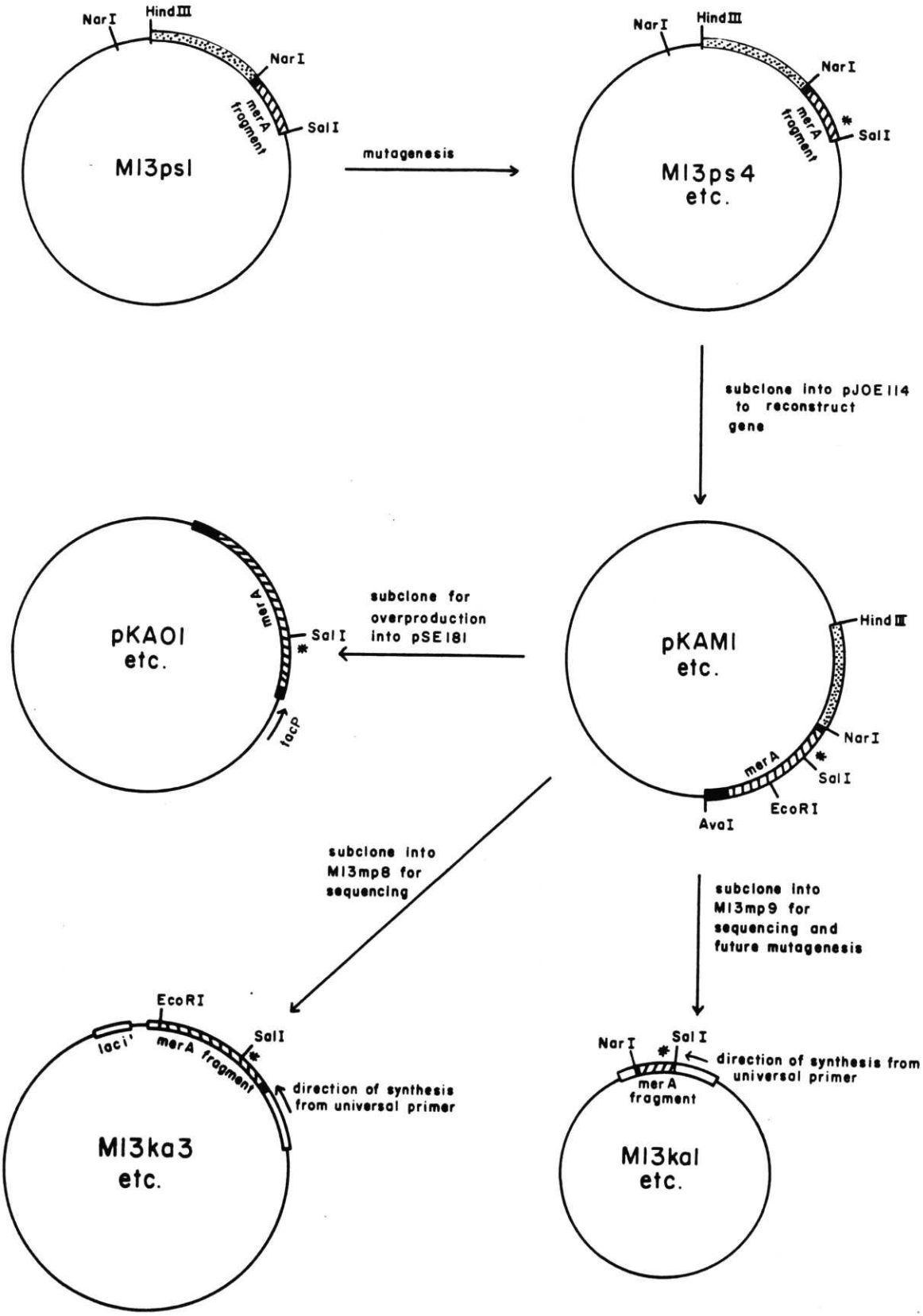
NarI
HindIII
NarI
merA fragment
SalI
M13psI
mutagenesis
NarI
HindIII
NarI
merA fragment
*
SalI
M13ps4 etc.
subclone into pJOE114 to reconstruct gene
pKAMI etc.
HindIII
NarI
merA
*
SalI
EcoRI
AvaI
subclone for overproduction into pSE181
pKAOI etc.
merA
SalI
*
tacp
subclone into M13mp8 for sequencing
subclone into M13mp9 for sequencing and future mutagenesis
EcoRI
SalI
lacI'
merA fragment
*
direction of synthesis from universal primer
M13ka3 etc.
NarI
SalI
*
direction of synthesis from universal primer
merA fragment
M13kaI etc.

Figure 2-15

Figure 2-16. SDS PAGE analysis of crude sonicate of W3110 $lacI^q$/pKA01 and pKA02 for overproduction of the mutant merA gene product. Samples were loaded as follows: lanes 1 and 2, purified native mercuric reductase, 15 µg; lanes 3 and 4, crude extract of W3110 $lacI^q$/pKA01, 100 µg; lanes 5 and 6, crude extract of W3110 $lacI^q$/pKA02, 100 µg.

Figure 2-16

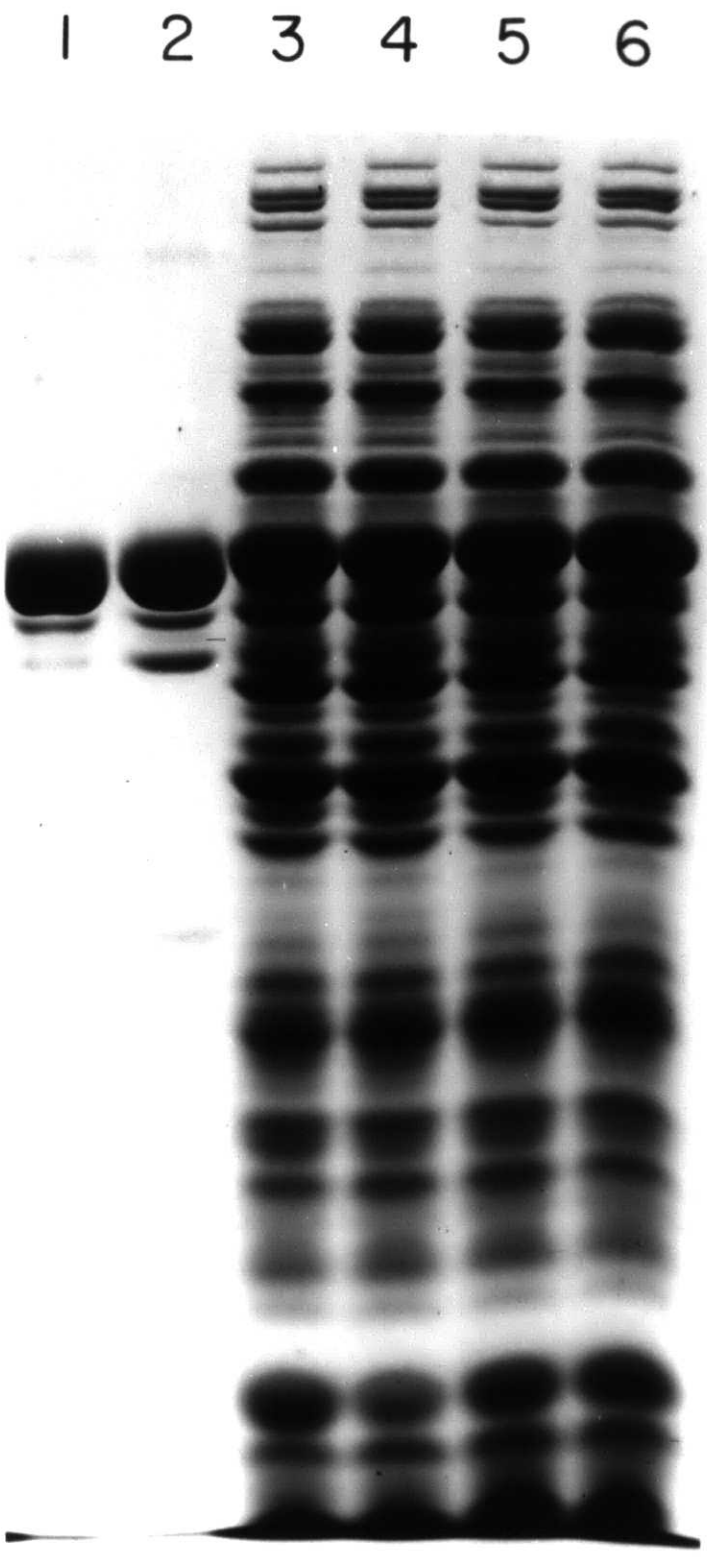

Discussion

The cys to ser and cys to ala mutant merA proteins are the first mutant enzymes produced in our laboratory for our studies on mercuric reductase. These mutations remove the redox active disulfide from the active site. The availability of stable cys to ala M13 templates allows the construction of a series of new active site mutants containing zero, one, or two cysteines in varying positions, such as ala_{135}, ala_{140}, and ala_{135}, cys_{139}, ala_{140}, and ala_{135}, cys_{139}, cys_{140}, work which is currently in progress (Distefano and Walsh, unpublished results).

Tn501 was selected over other sources for study of native mercuric reductase in this laboratory several years ago, principally because sequencing of the Tn501 gene by Brown et al. (1983) was then in progress. As expected, the availability of the gene sequence and primary structure plus the knowledge obtained from studies of the protein have proved to be extremely useful for mutagenesis studies. The pBR322-derived plasmid pJOE114 (Fig. 2-2), a gift from Dr. Nigel Brown, was our source of the Tn501 merA gene.

The method we chose to generate these mutant proteins, oligonucleotide-directed mutagenesis using recombinant M13 templates, is now a well established, widely used procedure. M13 is a filamentous, male-specific phage whose infectious cycle involves both a single-stranded and a double-stranded form of its DNA. The double-stranded form is useful for cloning; the single-stranded form is useful as a template for mutagenesis and sequencing. Messing's lab (1983) has developed a series of derivatives of M13, including the M13mp8 and M13mp9 used in this work, which have several very useful features. First, these vectors each contain a series of unique cloning sites. Second, since the cloning sites in these vectors are located

within a gene encoding a beta-galactosidase fragment which complements the defective beta-galactosidase produced by the host cell JM101, one can visually discriminate recombinant M13s from nonrecombinants by plaque color. This is accomplished by plating cells after transformation onto medium containing the chromogenic beta-galactosidase substrate Xgal and the lac operon inducer IPTG. Because insertion of a DNA fragment into the cloning region interferes with the production of a functional beta-galactosidase, recombinants give colorless plaques, whereas nonrecombinants generally give blue plaques.

Mutagenesis is accomplished by annealing an appropriate oligonucleotide to a recombinant M13 template and carrying out primer extension with Klenow fragment. The oligonucleotide serves two functions in the mutagenesis method used here. First, it functions as the mutagenesis primer. Second, it is labeled with ^{32}P and used as the probe in hybridization screening for the mutation. Since hybridization screening distinguishes primer hybridized to native M13 from primer hybridized to mutant M13 by differences in melting temperature, longer primers are not necessarily better primers for this method of mutagenesis. Besides length of the primer, factors which we considered in our choice of primers included number of mismatches, position of the mismatch(es) within the primer, and GC-richness.

Two major problems occurred in generating merA active site mutations. The first, the frequent deletion of a portion of the merA insert in M13, most likely resulted from the large size, 1.75 kb, of the insert (Inouye and Inouye, 1985) and may have also been aggravated by the high GC content of the cloned merA gene fragment. This problem appears to have been solved by removing 1.4 kb of excess DNA from the M13 template (Fig. 2-17), so that the size of the merA-containing insert is now 590 bp. (The remaining difference

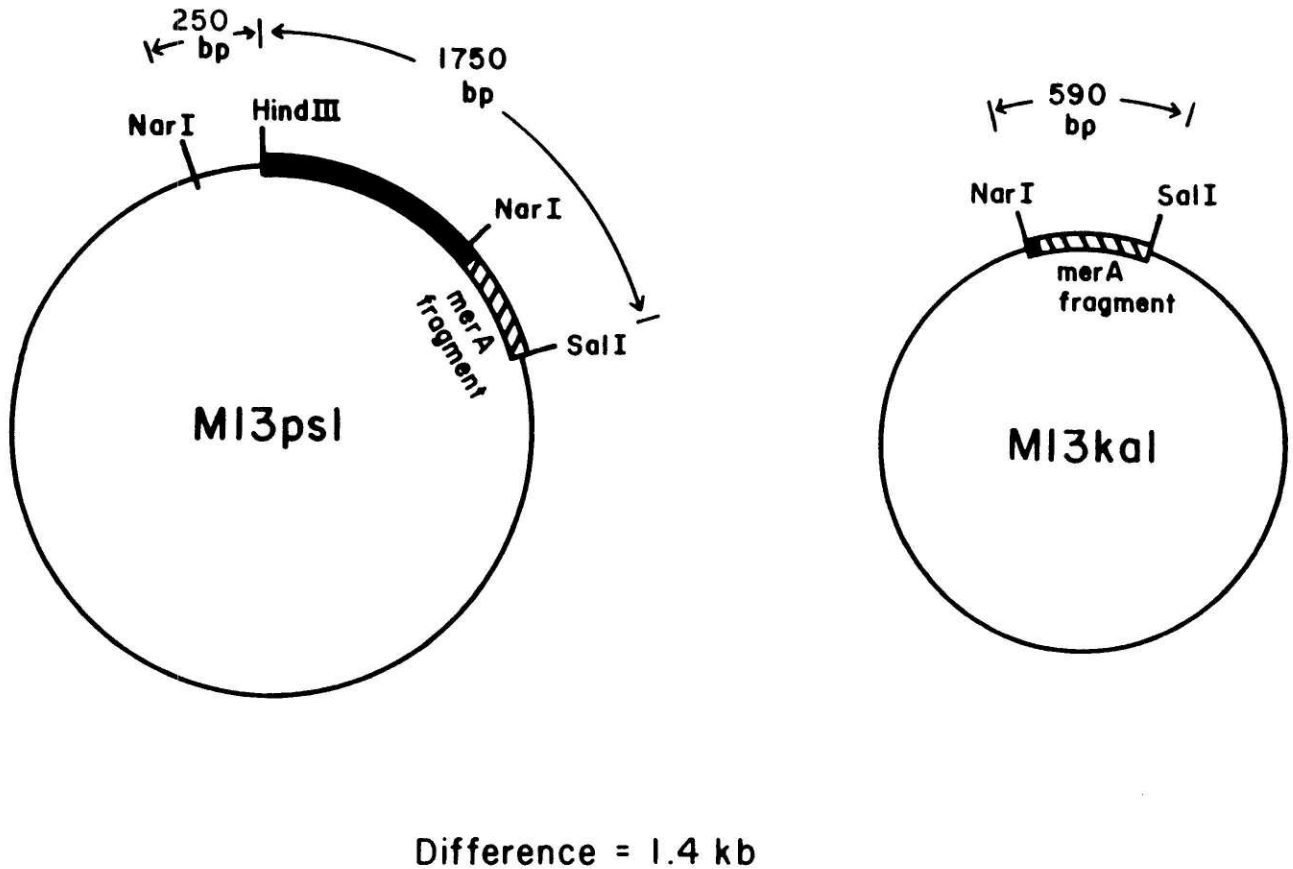

Figure 2-17. Comparison of the sizes of templates M13ps1-M13ps5 and M13ka1-M13ka2.

in size is due to the removal of approximately 250 bp of M13mp9 DNA.) The second problem, most evident with the cys to ala mutations, was low mutagenesis yields. This problem has been addressed in a number of ways in the literature. For example, mutagenesis efficiency may be reduced by 5'-3' exonuclease activity of the Klenow fragment during the *in vitro* mutagenesis reaction. The use of a second primer, such as the universal sequencing primer, which primes to the 5' side of the mutagenesis primer and thereby places the mismatch within the interior of an extended fragment has been reported to alleviate this problem; however, the influence of the proximity of the two primers upon mutagenesis yields is as yet unclear (Norris et al., 1983; Zoller and Smith, 1984). Yields may also be improved by methods which enrich the percentage of closed circular DNA after mutagenesis (Zoller and Smith, 1983; Norris et al., 1983). There is also evidence that mutagenesis efficiencies may be sequence-dependent, or at least dependent on the nature of the mismatched base pair(s) involved. The efficiency of post replicative mismatch repair in *E. coli* has been observed to vary with different mismatches (Kramer et al., 1984; Dohet et al., 1985). This repair system appears to be directed not only by the presence of an appropriate mismatch, but also by the lack of adenine methylation in 5'-GATC-3' sequences (Pukkila et al., 1983; Lu et al., 1983). Although the detailed mechanism for methyl-directed mismatch repair has yet to be reported, it may be significant to note that whereas the normal expected frequency of GATC sequences in DNA is about once per 250 bp (4^4 = 256) there are 3 such sequences within 66 bp around the *merA* active site. Kramer et al. (1982) have used a gapped hemimethylated heteroduplex M13 template to demonstrate that mutagenesis yields can be dramatically increased by preparing the M13 such that the template strand is the unmethylated strand. Kunkel (1985) has developed a

highly efficient site-directed mutagenesis procedure which uses template M13 DNA prepared from an E. coli dut⁻ ung⁻ strain. This strain produces increased amounts of dUTP, since it lacks dUTPase, the product of the dut gene, and it also incorporates and maintains uracil residues in its DNA, since it lacks uracil glycosylase, the product of the ung gene, which normally functions to remove such residues from DNA. The resulting template, which contains several uracil residues in place of thymine, is functional in the in vitro mutagenesis reaction, but undergoes degradation by uracil glycosylase when introduced into a wild type host cell. Thus, expression of the desired mutation is strongly favored. Both of the above methods give mutagenesis yields sufficiently high to allow one to bypass the hybridization screening step and instead, directly screen for mutants by Sanger sequencing. When using any strategy which bypasses the effects of in vivo mismatch repair, one should keep in mind that the efficiency of obtaining unwanted mutations also increases, since this repair system in E. coli apparently accounts for approximately a 10^3-fold increase in the fidelity of DNA replication over that observed with in vitro DNA replication systems (Cox, 1976; Hibner and Alberts, 1980). Our laboratory has recently produced two new active site mutations, ala_{135}, cys_{139}, cys_{140} and ala_{135}, ala_{140}, in the merA gene using the procedure of Kunkel, and sequencing of the entire NarI-SalI fragments of these mutant merA genes (i.e. the entire merA-containing insert in M13) is currently in progress (Distefano and Walsh, unpublished results).

Overproduction of the native and mutant merA gene products by use of the tac promoter proved to be relatively straightforward. The tac promoter is a very strong transcriptional initiation site composed of the -35 region of the trp promoter and the -10 region, operator, and ribosome binding site

of the *lac* UV-5 promoter and has been found to be a more efficient promoter than either of the parent promoters (de Boer et al., 1983). A second useful feature of the *tac* promoter is its regulation by the *lac* repressor. Undesirably high constitutive levels of transcription are avoided by using a host strain carrying the *lacI*^{q} mutation, which causes overproduction of the *lac* repressor. After an initial period of growth, IPTG is added to inactivate the *lac* repressor, thereby inducing the *tac* promoter. As will be described in the following chapter, this method of overproduction enables us to obtain 150 mg of pure native or mutant protein from 8 l of culture.

CHAPTER THREE

PURIFICATION AND CHARACTERIZATION OF THE MERCURIC REDUCTASE MUTANT ENZYMES

Introduction

The construction of four mercuric reductase mutants in which cys_{135} and cys_{140} have been altered independently to ser or ala and the overproduction of both the native and active site mutant proteins enable us to begin our studies to address the role of the redox active disulfide in Hg(II) binding and reduction. Provided that the mutant proteins, like the native protein, can be purified in high yield, we should now have available plentiful sources of both the native and mutant enzymes.

This chapter concerns the purification of mercuric reductase mutant proteins and their subsequent characterization in terms of physical and spectroscopic properties and redox states. Catalytic properties of these mutants will be discussed in Chapter 4. The spectral similarities and active site sequence homology among native mercuric reductase, lipoamide dehydrogenase, and glutathione reductase along with the known Xray crystal structure of human erythrocyte glutathione reductase allow us to define the initial experiments to be carried out on the mutant proteins. Spectroscopic studies should confirm that cys_{140}, analogous to cys_{63} of glutathione reductase (see Figure 1-6), is the residue involved in charge transfer interaction with the flavin and should allow titration of the pK_a of cys_{140} in those mutants lacking cys_{135}. Thiol titrations with DTNB and dithionite titrations of the mutants should reflect the loss of the redox active disulfide and the consequent two electron inventory (rather than the four electron inventory observed with the native protein). Finally, redox potential determinations should provide some indications of the effect of the mutations on the bound FAD reduction potential.

Experimental Procedures

Materials

E. coli W3110 $lacI^q$ carrying the plasmids pPS01, pPS02, pPS03, pKA01, or pKA02 were prepared as described in Chapter 2. Orange A Mātrex gel was purchased from Amicon Corp. Biogel P6DG was from BioRad. Ampicillin sodium salt, IPTG, TPCK, TLCK, and thio-$NADP^+$ were from Sigma. DTNB was purchased from Aldrich or from Boehringer Mannheim. Carba-1-deazariboflavin and 8-hydroxyriboflavin were generously provided by Merck, Sharp, and Dohme Research Laboratories, Rahway, New Jersey. Xanthine was from Sigma. Protocatechuic acid was purchased from Aldrich and recrystallized from water before use. Xanthine oxidase and protocatechuate dioxygenase were gifts from the laboratories of Drs. Vincent Massey and David Ballou, Department of Biological Chemistry, University of Michigan, Ann Arbor, Michigan.

Methods

Spectrometry

UV-visible spectra were recorded on a Perkin-Elmer 554 or Lambda 5 spectrophotometer at 25°C. Fluorescence spectra were recorded on a Perkin Elmer LS-3 fluorimeter. Unless otherwise noted, all enzymes used for spectroscopic studies were previously treated to remove enzyme-bound $NADP^+$ as described below, and were centrifuged to remove particulate matter.

Enzyme purification

The following procedure applies to native enzyme (pPS01) and the ser_{135}, cys_{140} (pPS02), cys_{135}, ser_{140} (pPS03), ala_{135}, cys_{140} (pKA01) and

cys_{135}, ala_{140} (pKA02) mutant enzymes. During purification, Hg(II) reductase and transhydrogenase (thioNADP$^+$/NADPH) activity was assayed in the case of the native enzyme, and transhydrogenase activity for mutant enzymes. Assay procedures for purifications are described below.

Cells (W3110 $\underline{lacI}^q$/pPS01; pPS02; pPS03; pKA01; pKA02) were grown in YT media at 37°C in a shaker bath. For each liter of medium, 20 ml of inoculum (from an overnight culture in YT plus 50 ug/ml ampicillin) was used. Native or mutant mercuric reductase was induced when A_{550} of the fermentation broth = 1.0 (approximately 2 hr after inoculation) by the addition of IPTG to a final concentration of 2 mM. Cells were harvested at late log phase, typically 4.5-5 hr after induction, by centrifugation for 10 min at 6000 x g. Typically, 30-40 g (wet weight) cells were harvested from 8 l of culture.

The remainder of the purification follows the procedures of Fox and Walsh (1982) with the following modifications: a) 0.01 mg/ml each of TPCK, TLCK, and leupeptin were added to the purification buffer; b) the heat precipitation step preceding Orange A Matrex Gel chromatography was omitted. After purification, the enzymes were dialyzed or passed through a Biogel P6DG column to remove excess NADP(H) introduced from Orange A column chromatography. Purified mercuric reductase (native and mutant) could be stored at 4°C over a period of weeks with little or no loss of activity. For extended periods, samples containing 10% w/v glycerol were frozen in liquid nitrogen and stored at -70°C.

Enzyme assays

For enzyme purifications, Hg(II)- and thioNADP$^+$-dependent NADPH oxidations were monitored at 37°C and 25°C, respectively, in 80 mM sodium

phosphate, pH 7.4 and 200 μM NADPH at 340 nm. Hg(II) reductase activity was monitored in the presence of 100 μM $HgCl_2$ and 1 mM 2-mercaptoethanol. Transhydrogenase activity was monitored in the presence of 1 mM 2-mercaptoethanol and 100 μM thioNADP$^+$. One unit of enzyme activity is defined as the amount of enzyme that catalyzes the Hg(II)- or thioNADP$^+$-dependent oxidation of 1 μmol of NADPH per minute.

Protein concentration

Protein concentrations were determined by the method of Lowry (1951) using bovine serum albumin as a standard. Routine determination of enzyme concentration was based on flavin content, using an extinction coefficient of 11.3 $mM^{-1}cm^{-1}$ at 458 nm for native enzyme, 11.3 $mM^{-1}cm^{-1}$ at 440 nm for cys_{135}, ser_{140} enzyme, 9.48 $mM^{-1}cm^{-1}$ at 440 nm for ser_{135}, cys_{140} enzyme, 11.9 $mM^{-1}cm^{-1}$ at 450 nm for cys_{135}, ala_{140} enzyme, and 8.57 $mM^{-1}cm^{-1}$ at 435 nm for ala_{135}, cys_{140} enzyme. These values were determined by comparison of the absorbance of an NADP-free sample of the enzyme at the visible absorption λ_{max} with the absorbance at 450 nm of free FAD at the same concentration. The sample of free FAD was generated from the sample of the NADP-free enzyme by boiling in a sealed vial for 5-15 min in 100 mM sodium phosphate (pH 7.4) and 10 mM $MgCl_2$ or in 100 mM sodium phosphate (pH 7.5) and 0.5 mM EDTA. The precipitated protein was removed by centrifugation, and the free flavin absorbance at 450 nm was measured. For comparison, a sample of free FAD boiled under these conditions lost 5% of its absorbance.

Molecular weight determination

Subunit molecular weight was determined by SDS-polyacrylamide gel electrophoresis as described by Laemmli (1970). Native molecular weight was

determined by polyacrylamide gel electrophoresis as described in Cooper (1977). Samples for native gel electrophoresis were loaded in 50 mM Tris-HCl, pH 7.0, 0.1% 2-mercaptoethanol, 20% w/v glycerol and 0.001% bromophenol blue.

Quantitation and removal of enzyme-bound $NADP^+$

Enzyme-bound $NADP^+$ was quantitated or removed as described by Fox and Walsh (1982). Since some loss of flavin is observed under the dialysis conditions for $NADP^+$ removal (V. Massey, unpublished), the following steps were added: a) after the KBr has been removed, the enzyme is incubated overnight at 4°C with excess FAD; b) the excess FAD is subsequently removed by chromatography through Biogel P6DG.

Thermal titrations

Enzyme was heated in 80 mM sodium phosphate buffer containing 0.1 mM EDTA and 0.1% 2-mercaptoethanol for 10 min in air-tight polypropylene tubes. Samples were then cooled to 0°C, centrifuged at 12,000 x g and assayed for transhydrogenase activity at 25°C.

Thiol titrations

Thiols were titrated with DTNB as described previously (Fox and Walsh, 1982).

Antibody preparation

Rabbit antiserum against wild type mercuric reductase was prepared from a New Zealand 2 kg white female rabbit. The rabbit was injected intramuscularly at 3-week intervals for 9 weeks with a 1:1 mixture of 1

mg/ml native mercuric reductase and 1 ml Freund's complete adjuvant (Difco) in 20 mM sodium phosphate, pH 7.4. Serum was frozen in liquid nitrogen and stored at -70°C until use. Routine precipitations were carried out by adding equal proportions of antisera and enzyme in 80 mM sodium phosphate, pH 7.4, incubating at 25°C for 10 min, and centrifuging at 12,000 x g for 5 min.

Anaerobic titrations

Anaerobic titrations were performed in rubber stoppered cuvettes or in anaerobic cuvettes similar to those described by Williams et al. (1979). To avoid formation of charge-transfer complexes with nicotinamides, $NADP^+$ was removed from all preparations of enzyme as previously described. Solutions were repeatedly evacuated and re-equilibrated with argon which had been scrubbed free of oxygen with an Oxisorb cartridge purchased from MG Scientific Gases. The buffer used was 100 mM NaPi, 0.5 mM EDTA, pH 7.5, with up to 10 μM methyl viologen added as mediator, since in its absence complete reduction of native enzyme was observed to occur extremely slowly (Fox and Walsh, 1982). Dithionite was typically used as a reductant. Dithionite solutions were made up with anaerobic buffer and were standardized by titration of an anaerobic solution of riboflavin. All additions were made with a repeating or threaded plunger gas tight syringe.

Redox titrations

Redox titrations of the mutant enzymes were performed as previously described in this laboratory (Fox and Walsh, 1982; Fox, 1983) or in the laboratory of Prof. Vincent Massey, University of Michigan, Department of Biological Chemistry, Ann Arbor, Michigan, using rubber stoppered or

anaerobic cuvettes (Williams et al., 1979) as described above. The redox indicator dyes 1-deazariboflavin ($E^{\circ\prime}$ = -280 mV (Walsh et al., 1978)), 8-hydroxyriboflavin ($E^{\circ\prime}$ = -340 mV (Light and Walsh, 1980)), methyl viologen ($E^{\circ\prime}$ = -449 mV (Wilson, 1978)), and benzyl viologen ($E^{\circ\prime}$ = -358 mV (Wilson, 1978)) were used to estimate oxidation-reduction potentials of the mutant mercuric reductases. For some measurements of redox potentials, protocatechuic acid and protocatechuate dioxygenase were included as an additional oxygen scrubbing system, and reducing equivalents were generated by xanthine oxidase and xanthine according to a procedure from Massey (unpublished). In such cases, titrations with methyl viologen as the redox indicator were carried out at pH 8.7 (100 mM sodium pyrophosphate) to allow complete titration of the methyl viologen, whose redox potential is independent of pH (Merck Index, 1976). Values were then corrected to pH 7 by -30 mV per pH unit increase for a two electron process (Dutton, 1978).

Results

Enzyme purifications

The purification procedure of Fox and Walsh (1982) has been modified to a one-step (Orange A Matrex dye column) procedure applicable to both native and mutant enzymes. Tables 3-I and 3-II summarize these purifications. Up to 150 mg of enzyme can be purified on a 2.5 x 20 cm Orange A column. Protease inhibitors TPCK, TLCK and leupeptin are added to the lysis buffer to reduce proteolysis during purification; however, results of recent purifications indicate that problems with proteolysis are mainly observed with longer growth times, so omission of such protease inhibitors may now be recommended. As was observed previously with native enzyme, a major band and a minor set of bands, corresponding to approximate molecular weights of 62,000 and 56,000, respectively, are observed for each mutant enzyme on denaturing gel electrophoresis (Figure 3-1). The DNA sequence of the Tn501 merA gene predicts a molecular weight of 58,660 for the unclipped enzyme (Brown et al., 1983). The lower molecular weight set of bands results from proteolytic removal of 85 amino acid residues from the amino terminus of the enzyme (Fox and Walsh, 1982). Fox and Walsh (1982) observed no apparent effect of this processing on the mercuric reductase activity or dimeric structure of the native enzyme.

Thiol titrations

Thiols in the native and mutant enzymes were titrated in the presence and absence of NADPH with DTNB. Enzymes were denatured prior to titration with 5 M guanidine-HCl. The presence in wild type enzyme of two titratable thiols per subunit in the oxidized form and four titratable thiols per

Table 3-I

Purification of native and cys to ser mutant mercuric reductases

Enzyme	Total protein (mg)[a]	Sp. activ. (U/mg)	Total activ. (U)	n-fold purification	Yield (%)
Native[b]					
Crude	4015	0.031	126	-	-
Orange A	142	0.96	137	30.7	108
Native[c]					
Crude	4015	0.235	944	-	-
Orange A	142	6.4	909	30.5	96
Ser_{135}, cys_{140}[b]					
Crude	3600	0.0044	15.8	-	-
Orange A	176	0.100	17.6	22.7	111
Cys_{135}, ser_{140}[b]					
Crude	3300	0.066	219	-	-
Orange A	146	1.42	207	21.4	95

[a]Protein was determined in crude extract by the method of Lowry (1951) and by flavin content for pure protein as described in Methods.

[b]Enzyme activity was determined by the thioNADP$^+$/NADPH transhydrogenase assay as described in Methods.

[c]Enzyme activity was determined by the mercuric ion reductase assay as described in Methods.

Table 3-II

Purification of cys to ala mutant mercuric reductases

Enzyme	Total protein (mg)[a]	Sp. activ. (U/mg)	Total activ. (U)	n-fold purification	Yield (%)
Ala_{135}, cys_{140}[b]					
Crude	1990	0.32	637	-	-
Orange A	185	3.0	555	9.4	87
Cys_{135}, ala_{140}[b]					
Crude	2050	0.42	861	-	-
Orange A	164	3.9	640	9.3	74

[a]Protein was determined by the method of Lowry (1951).

[b]Enzyme activity was determined by the thioNADP$^+$/NADPH transhydrogenase assay as described in Methods.

Figure 3-1. SDS PAGE of purified native and mutant mercuric reductases from W3110 $\underline{lacI}^q$/pPS01, pPS02, pPS03, pKA01, or pKA02. Samples were loaded left to right as follows: 35 μg of ser_{135}, cys_{140} mutant enzyme; 25 μg of cys_{135}, ser_{140} mutant enzyme; 25 μg of cys_{135}, cys_{140} native enzyme; 25 μg of ala_{135}, cys_{140} mutant enzyme; 25 μg of cys_{135}, ala_{140} mutant enzyme.

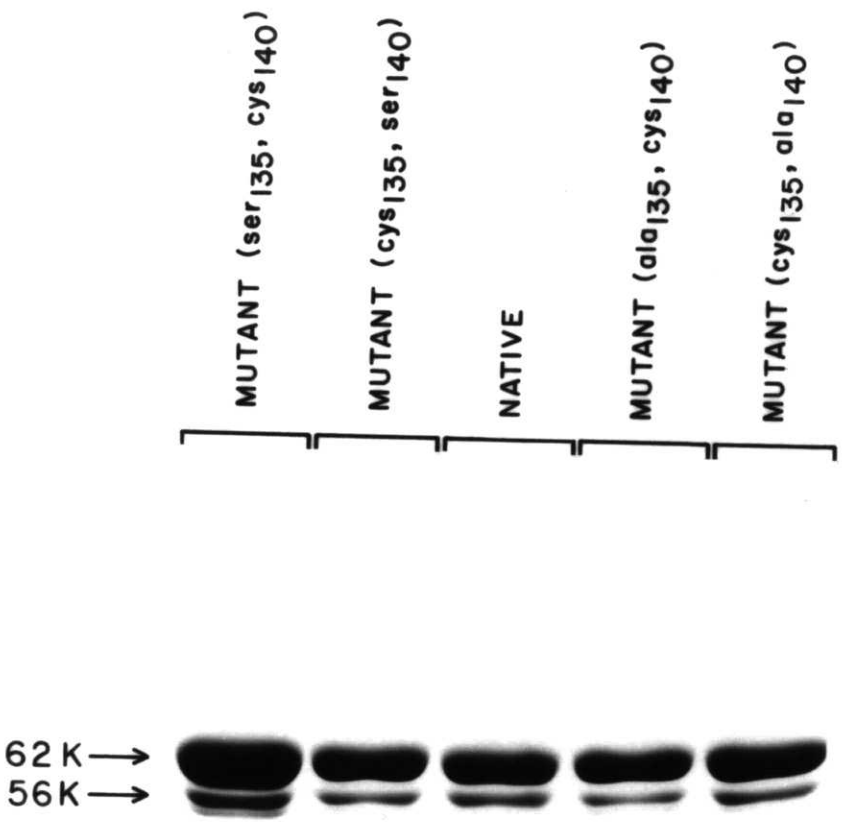
MUTANT (ser135, cys140)
MUTANT (cys135, ser140)
NATIVE
MUTANT (ala135, cys140)
MUTANT (cys135, ala140)
62K
56K

Figure 3-1

subunit upon reduction by NADPH (Fox and Walsh, 1982), confirmed here, is consistent with the presence of a redox-active disulfide. Native enzyme clipped with chymotrypsin to remove the 85 amino acid N-terminal arm by the method of Fox and Walsh (1983) gives the same result as the largely unclipped enzyme (Distefano, Au, and Walsh, unpublished). Miller et al. (1986) report the titration of four thiols per subunit for oxidized native enzyme and 6 per subunit for native EH_2, where two thiols per subunit in E and four thiols per subunit in EH_2 are titratable within minutes, and the remaining two thiols per subunit are titrable in 2-4 hrs. Both cys to ser mutants and both cys to ala mutants contain three titratable thiols in both the presence and absence of NADPH (Table 3-III). This result is as predicted by the DNA sequence of the mutants and is consistent with the substitution of one cysteine by serine or by alanine in each of the four mutants and with the absence of an NADPH-dependent redox active disulfide. In the case of oxidized nondenatured cys_{135}, ser_{140} mutant and cys_{135}, ala_{140} mutant, three thiols per subunit can be titrated with DTNB, indicative of aryl disulfide-thiol exchange at cys_{135} in the active site. Only two of the three thiols could be titrated in nondenatured ser_{135}, cys_{140} mutant enzyme. In the nondenatured ala_{135}, cys_{140} mutant enzyme, after rapid reaction of two enzyme thiols per subunit with DTNB, the absorbance at 412 nm continued to rise at a somewhat reduced but constant rate, and this increase in absorbance continued past the titration of a third thiol, for reasons as yet unclear.

Physical properties

The cys to ser and the cys to ala mutant enzymes share many physical properties with wild type enzyme. Both mutant and native enzymes have

Table 3-III

Titratable thiols in native and mutant mercuric reductases[a]

Enzyme	Titratable thiols in oxidized enzyme (-NADPH)	Titratable thiols in reduced enzyme (+NADPH)	Difference (reduced - oxidized)
Native	2.2	4.3	2.1
Ser_{135}, cys_{140}	3.2	3.2	0.0
Cys_{135}, ser_{140}	3.1	3.0	-0.1
Ala_{135}, cys_{140}	3.2	3.2	0.0
Cys_{135}, ala_{140}	3.2	2.8	-0.4

[a]Thiols were titrated with DTNB as described in Methods.

dimeric structures as observed by nondenaturing gel electrophoresis. The protein to flavin ratio, A_{272}/A_{458} for NADP-free native enzyme is 6.3-6.5. Similarly, the protein to flavin ratios for the NADP-free cys_{135}, ser_{140} mutant, A_{272}/A_{440}, and the NADP-free cys_{135}, ala_{140} mutant, A_{272}/A_{450} are 6.3-6.5. The ratio is slightly higher for the NADP-free enzymes carrying mutations at residue 135: A_{268}/A_{440} for the ser_{135}, cys_{140} mutant and A_{268}/A_{435} for the ala_{135}, cys_{140} mutant are 6.8-7.0. When FAD content of the NADP-free (FAD-reconstituted) enzymes is compared with protein concentration as determined by the method of Lowry, the stoichiometry of FAD binding is 0.85-0.9 FAD per subunit of protein. The stoichiometry of FAD to protein is approximately 25% lower in $NADP^+$-free enzyme which has not been reconstituted with FAD. Either significant amounts of FAD dissociate from the enzymes under the dialysis conditions used to remove enzyme-bound $NADP^+$, or the enzymes as isolated are underloaded with FAD.

$NADP^+$ is associated with the pure native and mutant enzymes, even after extensive dialysis. For native enzyme, the stoichiometry is 1 $NADP^+$ per 2.7 FAD (Fox and Walsh, 1982). For both the cys_{135}, ser_{140} and ser_{135}, cys_{140} mutants, the stoichiometry is 1 $NADP^+$ per 3.2 FAD. The stoichiometry for the ala_{135}, cys_{140} enzyme is 1 $NADP^+$ per 2.0 FAD, and that for the cys_{135}, ala_{140} enzyme is 1 $NADP^+$ per 10 FAD. The $NADP^+$ can be removed by KBr treatment as noted in Methods.

The thermal stabilities of the native and the cys to ser mutant enzymes are comparable. The midpoint of the heat inactivation curve for the cys_{135}, ser_{140} mutant is 76°C, for the ser_{135}, cys_{140} mutant, 78.5°C, and for oxidized native enzyme, 83°C. The disulfide bridge has relatively little effect on the thermal stability of the enzyme toward heat denaturation, not too surprisingly, since the cystine disulfide bridges only four amino acid

residues. The thermal stabilities of the cys to ala mutant enzymes was not tested.

Antibodies raised against native enzyme cross-react with both cys to ser mutants. All three enzymes lost greater than 90% of the transhydrogenase activity when titrated with antiserum. In the case of highly homologous glutathione reductase, evidence points to an antigenic determinant at the nicotinamide binding domain of the enzyme (Carlberg et al., 1981). Antibody crossreactivity of the cys to ala mutants was not tested.

Spectroscopic properties

The presence of enzyme bound $NADP^+$ in the native and mutant enzymes (see above) results in unusual UV-visible spectra for some of these enzymes after elution from Orange A and subsequent dialysis. Native enzyme showed a broad long wavelength absorbance, extending to 700 nm, with a maximum around 580 nm (Figures 3-2 and 3-5), which gave the enzyme a somewhat greenish color. After dialysis to remove excess NADP(H) introduced by Orange A chromatography (but not enzyme-bound $NADP^+$), the enzyme appears yellow. The long wavelength absorbance is no longer observed after the enzyme is dialyzed against 2 M KBr to remove enzyme-bound $NADP^+$. The ser_{135}, cys_{140} and ala_{135}, cys_{140} mutants appear dark red and deep green, respectively, after elution from Orange A and subsequent dialysis (Figures 3-3 and 3-5). Upon removal of the enzyme-bound $NADP^+$, the latter two mutants take on, respectively, a less intense reddish brown and less intense greenish brown color. These unusual colors are due to charge transfer interactions of flavin with the nicotinamide cofactor and/or cys_{140} thiolate, as discussed below. In contrast, the cys_{135}, ser_{140} and the cys_{135}, ala_{140} mutants,

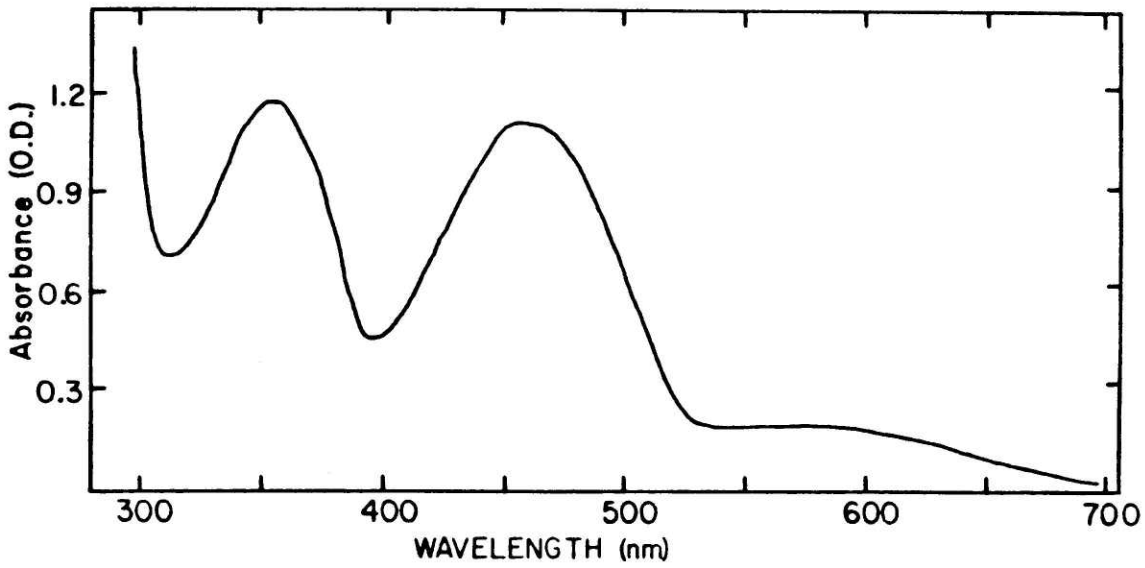

Figure 3-2. Spectrum of native mercuric reductase as isolated (from Fox, 1983). The enzyme was eluted from Orange A and then concentrated on an Amicon PM10 membrane.

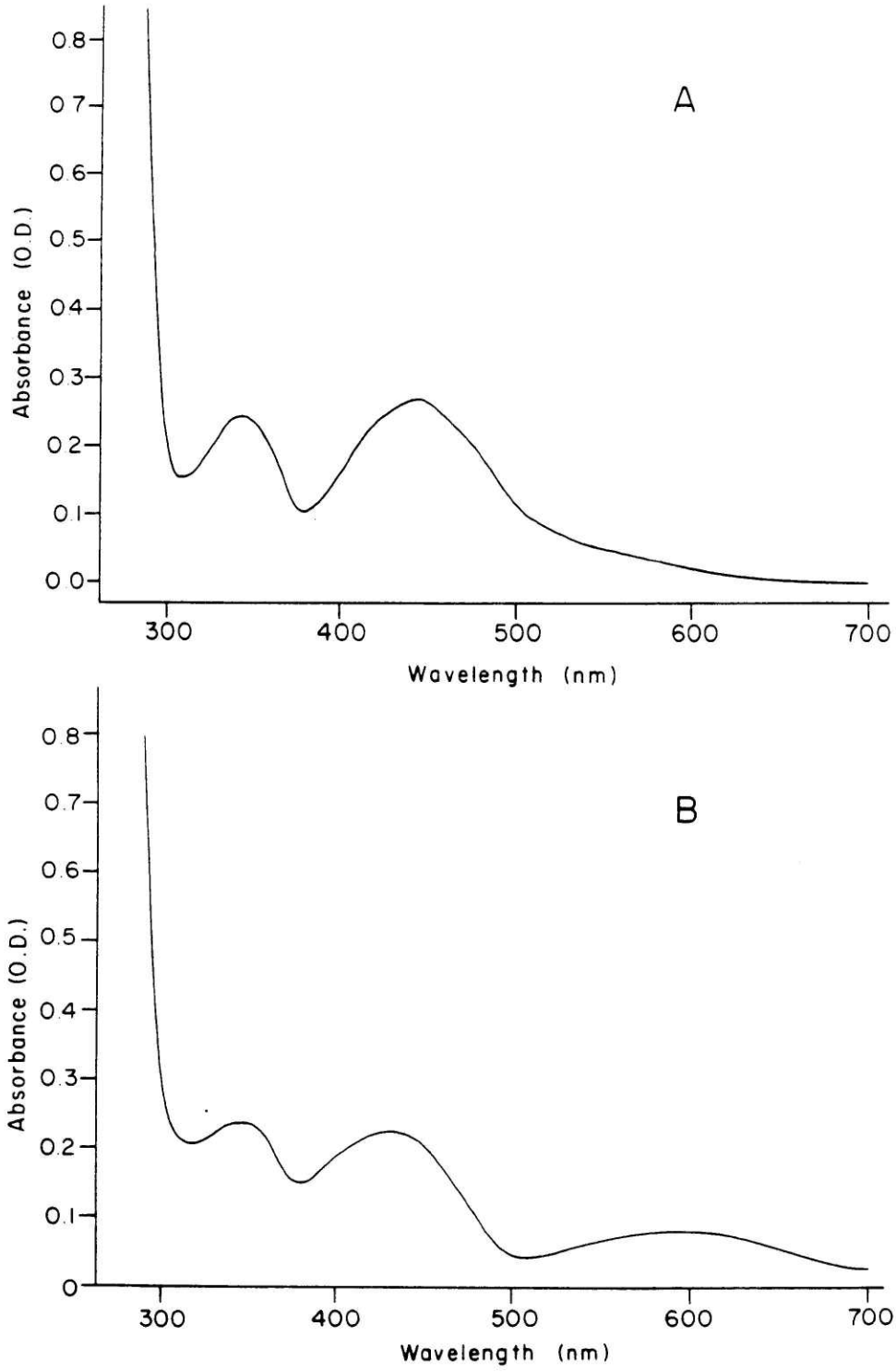

Figure 3-3. Spectra of mutant mercuric reductases after elution from Orange A and subsequent dialysis, which removes $NADP(H)^+$ introduced by Orange A chromatography but not enzyme bound $NADP^+$. A) Spectrum of the ser_{135}, cys_{140} mutant enzyme. B) Spectrum of the ala_{135}, cys_{140} mutant enzyme.

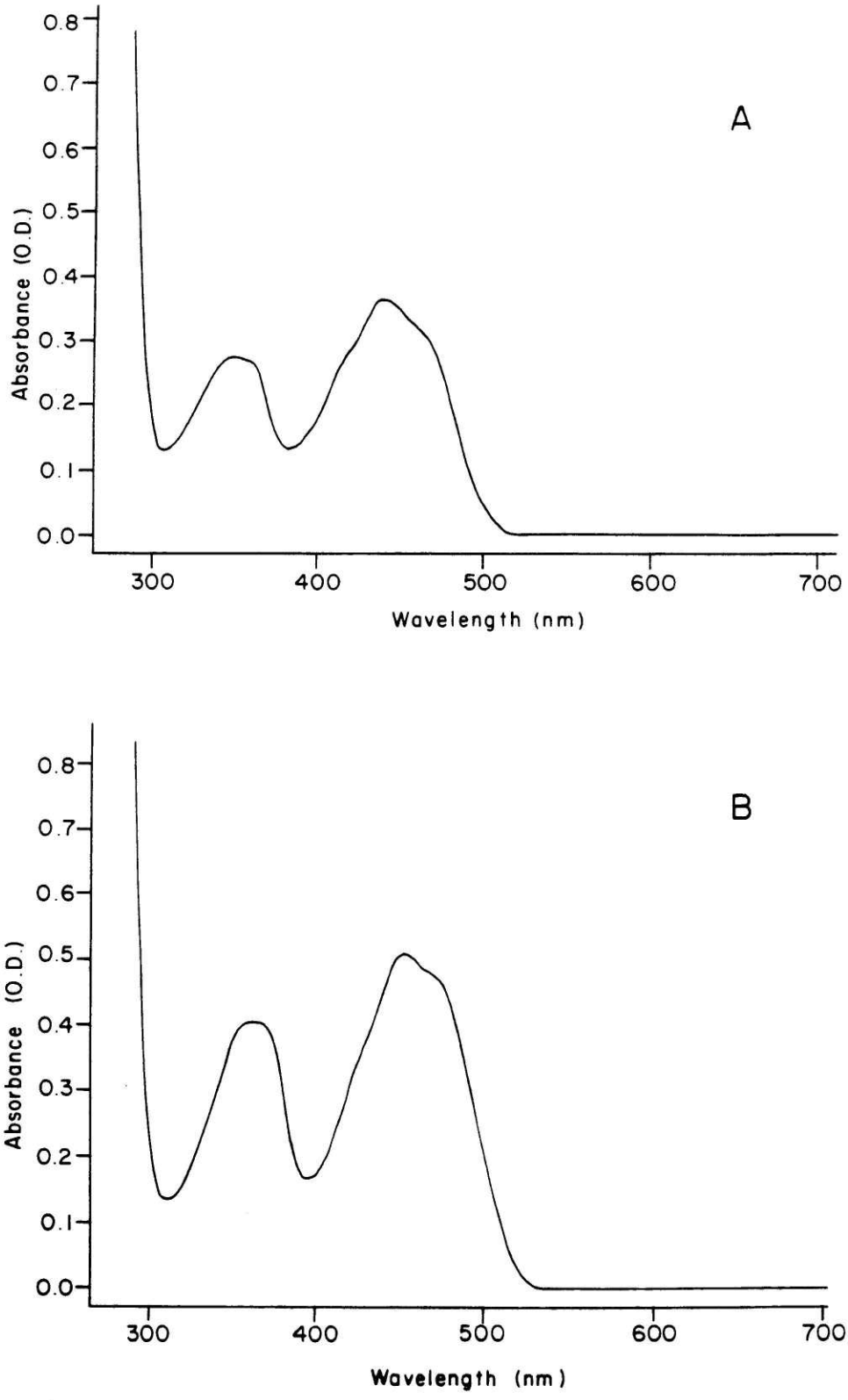

Figure 3-4. Spectra of mutant mercuric reductases after elution from Orange A and subsequent dialysis, which removes NADP(H) introduced by Orange A chromatography but not enzyme bound $NADP^+$. A) Spectrum of the cys_{135}, ser_{140} mutant enzyme. B) Spectrum of the cys_{135}, ala_{140} mutant enzyme.

Figure 3-5. Color photograph of the native and mutant mercuric reductase enzymes after elution from Orange A and subsequent dialysis, which removes NADP(H) introduced by Orange A chromatography but not enzyme bound $NADP^+$. These samples were concentrated by ultrafiltration with an Amicon PM30 membrane and are approximately 5-10 mg/ml in protein concentration.

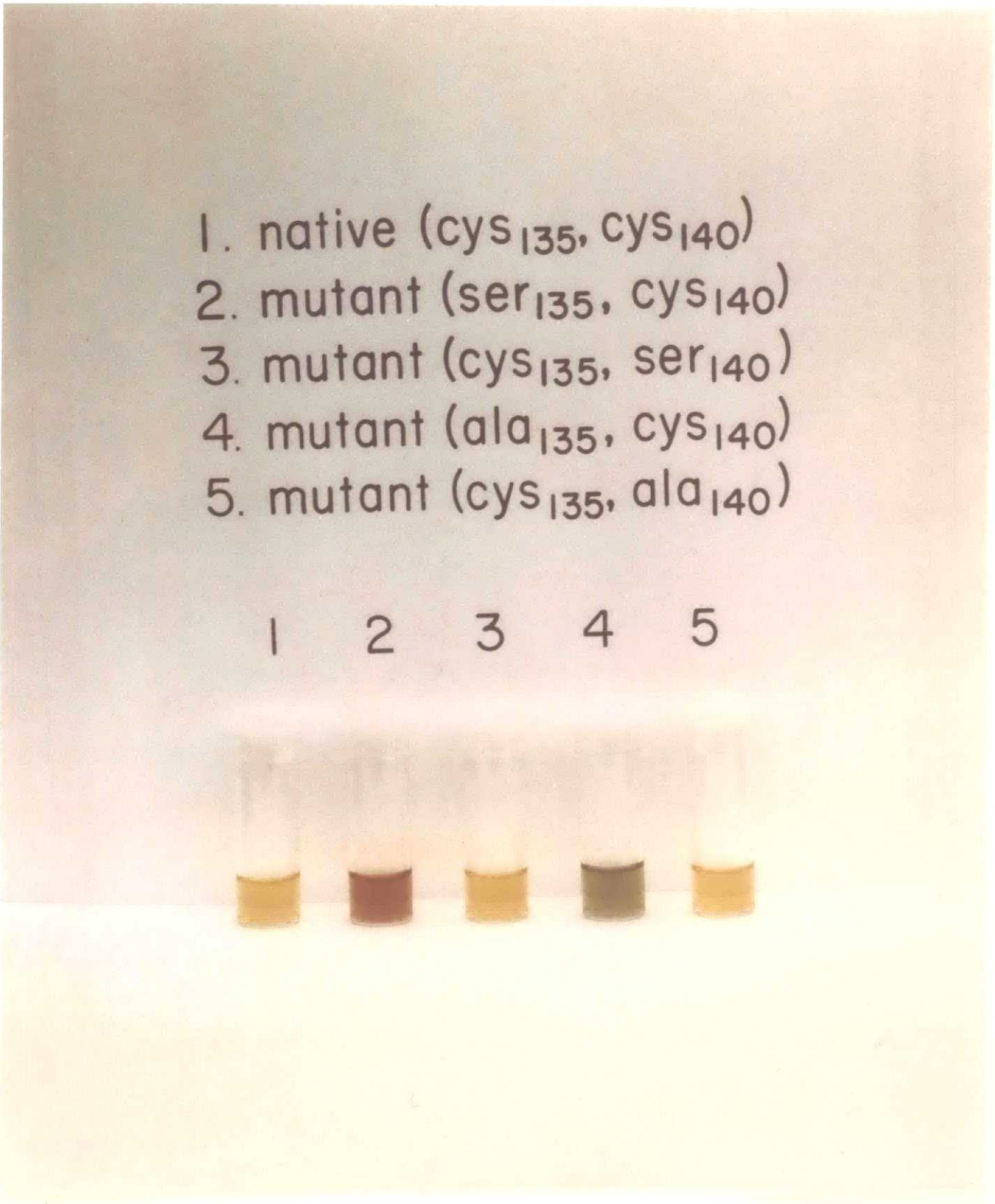
1. native (cys_{135}, cys_{140})
2. mutant (ser_{135}, cys_{140})
3. mutant (cys_{135}, ser_{140})
4. mutant (ala_{135}, cys_{140})
5. mutant (cys_{135}, ala_{140})
1 2 3 4 5

Figure 3-5

after elution from Orange A and subsequent dialysis, display a yellow color typical of flavoproteins (Figures 3-4 and 3-5).

Native mercuric reductase can exist in an oxidized state (E), a two electron reduced state (EH_2) and a four electron reduced state (EH_4) (Figure 1-7), each of which have distinctive electronic absorption spectra (Figure 3-6A). The oxidized state is characterized by a λ_{max} in the visible region at 458 nm with pronounced shoulders on this peak, indicating that the flavin is bound in a hydrophobic environment (Fox and Walsh, 1982; Massey and Ganther, 1965). EH_2 contains oxidized flavin and reduced disulfide (cys_{135} and cys_{140}) at the active site. This change is reflected in a 28% decrease in the 458 nm absorbance in the $NADP^+$-free enzyme, a shift of λ_{max} to 440 nm, and a new absorbance band at 540 nm. This long wavelength absorbance is ascribed to a charge transfer complex between one of the thiolate anions in the active site and oxidized flavin (Fox and Walsh, 1982; Thorpe and Williams, 1981). Further addition of electrons results in the loss of absorbance in both the long wavelength absorbing chromophore and the flavin, consistent with net four electron reduction of the disulfide and the flavin.

The cys to ser and the cys to ala mutant enzymes lack the redox active disulfide and consequently have only a two electron reduction capacity. The spectrum of the oxidized ser_{135}, cys_{140} enzyme (Fig. 3-6B), with a λ_{max} at 440 nm (ε = 9.48 $mM^{-1}cm^{-1}$) and long wavelength absorption at 540 nm, resembles that of EH_2 in native enzyme (Fig. 3-6A). The presence of the 540 nm band in this mutant clearly demonstrates the involvement of cys_{140} in the thiolate-flavin charge transfer complex. The absorbance spectra of native EH_2 and oxidized ser_{135}, cys_{140} enzyme differ in the charge transfer region, possibly through the influence of the residue at position 135 on the charge transfer complex. Reduction of oxidized ser_{135}, cys_{140} enzyme by two

Figure 3-6. Absorbance spectra of oxidized and reduced native and cys to ser mutant enzymes. In A-C, spectrum 1 is oxidized enzyme, spectrum 2 is two electron reduced enzyme, and spectrum 3 is four electron reduced enzyme. A) Native enzyme (cys_{135}, cys_{140}) (from Fox, 1983). B) Ser_{135}, cys_{140} mutant enzyme. C) Cys_{135}, ser_{140} mutant enzyme.

Figure 3-6

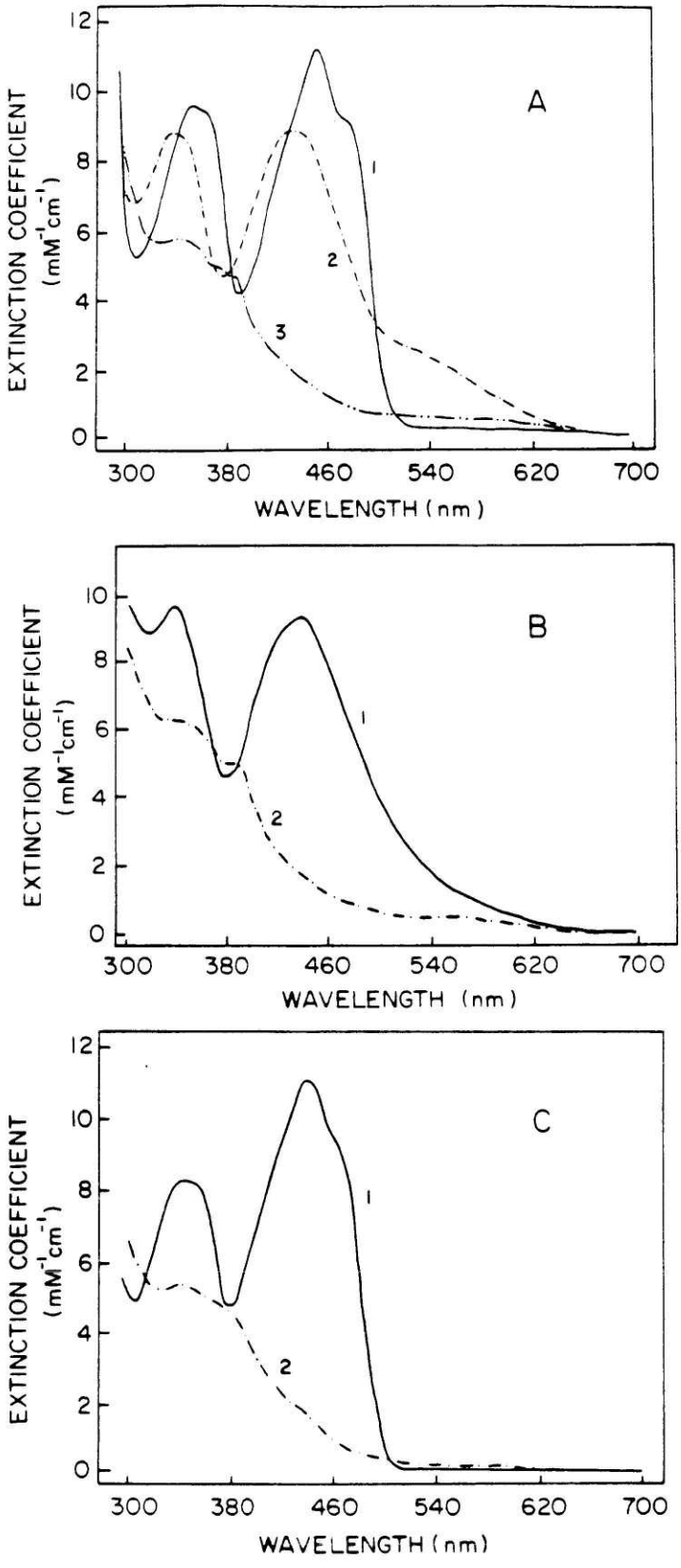
A
B
C
EXTINCTION COEFFICIENT
(mM⁻¹cm⁻¹)
WAVELENGTH (nm)
1
2
3
0
2
4
6
8
10
12
300
380
460
540
620
700

electrons results in the loss of the charge transfer and flavin band, consistent with formation of $FADH_2$.

The absorption spectrum (Fig. 3-6C) of oxidized cys_{135}, ser_{140} mutant mercuric reductase, which has λ_{max} at 440 nm (ε = 11.3 $mM^{-1}cm^{-1}$), resembles that of oxidized native enzyme. The shift in λ_{max} to higher energy (458 to 440 nm) in the mutant versus native enzyme may indicate partial stabilization of the flavin by the hydroxyl group at residue 140. Dithionite reduction of the oxidized cys_{135}, ser_{140} enzyme again results in the loss of the 440 nm absorbance, indicative of $FADH_2$ formation. The lack of a charge transfer complex in this mutant suggests that cys_{135} is not in close proximity to the bridgehead C-4a position of the flavin.

Like the cys_{135}, ser_{140} mutant, the cys_{135}, ala_{140} mutant has a spectrum (Fig. 3-7B) similar to that of oxidized native enzyme. The λ_{max} is at 450 nm (ε = 11.9 $mM^{-1}cm^{-1}$), with a more pronounced shoulder than observed with the cys_{135}, ser_{140} mutant enzyme. This flavin absorbance is lost upon two electron reduction by dithionite.

The spectrum of the ala_{135}, cys_{140} enzyme (Fig. 3-7C), with a λ_{max} at 435 nm (ε = 8.57 $mM^{-1}cm^{-1}$) and broad, long wavelength absorption at 550 nm, resembles that of native enzyme monoalkylated at cys_{135} with iodoacetamide (EHR) (Fig. 3-7A), which shows a long wavelength band around 560 nm. Again, this demonstrates the involvement of cys_{140} in the thiolate-flavin charge transfer complex; however, in this case, as with native EHR, the long wavelength absorbance band differs in character when compared to that in native EH_2. Fox and Walsh (1983) have noted the resemblance of the spectrum of native EHR to several species: a complex between lipoamide dehydrogenase EH_2 and NAD^+, a complex between lipoamide dehydrogenase EHR and nicotinamide analogue 3-aminopyridine adenine dinucleotide, lipoamide dehydrogenase EH_2

Figure 3-7. Absorbance spectra of oxidized and reduced native, alkylated native, and cys to ala mutant enzymes. In A-C, spectrum 1 is oxidized enzyme, spectrum 2 is two electron reduced enzyme, spectrum 3 is iodoacetamide alkylated enzyme, and spectrum 4 is four electron reduced enzyme. A) Native enzyme (cys_{135}, cys_{140}) (from Fox, 1983). B) Cys_{135}, ala_{140} mutant enzyme. C) Ala_{135}, cys_{140} mutant enzyme.

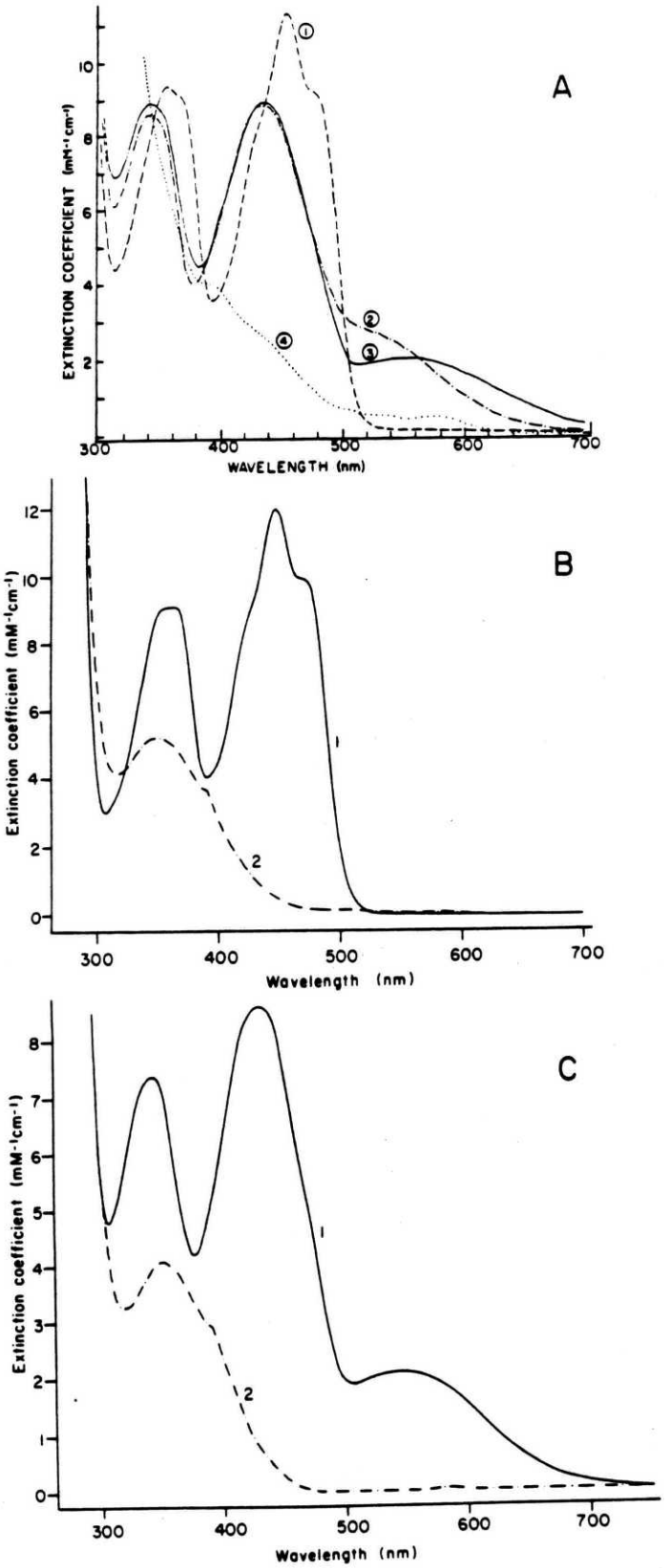
A
EXTINCTION COEFFICIENT (mM⁻¹cm⁻¹)
WAVELENGTH (nm)
B
Extinction coefficient (mM⁻¹cm⁻¹)
Wavelength (nm)
C
Extinction coefficient (mM⁻¹cm⁻¹)
Wavelength (nm)

Figure 3-7

in the presence of 0.2 M guanidinium chloride, and a complex between mercuric reductase EH_2 and $NADP^+$ (Fox, 1983). Dithionite reduction of the ala_{135}, cys_{140} enzyme by two electrons results in the loss of the charge transfer and flavin band.

For native enzyme, the fluorescence emission maximum of the native enzyme at 30°C is at 520 nm and the excitation maximum is at 483 nm (Fox and Walsh, 1982). The fluorescence of the native enzyme is 3.1 times more intense than that of a sample of free FAD at the same concentration. With free FAD, the adenine ring stacks over the isoalloxazine ring and quenches the fluorescence; this quenching decreases when the FAD binds to the enzyme (Fox, 1983). The fluorescence emission and excitation maxima at 20°C of the ser_{135}, cys_{140} mutant enzyme are at 518 nm and 475 nm, respectively, with an intensity one-third that of free FAD. The emission and excitation maxima for the cys_{135}, ser_{140} enzyme at 20°C are at 508 nm and 468 nm, respectively (intensity 1.7 times that for free FAD). The emission and excitation maxima for the ala_{135}, cys_{140} enzyme at 25°C are at 516 nm and 470 nm, respectively (intensity one-half that of free FAD). The emission and excitation maxima for the cys_{135}, ala_{140} enzyme at 25°C are at 516 nm and 475 nm, respectively (intensity three times that of free FAD). The fluorescence spectra of the mutant enzymes are shown in Figure 3-8. The fluorescence is clearly quenched in those mutants which contain a cys_{140} thiolate residue.

Cys_{140} pK_a determination

The ser_{135}, cys_{140} mutant and the ala_{135}, cys_{140} mutant enable us to determine the pK_a of the thiolate anion involved in the charge transfer complex by monitoring the extinction coefficient of the 540 nm absorbance as a function of pH. As the pH is lowered, the spectrum of each oxidized

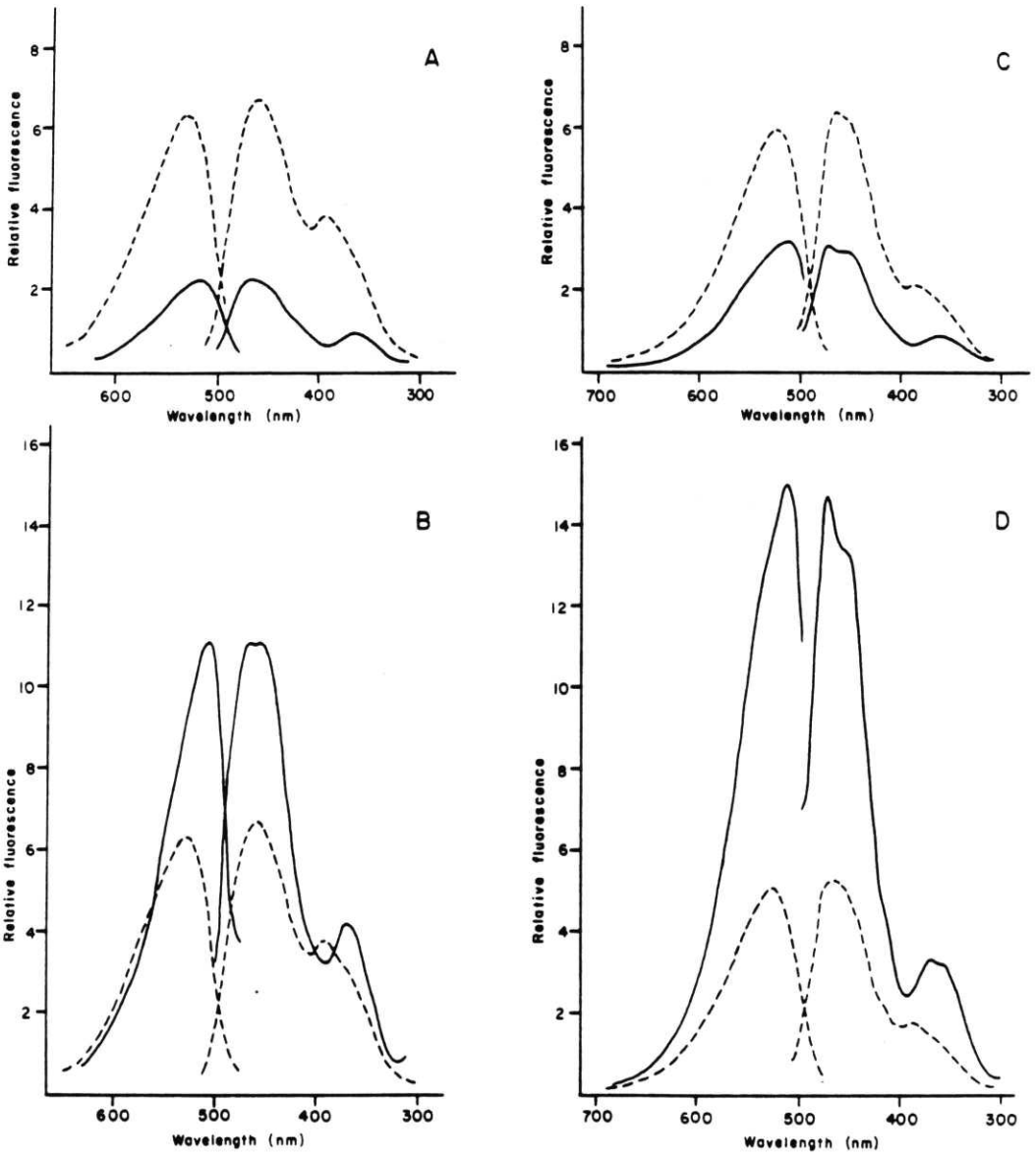

Figure 3-8. Fluorescence spectra of the mutant mercuric reductases. In each case, the solid line is the fluorescence spectrum of the enzyme bound FAD, and the dashed line is the fluorescence spectrum of free FAD presumed to be at the same concentration, obtained by boiling the corresponding enzyme sample in a sealed vial for 15 min. A) Ser_{135}, cys_{140} enzyme. B) Cys_{135}, ser_{140} enzyme. C) Ala_{135}, cys_{140} enzyme. D) Cys_{135}, ala_{140} enzyme.

enzyme approaches that of free FAD (Figures 3-9 and 3-10). These absorption changes are compatible with protonation of the anionic electron donor, with consequent loss in the charge transfer band. The titration curve for the ser_{135}, cys_{140} enzyme is reversible down to pH 3.0 and affords a pK_a for cys_{140} of 5.1. For comparison, the pK_a of the corresponding cysteine in two electron reduced pig heart lipoamide dehydrogenase is 5.2 (Matthews and Williams, 1976) and 4.8 for two electron reduced glutathione reductase (Arscott et al., 1981). Relatively little difference is seen in the long wavelength region of the absorption spectrum of the cys_{135}, ser_{140} mutant from pH 6.0 to 12, and there is no optical indication of titration of an acid-base group.

For the ala_{135}, cys_{140} mutant, the titration curve is reversible to about pH 5 and affords a higher pK_a value of 6.3, one pK_a unit higher than in the ser_{135}, cys_{140} case. Between pH 4 and 5, the flavin appears to dissociate from the protein, since the spectrum starts to resemble that of free flavin, and the protein precipitates when the pH is then raised to 7.0.

For comparison, a preliminary pK_a value measured for the native enzyme is about 5.1 (Miller et al., unpublished).

Oxidation-reduction potentials

The oxidation-reduction potentials of the mutant enzymes were estimated by dithionite or xanthine oxidase titration, as described in Methods, in 80 mM sodium phosphate (pH 7.4) in the presence of the redox indicator dyes 1-deazaflavin or benzyl viologen (cys_{135}, ser_{140} and cys_{135}, ala_{140}), 8-hydroxyriboflavin or methyl viologen (ser_{135}, cys_{140}), and methyl viologen or benzyl viologen (ala_{135}, cys_{140}). The midpoint potential in native enzyme of the E/EH_2 couple is -269 mV and -335 mV for the EH_2/EH_4 couple

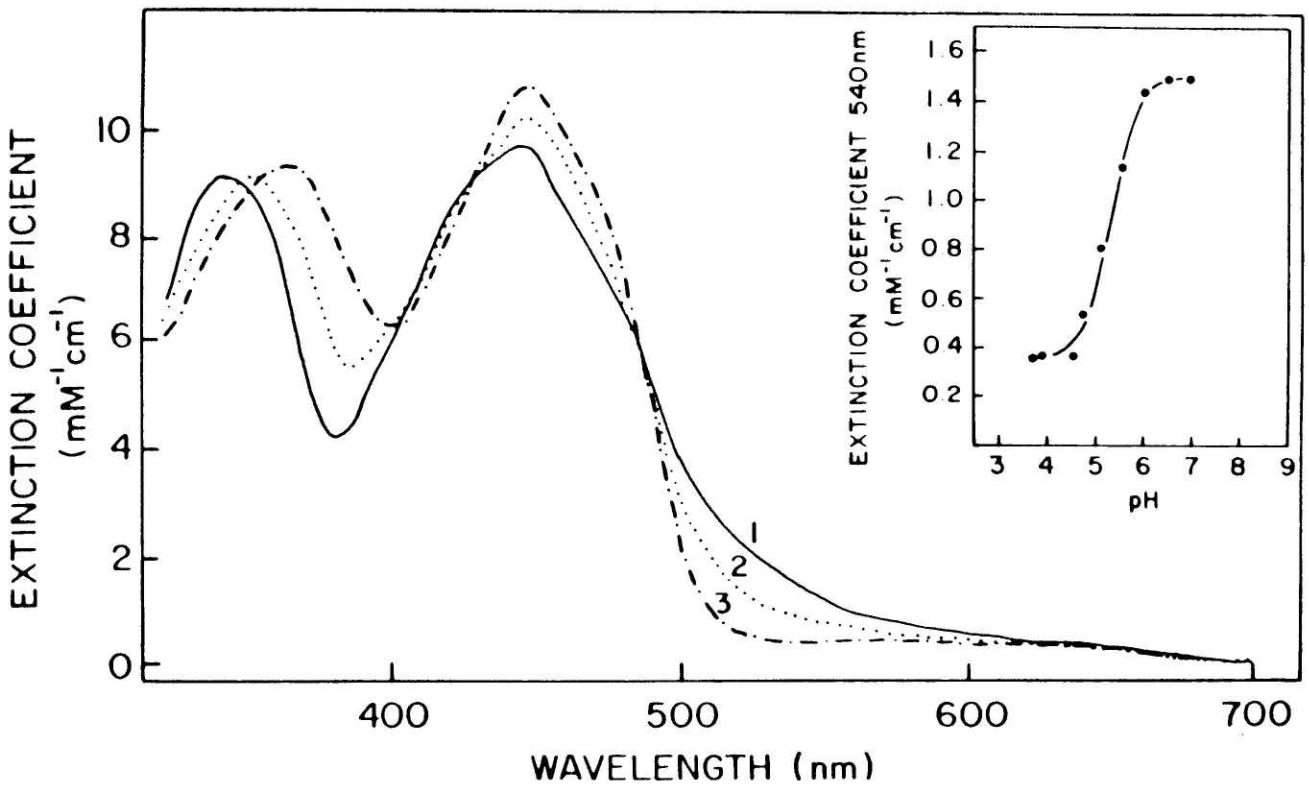

Figure 3-9. Determination that the pK_a of cys_{140} in the ser_{135}, cys_{140} mutant enzyme is 5.1. This value was determined from a replot of the data shown as $1/\Delta A$ vs. $1/[H^+]$ where the value for K_a is taken from the negative reciprocal of the x-intercept. A few representative spectra from the titration are shown. 1) pH 7.60. 2) pH 5.08. 3) pH 3.95.

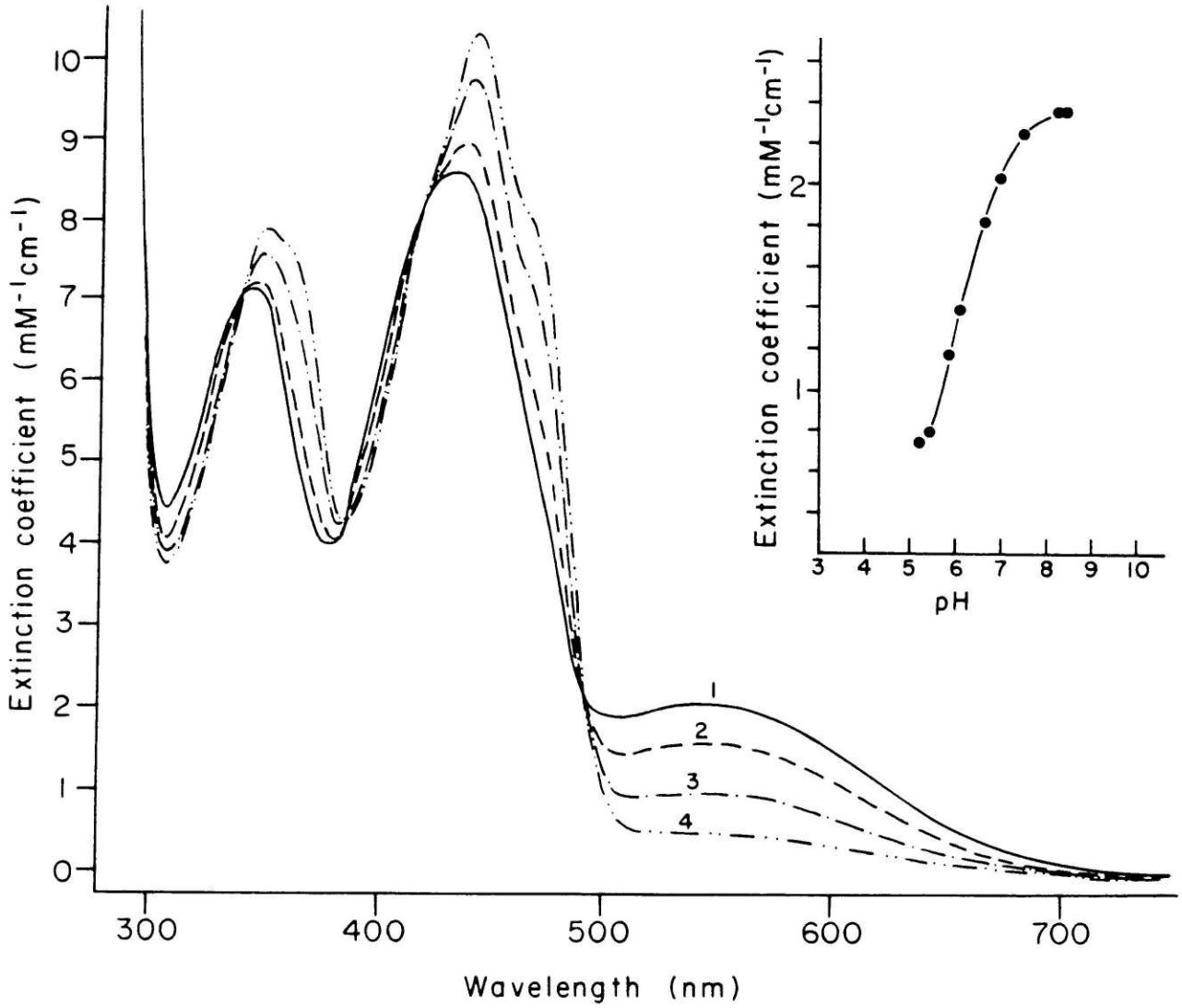

Figure 3-10. Determination that the pK_a of cys_{140} in the ala_{135}, cys_{140} mutant enzyme is 6.3. This value was determined from a replot of the data shown as $1/\Delta A$ vs. $1/[H^+]$ where the value for K_a is taken from the negative reciprocal of the x-intercept. A few representative spectra from the titration are shown. 1) pH 7.50. 2) pH 6.63. 3) pH 5.83. 4) pH 5.23.

(Fox and Walsh, 1982). The latter value was calculated from the extent of disproportionation of EH_2 at equilibrium as described by Matthews and Williams (1976). For native enzyme, the slope of a plot of E' versus log E/EH_2 was 28 mV, which compared favorably with the theoretical value of 30 mV for a two electron process (derived from the Nernst equation, $E' = E°' + (RT/(nF))\log(ox/red)$; when n = 2, RT/(nF) = 30 mV). In contrast, plots of E' vs. log E/EH_2 (or more conveniently, plots of log E/EH_2 vs. log dye_{ox}/dye_{red}) for the mutant enzymes resulted in n values closer to 1 than to 2. Massey et al. (unpublished) have suggested that determinations of these redox potentials are complicated by the possibility that the flavins on the two subunits display cooperativity. Accordingly, when the data are replotted with the assumptions that the two subunits contribute equally toward the absorbance spectra and that their redox potentials are sufficiently different to allow the titration of the first subunit to go essentially to completion before the other subunit is titrated, slopes which give n values closer to 2 are obtained. As the validity of these assumptions is not yet established, the values measured for the redox potentials in Table 3-IV should be regarded as preliminary. Nevertheless, it seems reasonable to conclude that the redox potential of the ser_{135}, cys_{140} mutant enzyme is substantially lower than that of any of the other mutants, as well as that of the native EH_2/EH_4 couple. Figures 3-11 and 3-12 show the results of redox titrations obtained with the cys to ala mutant enzymes.

Table 3-IV

Bound flavin redox potentials

in the native and active site mutant mercuric reductases

Mutant enzyme[a]		Redox potential[b] (E/EH_2)
ser_{135}, cys_{140}[c]	-	-393 mV, -428 mV
cys_{135}, ser_{140}[c]	-	-326 mV, -375 mV
ala_{135}, cys_{140}	-	-321 mV, -369 mV
cys_{135}, ala_{140}	-	-307 mV, -351 mV
Native enzyme[d]	**Redox potential (E/EH_2)**	**Redox potential (EH_2/EH_4)**
cys_{135}, cys_{140}	-269 mV	-335 mV

[a]Values for mutant redox potentials are preliminary, as discussed in text.

[b]Two redox potentials are reported for each of the mutant enzymes under the assumption of subunit cooperativity, as discussed in text.

[c]Massey et al., unpublished.

[d]Fox and Walsh, 1982.

Figure 3-11. Redox titration of the ala_{135}, cys_{140} mutant enzyme in the presence of benzyl viologen. For simplicity, approximately half of the spectra used for the plot in the inset are shown. The final absorbances at 435 nm and 602 nm are marked. Inset: determination of midpoint potential from treating the data shown as the titration of two different subunits, as described in the text (solid triangles). Data points in the middle of the titration are presumed to be subject to the largest error in this analysis and are omitted from calculation of the best fitting lines. Solid circles represent data points calculated under the assumption of a single redox active site.

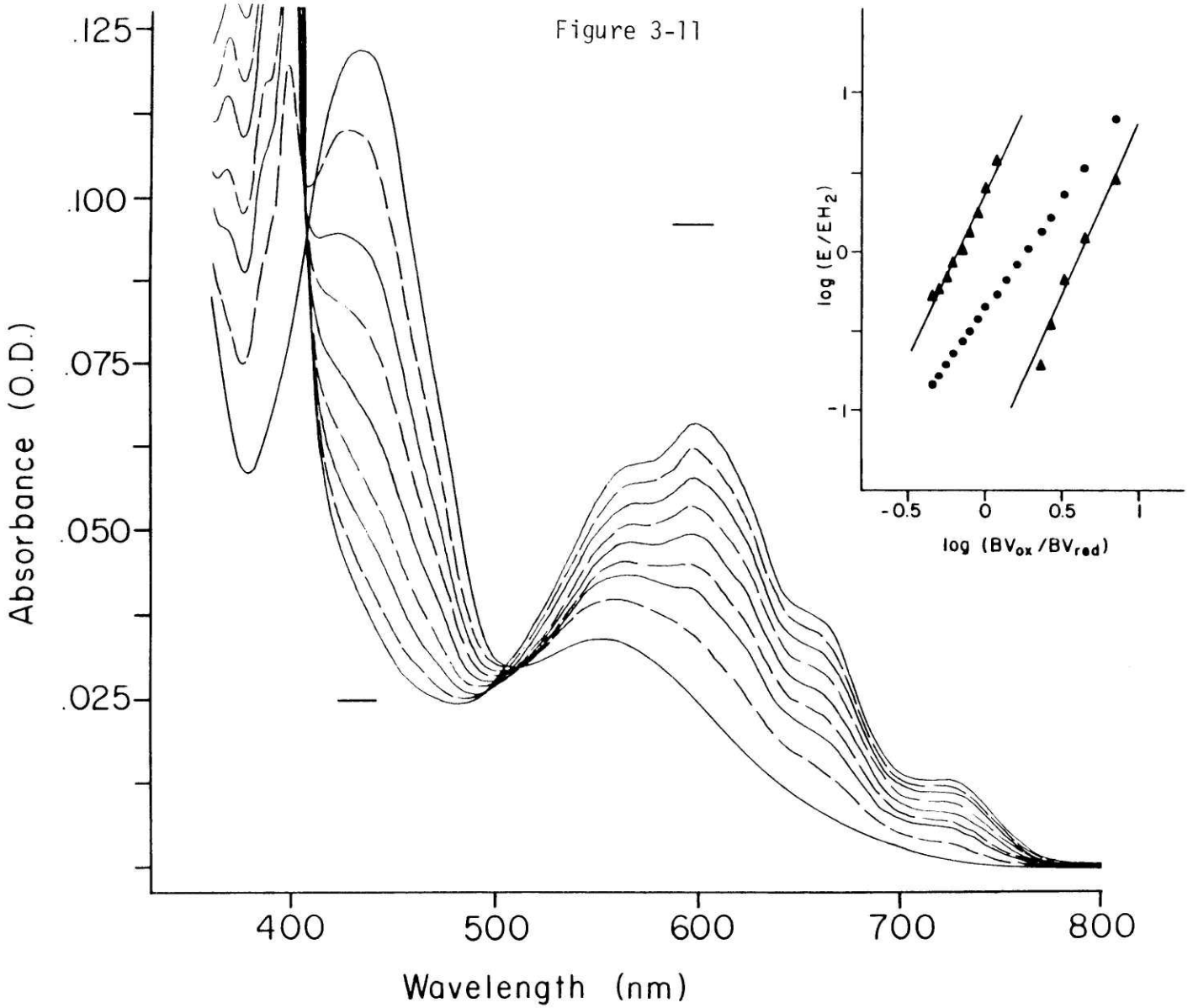
Figure 3-11
Absorbance (O.D.)
.125
.100
.075
.050
.025
400
500
600
700
800
Wavelength (nm)
log (E/EH2)
1
0
-1
-0.5
0
0.5
1
log (BVox/BVred)

Figure 3-12. Redox titration of the cys_{135}, ala_{140} mutant enzyme in the presence of benzyl viologen. For simplicity, approximately half of the spectra used for the plot in the inset are shown. The final absorbances at 450 nm and 602 nm are marked. Inset: determination of midpoint potential from treating the data shown as the titration of two different subunits, as described in the text (solid triangles). Data points in the middle of the titration are presumed to be subject to the largest error in this analysis and are omitted from calculation of the best fitting lines. Solid circles represent data points calculated under the assumption of a single redox active site.

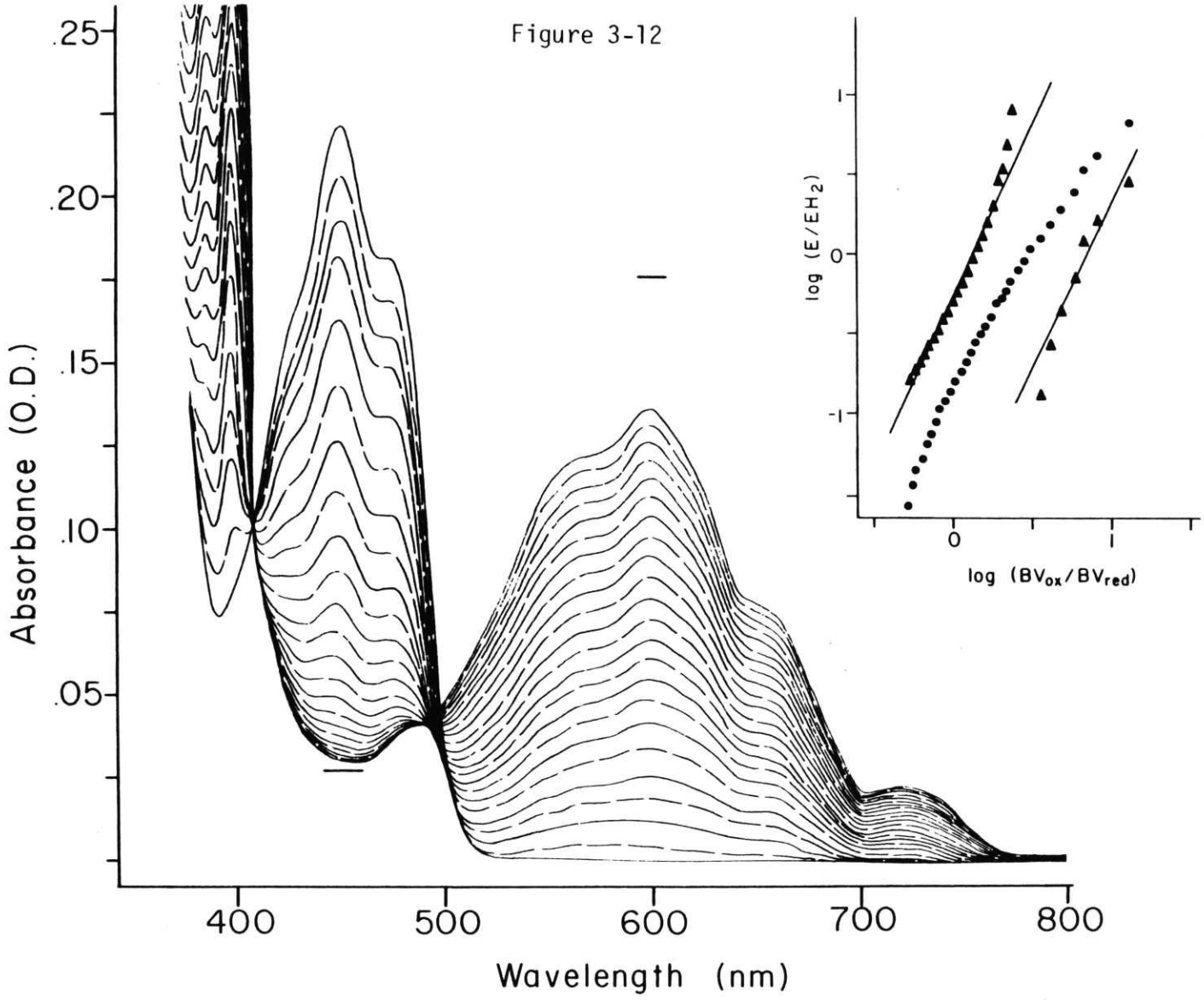
.25
.20
.15
.10
.05
Absorbance (O.D.)
400
500
600
700
800
Wavelength (nm)
log (E/EH2)
1
0
-1
0
1
log (BVox/BVred)

Figure 3-12

Discussion

In order to understand the unique structural properties of mercuric reductase which make possible Hg(II) reduction, we have begun to construct active site mutants and characterize their physical and catalytic properties. We have therefore constructed four active site mutants, the cys_{135}, ser_{140} and ser_{135}, cys_{140} mutants, in which cys_{140} and cys_{135}, respectively, have been altered to serine residues, and the cys_{135}, ala_{140} and ala_{135}, cys_{140} mutants, in which cys_{140} and cys_{135}, respectively, have been altered to alanine residues (Figure 2-11).

The native and mutant merA genes have been placed behind the hybrid tac promoter (see Chapter 2), and the expressed enzymes have been purified in high yield in one step by affinity chromatography. The specificity of the key Orange A column used in this protocol appears to due in large part to its affinity for the enzymes' $NADP^+$ binding site (Clonis and Lowe, 1980). Furthermore, the transhydrogenase assay used need not require the presence of a redox active disulfide. Consequently, on the basis of our working model for the active site geometry of mercuric reductase (Figure 3-13), we expect that this column and assay should be useful for the purification of future active site mutant enzymes involving mutations around the redox active disulfide.

Like glutathione reductase and lipoamide dehydrogenase, native mercuric reductase is isolated with both FAD and the active site cysteines oxidized as the intramolecular disulfide. This is termed the oxidized (E) form of the enzyme. Two electron reduction of oxidized enzyme generates EH_2 which, when first formed, is likely to contain $FADH_2$, based on the X-ray structure of glutathione reductase in which FAD is sandwiched between $NADP^+$ and cys_{58}-S-S-cys_{63} (Figure 1-5). The electrons, however, are rapidly

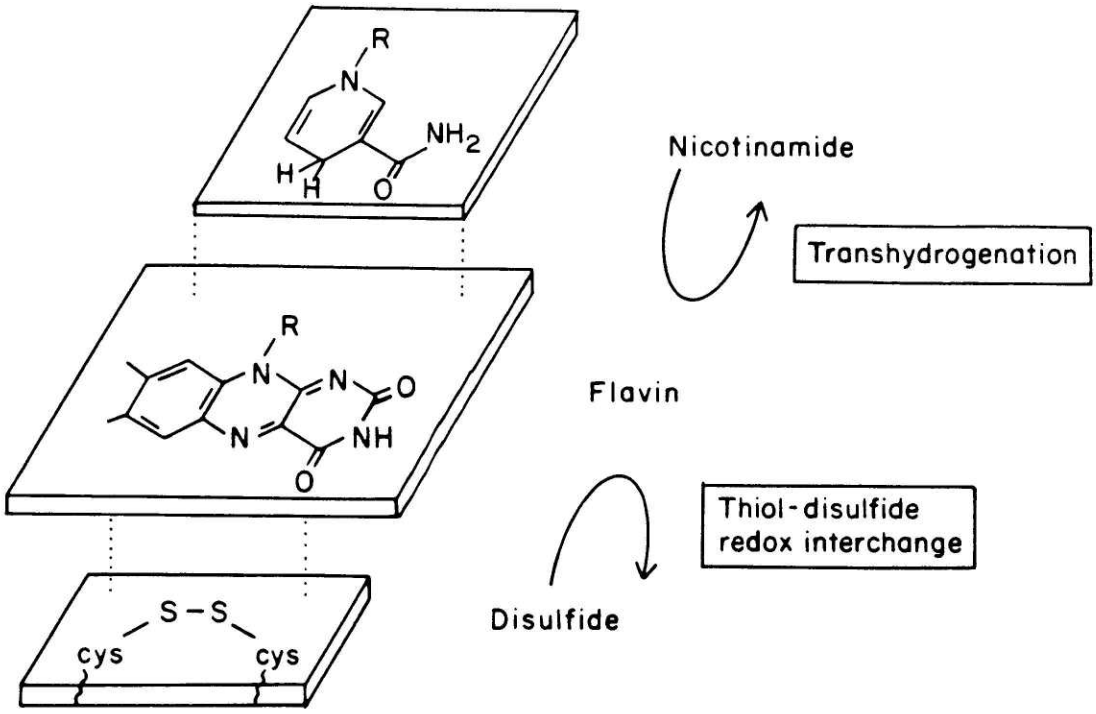

Figure 3-13. Working model for the active site geometry of mercuric reductase, which is based on the known structure of the active site in glutathione reductase (adapted from Fox, 1983).

transferred from $FADH_2$ to the active site disulfide, and the equilibrium form of EH_2 is characterized by a charge transfer complex between one of the cysteine thiols and FAD.

Iodoacetamide treatment of the active site cysteines in EH_2 affords an 18/1 regioselective labelling of cys_{135} versus cys_{140} (Fox and Walsh, 1983), a selectivity for the amino proximal cysteine of the dithiol pair mirroring that seen with glutathione reductase (Arscott et al., 1981). Since the oxidized, alkylated native mercuric reductase displayed a charge transfer band, provisionally assigned to cys_{140} and oxidized FAD, we anticipated that of the four mutants, only the oxidized ser_{135}, cys_{140} and ala_{135}, cys_{140} mutants would show a charge transfer band. This is in fact the case and is consistent with the use of the glutathione reductase X-ray structure as a predictive guide in which the carboxy proximal cysteine is in close proximity (3.6 Å (Schulz et al., 1982)) to the C-4a locus of bound FAD.

The presence of the charge transfer band in the spectrum of the ser_{135}, cys_{140} and the ala_{135}, cys_{140} mutant enzymes permitted the facile titration of the cys_{140} thiol pK_a. The value of 5.1 for the ser_{135}, cys_{140} mutant reflects a three order of magnitude stabilization of the thiolate in its active site geometry compared with a cysteine free in solution (pK_a = about 8). The thiolate stabilization is due at least in part to the stabilization provided by interaction with FAD in the charge transfer complex and may also indicate the involvement of an active site base in conversion of cys_{140}-SH to cys_{140}-S^- (Williams, 1976; Matthews and Williams, 1976; Untucht-Grau et al., 1979). Furthermore the reduction potential for the $FAD/FADH_2$ couple in the ser_{135}, cys_{140} mutant (near -400 mV) is substantially more negative than that of the EH_2/EH_4 couple (-335 mV) in the native enzyme. The higher pK_a value of 6.3 for cys_{140} and the less negative bound flavin redox potential

in the ala_{135}, cys_{140} mutant enzyme, as compared to the ser_{135}, cys_{140} mutant enzyme, could reflect the loss of a stabilizing charge interaction involving an active site base and residues 135 and 140 and/or it may reflect an alteration of the thiol-flavin charge transfer interaction which results in weaker stabilization of the cys_{140} thiolate anion. Alteration of the charge transfer interaction between these two mutants is suggested by differences in their spectra as well.

On addition of two additional electrons to the EH_2 form of native mercuric reductase, the four electron capacity of the enzyme is saturated and E-$FADH_2$ accumulates. This change is reflected in the disappearance of the 458 nm FAD absorption in the four electron reduced enzyme, EH_4 (figure 3-6A). It is worth explicit note that the mutation of either cys_{135} or cys_{140} to serine or alanine produces mutant mercuric reductases which in their fully oxidized state, E, are functionally equivalent to the EH_2 form of the native enzyme. These mutants contain oxidized FAD and an active site thiol. Correspondingly, the two electron reduced mutant enzymes, with $FADH_2$ in the active site, are functionally equivalent to the EH_4 form of native enzyme, the only form of native enzyme with a significant content of $FADH_2$. This relationship is reflected in the electronic absorption spectra of the EH_2 mutant enzymes, which resemble that of native EH_4 (Figures 3-6 and 3-7).

The work in this chapter has demonstrated that the native enzyme and the four active site mutant enzymes are each unique with respect to their physical and redox characteristics. The influence of these differences on catalytic properties will be explored in the following chapter.

CHAPTER FOUR

CATALYTIC PROPERTIES OF THE ACTIVE SITE MUTANT MERCURIC REDUCTASES

Introduction

The Tn501-encoded native mercuric reductase, like the related flavin-containing pyridine nucleotide disulfide oxidoreductases, catalyzes oxidation reduction reactions of several different substrates. For example, the transhydrogenase activity monitored during native or mutant mercuric reductase purifications, as described in Chapter 3, involves the transfer of electrons from NADPH to thioNADP$^+$. As diagrammed in Figure 3-13, this activity is not expected to require the presence of the redox active disulfide. Reduction of O_2 to H_2O_2, resulting from the reaction of O_2 with enzyme-bound dihydroflavin, is low but measurable in the native enzyme (Fox and Walsh, 1982). Again, this activity is not expected to require the involvement of a redox active disulfide. Rinderle et al. (1983) have reported the reduction of DTNB by the closely related R100-encoded mercuric reductase. Fox (1983) has also previously observed DTNB reductase activity in the Tn501 enzyme. Catalytic disulfide reduction, as in the case of DTNB, is a striking similarity between mercuric reductase and the pyridine nucleotide disulfide oxidoreductases. On the other hand, although two electron reduction of mercuric reductase, glutathione reductase, and lipoamide dehydrogenase results in the formation of an active site dithiolate capable of complexing mercuric ions (Massey and Williams, 1965; Casola and Massey, 1966), mercuric reductase is unique among this class of flavoenzymes in its ability to catalyze the reduction of Hg(II) to Hg(0) (Fox and Walsh, 1982).

This chapter describes investigations of the behavior of the native enzyme and the four active site mutant enzymes toward the native enzyme substrates thioNADP$^+$, O_2, DTNB, and various complexes of Hg(II). The active site cysteines are believed to play an important role in the binding and/or

reduction of Hg(II) complexes and DTNB, and they may also influence the behavior of the enzyme in O_2 reduction and transhydrogenation. The replacement of each active site cysteine independently with serine or alanine and the resulting absence of the redox active disulfide provides us with an approach for studying the role of these cysteines in substrate binding and reduction.

Experimental Procedures

Materials

$Hg(CN)_2$ was purchased from Alfa or from Aldrich. Sources for all other materials used are described in Chapter 3.

Methods

Spectrometry

Absorbance was monitored on a Perkin Elmer 554 or Perkin Elmer Lambda 5 UV-visible spectrophotometer, both equipped with thermostated sample compartments. Fluorescence was measured on an unthermostated Perkin Elmer LS-3 fluorimeter. Anaerobic assays were performed in anaerobic cuvettes with two side arms similar in construction to those described by Williams et al. (1979).

Protein concentration

Protein concentration was determined by flavin content as described in Chapter 3.

Enzyme assays

ThioNADP$^+$-dependent oxidation of NADPH (transhydrogenation) was monitored at 340 nm (absorbance) or 470 nm (emission; excitation set to 340 nm) at 25°C in 80 mM sodium phosphate, pH 7.5, 1 mM 2-mercaptoethanol, 200 μM NADPH, and 100 μM thioNADP$^+$, using enzyme samples treated as indicated below. Reaction was initiated by the addition of thioNADP$^+$. O_2 consumption assays were performed at 37°C on a Yellow Springs Instrument Co. biological

oxygen monitor model 53 using air saturated buffer (50 mM sodium phosphate, pH 7.5) and 200 μM NADPH, which was added to initiate the reaction. Enzyme samples used in O_2 consumption assays had been previously treated by KBr dialysis as described in Chapter 3. DTNB reduction was monitored at 412 nm (ε = 13.6 $mM^{-1}cm^{-1}$) at 25°C in the presence of 1 mM DTNB in 80 mM sodium phosphate, pH 7.5, with 200 μM NADPH added to initiate turnover, using enzyme samples which had been treated by passage through Biogel P6DG to remove excess thiols or by KBr dialysis as described in Chapter 3. Hg(II) reductase assay mixtures were monitored at 340 nm at 37°C and contained 80 mM sodium phosphate, pH 7.5, 200 μM NADPH, and one of the following Hg(II) complexes: 100 μM $HgCl_2$ plus 1 mM 2-mercaptoethanol for $Hg(SR)_2$ (R = CH_2CH_2OH), 100 μM $HgCl_2$ plus 0.5 mM EDTA for Hg(EDTA) (the high stability constant of Hg(EDTA) that all Hg(II) is present as the EDTA chelate (Sillen and Martell, 1964; Rinderle et al., 1983)), or 200 μM $Hg(CN)_2$. Reaction was initiated by the addition of the mercuric compound. Enzymes used for $Hg(SR)_2$ reductase assays were stored in the presence of 0.1% 2-mercaptoethanol and 0.5 mM EDTA. Enzymes used for Hg(EDTA) and $Hg(CN)_2$ reductase assays had been treated as described above for DTNB reductase assays. All changes in absorbance were monitored over at least several turnovers.

Enzyme activities are expressed as turnover numbers where turnover of 1 nmol is defined as 1 nmol of NADPH or O_2 consumed (for HgX_2 reductase, O_2 reductase, and transhydrogenase assays) or 1 nmol of 5-thio-2-nitrobenzoate dianion produced (for DTNB reductase assays) and where 1 nmol of enzyme is equivalent to 1 nmol of enzyme-bound FAD.

Results

We have assayed the following activities in both the native and the four mutant mercuric reductases: $Hg(SR)_2$-, Hg(EDTA)-, and $Hg(CN)_2$-dependent NADPH oxidation, aryl disulfide reduction, transhydrogenation (thioNADP$^+$/NADPH), and O_2 reduction.

Behavior toward mercuric complexes

All mercuric reductase enzymes isolated to date show a requirement of exogenous thiols for sustained Hg(II) reduction (Robinson and Tuovinen, 1984). For example, native mercuric reductase (Tn501) shows Hg(II) reductase activity in the presence of exogenous 1 mM 2-mercaptoethanol (Fox and Walsh, 1982). The kinetics of NADPH oxidation for the Tn501-encoded mercuric reductase have been shown to be biphasic with V_{max} of 800 min^{-1} per FAD (first phase), 380 min^{-1} per FAD (second phase), and K_m for $HgCl_2$ of 12 μM (Fox and Walsh, 1982). As observed previously by Rinderle et al. (1983) with the R100 mercuric reductase, native enzyme is rapidly inactivated by Hg(EDTA) in the absence of thiol reagents, as indicated by the decrease in the rate of NADPH oxidation (data not shown). Subsequent incubation with thiols reactivates the HgEDTA-inactivated enzyme complex.

The cys to ser and cys to ala mutant mercuric reductases show no reductase activity toward Hg(II) in the presence of 1 mM 2-mercaptoethanol or 0.5 mM EDTA (turnover number < 1 min^{-1}). However, on screening a number of HgX_2 salts, many of which were not usable because they formed complexes with NADPH (McGary et al., 1968; Marshall et al., 1984), it was found that the ser_{135}, cys_{140} mutant catalyzes $Hg(CN)_2$-dependent oxidation of NADPH. The kinetics in this case were not biphasic. The V_{max} was 7 min^{-1} and K_m for $Hg(CN)_2$ was 48 μM (Figure 4-1). Addition of 1 mM 2-mercaptoethanol to

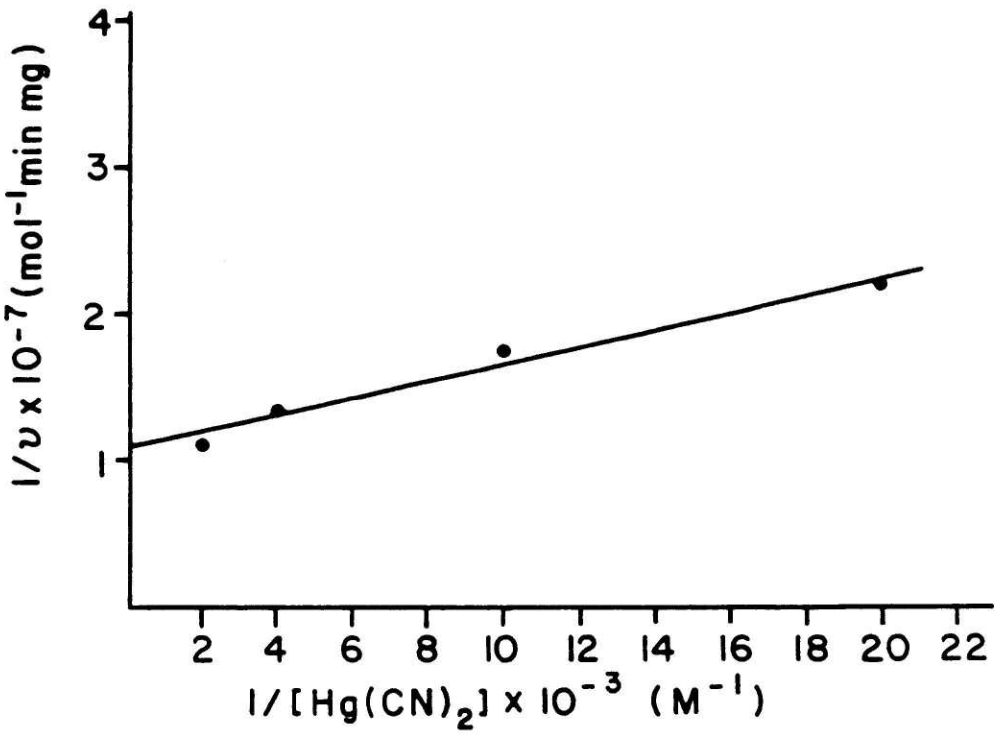

Figure 4-1. Kinetics of $Hg(CN)_2$-dependent NADPH oxidation by the ser_{135}, cys_{140} mutant enzyme.

the assay solution completely inhibited this NADPH oxidation. Native enzyme, the cys_{135}, ser_{140} mutant enzyme, and the ala_{135}, cys_{140} mutant enzyme, but not the cys_{135}, ala_{140} mutant enzyme, also showed a small amount of $Hg(CN)_2$-dependent NADPH oxidation, but in these cases, the rate quickly decreased to background or below. Subsequent addition of 1 mM 2-mercaptoethanol to the assay mixture containing native enzyme and $Hg(CN)_2$ resulted in turnover, as was observed with Hg(EDTA)-inactivated native enzyme.

Addition of $Hg(CN)_2$ to oxidized ser_{135}, cys_{140} enzyme (Figure 4-2) in the absence of NADPH at pH 7.5 decreases the absorbance of the charge transfer band. The decrease in absorbance of the charge transfer band suggests the formation of a monodentate cys_{140}-S-Hg-CN or bidentate cys_{140}-S-Hg-O-ser_{135} adduct. Dissipation of the charge transfer band upon addition of $Hg(CN)_2$ was observed in the ala_{135}, cys_{140} enzyme (Figure 4-3). In this case, additions of $Hg(CN)_2$ were made in smaller increments than for the ser_{135}, cys_{140} titration, and it was then noticed that the initial additions led to a small rise in the charge transfer absorbance, possibly due to Hg(II) binding at a second site, although subsequent additions led to the disappearance of the charge transfer band. In the presence of 1 mM 2-mercaptoethanol or 0.5 mM EDTA, very little decrease in the charge transfer absorbance of the ser_{135}, cys_{140} mutant enzyme was observed until greater than 0.5 mM $HgCl_2$ had been added. This suggests that cys_{140} in the ser_{135}, cys_{140} mutant is unable to bind Hg(II) effectively in the presence of excess EDTA or 2-mercaptoethanol and could explain the differences in catalytic behavior of this mutant toward the various mercuric complexes tested. In native enzyme, iodoacetamide shows an 18/1 preference for alkylation of cys_{135} over cys_{140} in native EH_2 (Fox and Walsh, 1983). This

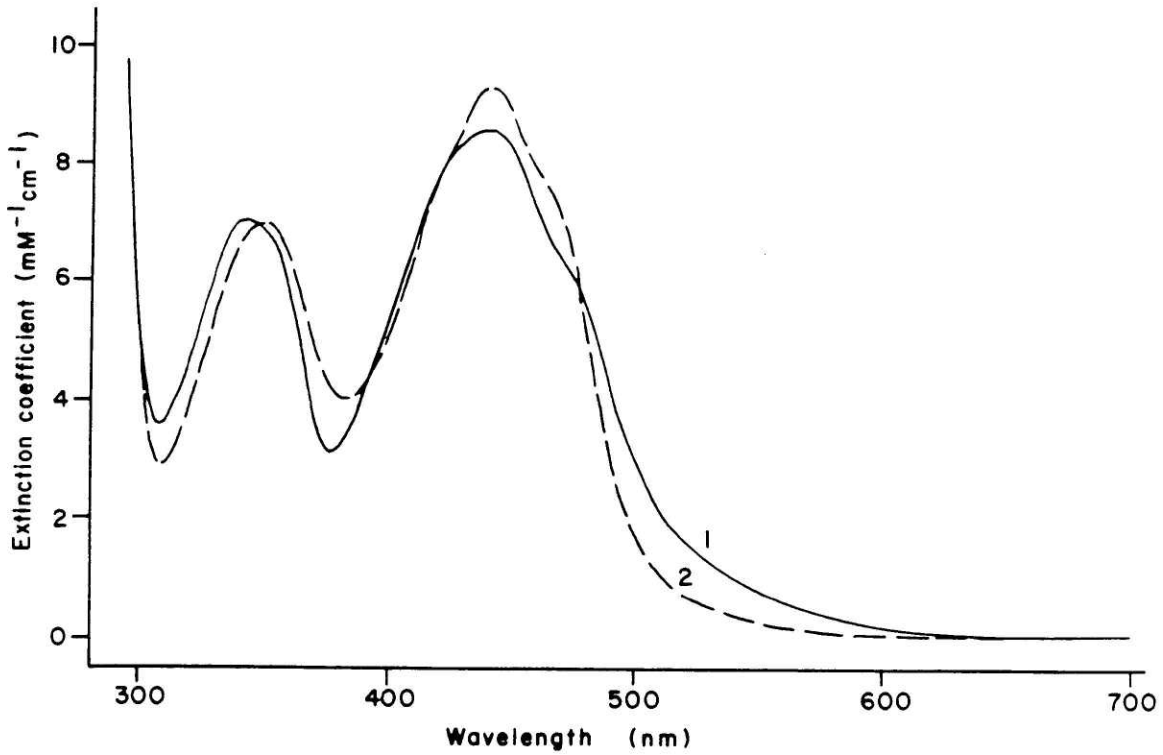

Figure 4-2. $Hg(CN)_2$-dependent decrease of charge transfer band in the ser_{135}, cys_{140} mutant enzyme.

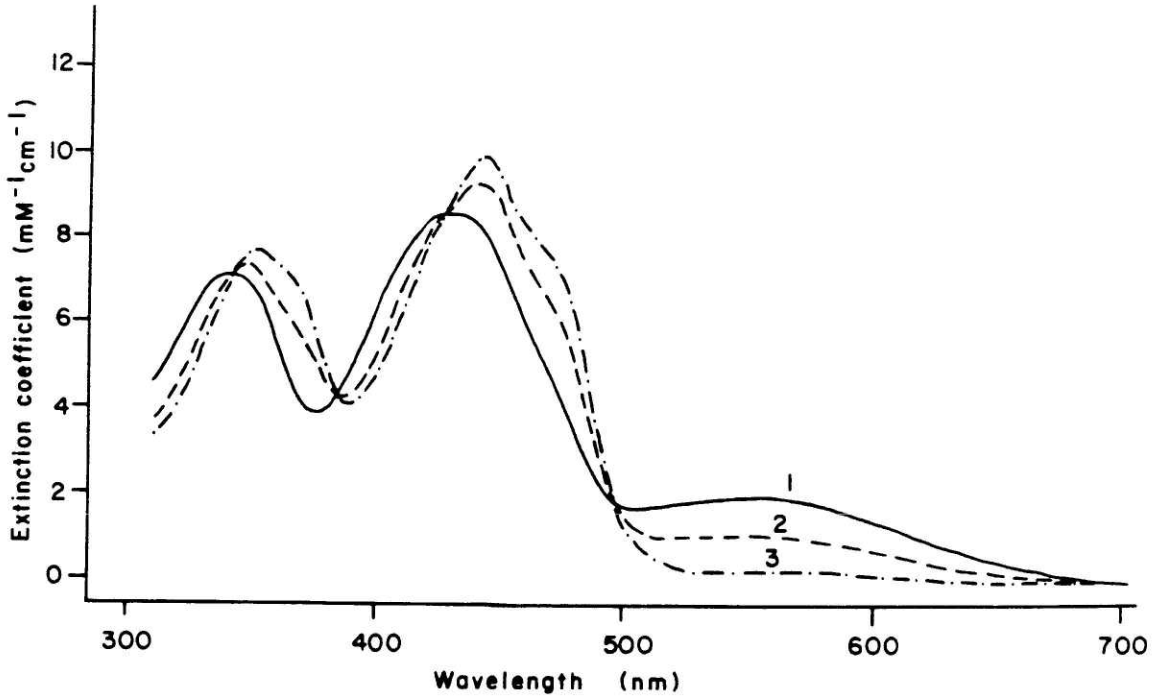

Figure 4-3. $Hg(CN)_2$-dependent loss of charge transfer band in the ala_{135}, cys_{140} mutant enzyme.

preference is likely to reflect steric accessibility. Accordingly, differences in size among the various mercuric complexes could account for the observed differences in binding properties of cys_{140} in the ser_{135}, cys_{140} mutant. Interestingly, Miller et al. (1986) have observed some residual EH_2-type spectroscopic character, but largely E_{ox}-type character for two electron reduced native enzyme in the presence of 100 μM $HgCl_2$ and 1 mM 2-mercaptoethanol. In contrast, only E_{ox}-type character is observed in the absence of 2-mercaptoethanol (Miller et al., 1986). This raises the possibility that under standard $Hg(SR)_2$ reductase assay conditions (200 μM NADPH, 100 μM $HgCl_2$, and 1 mM 2-mercaptoethanol) some mercuric ion complexation involving cys_{140} of the native enzyme may occur (unless the Hg(II) is reduced before binding to cys_{140}) and that such complexation can be reversed in the presence of excess thiol.

Although reduction of $Hg(CN)_2$ to Hg(0) plus $2CN^-$ is the most obvious explanation for $Hg(CN)_2$-dependent NADPH oxidation catalyzed by the ser_{135}, cys_{140} mutant enzyme, an alternative explanation must be considered. The turnover number for this activity (7 min^{-1}) is much more similar to O_2 reductase turnover numbers in some of the other mutants (e.g. cys_{135}, ala_{140}; see below) than it is to the turnover number for $Hg(SR)_2$ reduction in the native enzyme. This suggests that the $Hg(CN)_2$-dependent NADPH oxidation in the ser_{135}, cys_{140} mutant might be due to an increase in O_2 reductase activity (O_2 --> H_2O_2) upon binding of $Hg(CN)_2$ to the enzyme, rather than to actual reduction of mercuric ion. This possibility was tested and confirmed in two ways. First, the O_2 reductase activity, as observed by oxygen electrode, increased from 0.2 min^{-1} to 7 min^{-1} when 200 μM $Hg(CN)_2$ was added to the assay solution. Second, no significant $Hg(CN)_2$-dependent oxidation of NADPH was observed under anaerobic conditions. Upon

opening the cuvette and bubbling air through the assay solution, turnover was observed. No significant NADPH oxidation was detected under anaerobic conditions with the other three mutants nor with native enzyme; therefore, it is likely that any changes observed aerobically are due to perturbations of the O_2 reductase activities of these proteins as well. In contrast, turnover of Hg(EDTA) followed by inactivation of native enzyme proceeded under anaerobic conditions.

DTNB reduction

The native and the two cys to ser mutant mercuric reductases show no detectable (< 1 min^{-1}) NADPH oxidation activity in the presence of the disulfides glutathione and lipoamide. The cys to ala mutants showed no activity toward glutathione; activity of the cys to ala mutants toward lipoamide was not tested. Native mercuric reductase, however, does reduce the aryl disulfide 5,5'-dithiobis-(2-nitrobenzoate) (DTNB) in the presence of NADPH at the rate of 20 min^{-1} at 1 mM DTNB, under anaerobic conditions. Anaerobic conditions were employed to avoid possible complications from H_2O_2 production resulting from O_2 reductase activities. The R100-encoded Hg(II) reductase has been reported to have a K_m of 3 mM for DTNB and V_{max} of 10 min^{-1}, 1% of the Hg(II) reduction rate (Rinderle et al., 1983). A previously reported value from our laboratory (220 min^{-1} per FAD) (Schultz et al., 1985) was not reproducible.

The cys_{135}, ser_{140} mutant, cys_{135}, ala_{140} mutant, and ala_{135}, cys_{140} mutant also reduce DTNB in the presence of NADPH with activities of 3, 1, and 2 min^{-1}, respectively, at 1 mM DTNB under anaerobic conditions. In the absence of NADPH the cys_{135}, ser_{140} and cys_{135}, ala_{140} mutants release a stoichiometric amount of 5-thio-2-nitrobenzoate dianion (see Chapter 3),

suggesting DTNB disulfide exchange with cys_{135} leading to the formation of the cys_{135}-S-S-nitrobenzoate mixed disulfide. The ser_{135}, cys_{140} mutant initially shows no NADPH oxidation activity anaerobically in the presence of 1 mM DTNB, nor is the active site thiol titratable in nondenatured enzyme. However, after a 1-2 minute lag after addition of 200 μM NADPH, DTNB reduction is observed at a very low rate of 0.2-0.3 min^{-1}. The ala_{135}, cys_{140} mutant appears to reduce DTNB anaerobically at a rate of 2 min^{-1} in the presence of 1 mM DTNB and 200 μM NADPH. In nondenatured ala_{135}, cys_{140} mutant enzyme, the active site thiol appears to be slowly titratable, but the nondenaturing titration results are ambiguous, as discussed in Chapter 3. Differences in the spectra, redox potentials, and pK_a's of cys_{140} in the ala_{135}, cys_{140} and ser_{135}, cys_{140} mutants (see Chapter 3) suggest that the two mutants have significant physical differences and that they need not show identical behavior toward substrates like DTNB.

Transhydrogenation

The native and mutant enzymes all show transhydrogenase activity (thioNADP$^+$/NADPH) as do glutathione reductase and lipoamide dehydrogenase. For the native enzyme, the V_{max} is 23 min^{-1}, and K_m for NADPH is 0.8 μM; for the cys_{135}, ser_{140} mutant, V_{max} is 28 min^{-1}, and K_m is 0.8 μM; for the ser_{135}, cys_{140} mutant, V_{max} is 10 min^{-1}, and K_m is 3 μM (Figure 4-4). These values were measured on enzymes treated by KBr dialysis to remove enzyme-bound NADP$^+$ as described in Chapter 3. The rates measured for enzymes not treated by KBr dialysis in the presence of 200 μM NADPH are 56 min^{-1}, 6 min^{-1}, and 84 min^{-1} for native, the ser_{135}, cys_{140} mutant, and the cys_{135}, ser_{140} mutant, respectively. For the ala_{135}, cys_{140} mutant, V_{max} is 252 min^{-1} and K_m for NADPH is 4.9 μM. For the cys_{135}, ala_{140} mutant, V_{max} is

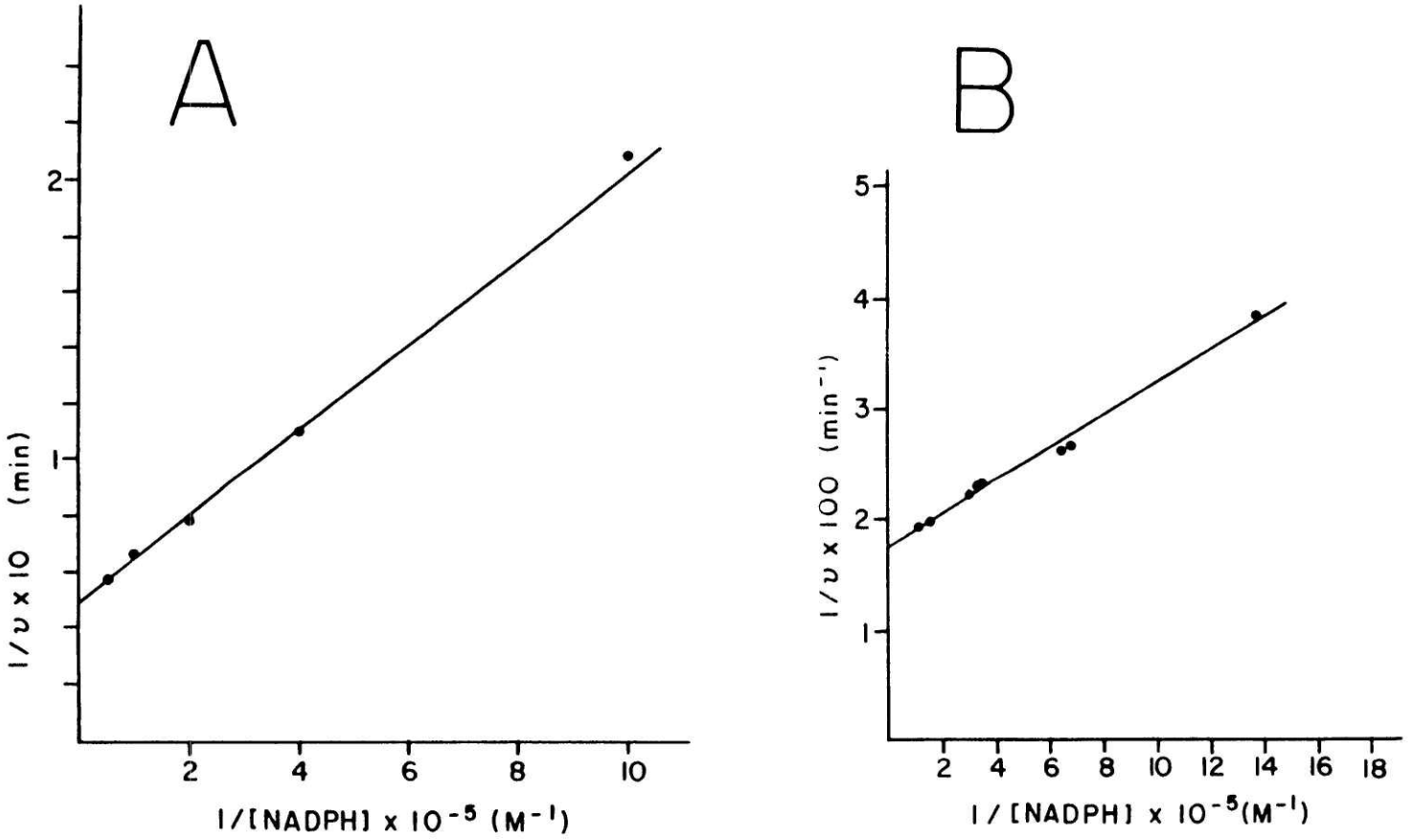

Figure 4-4. Kinetics of thioNADP$^+$-dependent NADPH oxidation by the cys to ser mutant enzymes. A) Ser_{135}, cys_{140} mutant enzyme. B) Cys_{135}, ser_{140} mutant enzyme.

328 min^{-1} and K_m is 4.0 μM (Figure 4-5). The cys to ala mutants used for these measurements were not treated by KBr dialysis. The transhydrogenase activity of the mutants is not too surprising, since the iodoacetamide cys_{135}-alkylated native enzyme has a V_{max} of 220 min^{-1} for transhydrogenation, a value 2.5 to 6-fold that measured for the native enzyme (Fox and Walsh, 1983). The absence of any correlation between transhydrogenase activity in the mutant and alkylated enzymes with Hg(II) reductase activity is consistent with independent nicotinamide and Hg(II) binding domains (Figure 3-13). Since these enzymes have only a two electron capacity and only one nicotinamide binding site, transhydrogenation is likely to result from intermediate reduction and reoxidation of FAD.

O_2 reduction

The native and mutant mercuric reductases all show O_2-dependent NADPH oxidation activity. Native enzyme has a k_{cat} of 2 min^{-1}, ser_{135}, cys_{140} enzyme a k_{cat} of 0.2 min^{-1}, and cys_{135}, ser_{140} enzyme a k_{cat} of 2 min^{-1} in air-saturated buffer at 37° in the presence of 200 μM NADPH. (An earlier value of 8.5 min^{-1} was not reproducible in a new preparation of cys_{135}, ser_{140} enzyme.) Ala_{135}, cys_{140} has a k_{cat} of 3.4 min^{-1}, and cys_{135}, ala_{140} enzyme has a k_{cat} of 7.2 min^{-1}. Production of H_2O_2 was confirmed by the addition of catalase to the assay solutions.

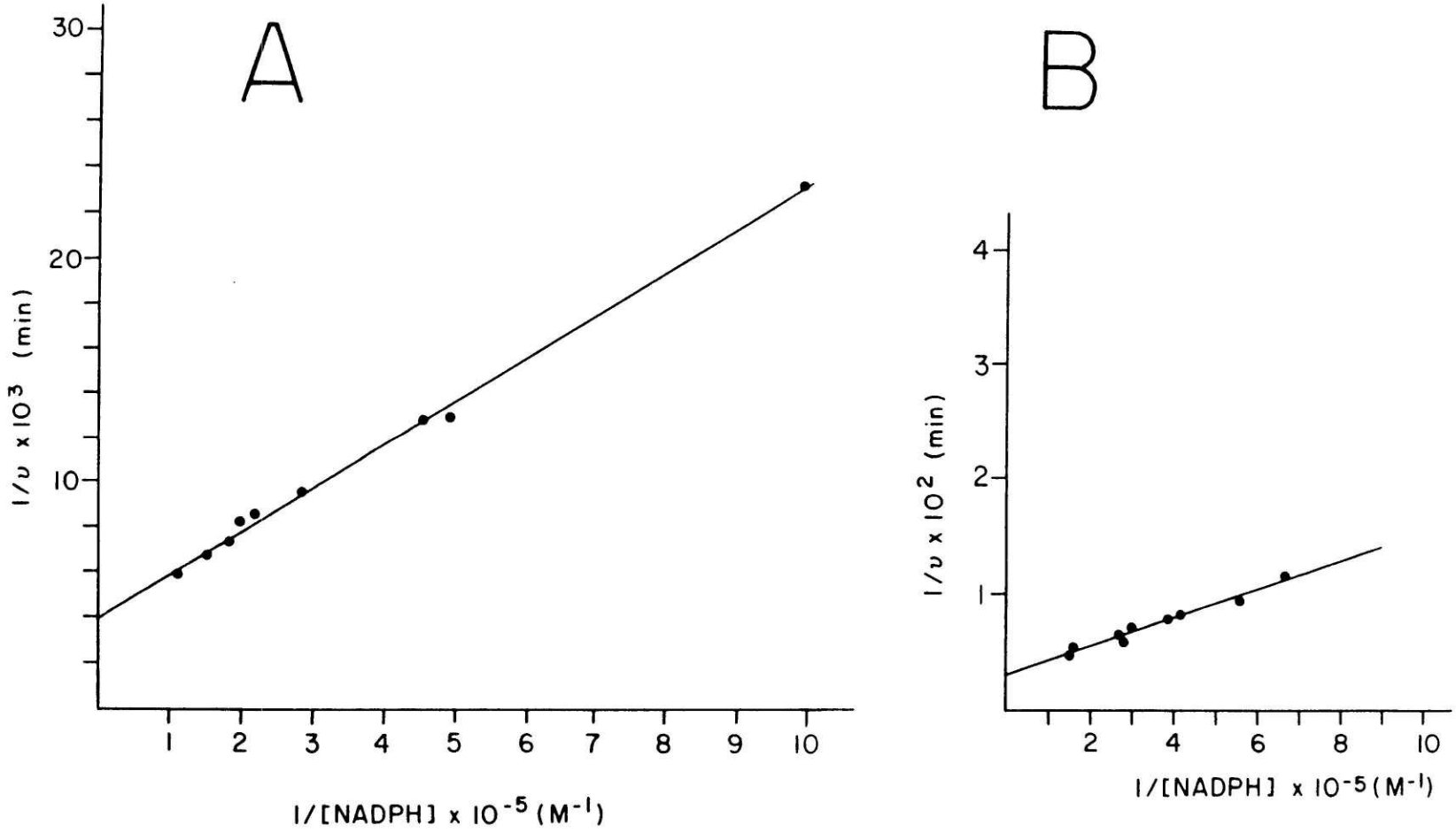

Figure 4-5. Kinetics of thioNADP$^+$-dependent NADPH oxidation by the cys to ala mutant enzymes. A) Ala_{135}, cys_{140} mutant enzyme. B) Cys_{135}, ala_{140} mutant enzyme.

Discussion

The active site cys to ser and cys to ala mutations have converted mercuric reductase into a catalyst with only a two electron redox inventory rather than a four electron redox inventory. This fact coupled with the different loci of the remaining active site cysteine residue is a useful context for analysis of the catalytic properties of the four mutant mercuric reductases.

We have assayed four types of catalytic activities in this work: (a) transhydrogenation from NADPH to thioNADP$^+$, (b) reduction of the aryl disulfide 5,5'-dithiobis-(2-nitrobenzoic acid), (c) reduction of O_2 to H_2O_2, and (d) NADPH oxidation in the presence of mercuric complexes $Hg(SR)_2$, Hg(EDTA), and $Hg(CN)_2$. All of these redox reactions involve the bound FAD, but it is likely that only reactions (b) and (d) require participation of either active site cysteine.

Fox and Walsh (1983) previously found that mercuric reductase, monoalkylated at cysteine 135 and therefore incompetent for Hg(II) reduction still catalyzed hydride transfer between NADPH and thioNADP$^+$. In fact, the V_{max} for this activity was 2.5 to 6-fold the V_{max} of the native enzyme. These results were consistent with the active site geometry found in glutathione reductase in which NADPH and the cystine disulfide lie on opposite faces of the bound FAD (Pai and Schulz, 1983). Thus we anticipated that all four mutants would be competent in the transhydrogenase half reaction. The nicotinamide-flavin half reaction, as assayed by transhydrogenation, does in fact survive both cys to ser and cys to ala mutations, with all mutants except the ser_{135}, cys_{140} mutant having a V_{max} higher than that in native enzyme.

Transhydrogenation in mercuric reductase requires the involvement of an

enzyme species containing $FADH_2$, since mercuric reductase apparently has only one nicotinamide binding site per subunit (Fox, 1983). Stimulation of transhydrogenase activity in EHR and in 5-deazaFAD reconstituted native enzyme was largely explained as the result of the modified enzyme's inability to transfer electrons from the flavin to a redox active disulfide and a therefore greater population of enzyme species containing $FADH_2$ (Fox, 1983). The cys to ser and cys to ala mutants have no redox active disulfide in the active site to influence transhydrogenation rates. In fact, the transhydrogenation rates to some extent correlate with bound flavin redox potential, as presented in Table 4-I. If one considers only the less negative of the two redox potentials for each mutant, the transhydrogenation rate of native enzyme can also fit this correlation, with the assumption that the native EH_2/EH_4 midpoint potential is more relevant than that for the native E/EH_2 couple, since native EH_2 contains very little $FADH_2$. Since some differences in K_m and in levels of enzyme-bound $NADP^+$ are observed among the native, cys to ser mutants, and cys to ala mutants, it would not be unreasonable for these active site mutations to result in some differences in nicotinamide binding that could also contribute to differences in transhydrogenase activities.

Although rapid reduction of O_2 to H_2O_2 is a property of dihydroflavins free in solution, in many flavoproteins reaction of bound dihydroflavin with O_2 is strongly suppressed. This is the case with native mercuric reductase where O_2 reduction at 2 min^{-1} is only about 0.5% the k_{cat} for Hg(II) reduction. As with transhydrogenation (see above), factors influencing O_2 reduction rates include redox potential of the bound flavin, partitioning of electrons between FAD and a redox active disulfide (which we assume is relevant only for native enzyme), and accessibility of reduced flavin to

Table 4-I

Comparison of transhydrogenase and O_2 reductase rates with estimates of bound flavin redox potentials

Mutant enzyme	E°'	Transhydrogenase[b] rate	O_2 reductase rate
ser_{135}, cys_{140}[a]	-393, -428 mV	6 min^{-1}	0.2 min^{-1}
cys_{135}, ser_{140}[a]	-326, -375 mV	84 min^{-1}	2.0 min^{-1} [c]
ala_{135}, cys_{140}	-321, -369 mV	252 min^{-1}	3.4 min^{-1}
cys_{135}, ala_{140}	-307, -351 mV	328 min^{-1}	7.2 min^{-1}
Native enzyme[d]			
cys_{135}, cys_{140}	-335 mV (EH_2/EH_4)	56 min^{-1}	2.0 min^{-1}

[a]Redox potentials for cys to ser mutant enzymes were measured by Massey et al. (unpublished).

[b]Rates measured for enzymes not treated by KBr dialysis.

[c]Our previously reported value of 8.5 min^{-1} (Schultz et al., 1985) was not reproducible.

[d]Fox and Walsh, 1982.

dissolved O_2. Again, some qualitative correlation can be made between O_2 reduction rates and redox potential (Table 4-I). It should be stressed that the redox potentials reported here are preliminary numbers. Nevertheless, it seems reasonably clear that the ser_{135}, cys_{140} mutant has a particularly low redox potential and that this is likely to be a major contributor to the particularly low rates of transhydrogenation and O_2 reduction in this mutant when compared with native and the other mutant enzymes.

The remaining activities, aryldisulfide and mercuric complex reduction focus more specifically on the role of cys_{135} and cys_{140} in mercuric ion reduction by this unique enzyme. Reduction of the chromogenic aryl disulfide 5,5'-dithiobis-(2-nitrobenzoate) at 1 mM concentration occurs in the native enzyme at the rate of 20 min^{-1}. The cys_{135}, ser_{140} mutant, cys135, ala140 mutant, and ala135, cys140 mutant can also reduce DTNB (at 1 mM) catalytically with rates of 3 min^{-1}, 1 min^{-1}, and 2 min^{-1}, respectively. The detection of catalytic DTNB reduction in these mutants suggests that in the absence of a redox active disulfide, $FADH_2$ is directly supplying reducing equivalents to the mixed cys-S-S-aryl disulfide to produce ArS- and oxidized mutant enzyme. The diminished rate of DTNB reduction by these mutants relative to native mercuric reductase may reflect either altered FAD redox properties, altered binding geometries in the active site, or a change in mechanism for DTNB reduction. If the mechanism for DTNB reduction in native mercuric reductase is analogous to that for disulfide reduction by the disulfide oxidoreductases, where the enzyme cycles between E and EH_2 (Williams, 1976), then it is necessary to postulate a change in mechanism for these active site mutants. The ser_{135}, cys_{140} mutant enzyme shows very low activity (0.2-0.3 min^{-1}) toward 1 mM DTNB, which is detectable only after a lag of 1-2 minutes. Nondenaturing thiol titrations indicate that

cys_{140} in the ser_{135}, cys_{140} mutant is inaccessible to DTNB in the absence of NADPH. One may speculate that binding of NADPH is some way leads to accessibility of cys_{140} to DTNB.

A primary objective in the study of mercuric reductase is to elucidate the mechanism by which this enzyme is able to reduce Hg(II) to Hg(0). A central issue is whether the enzyme cycles between E and EH_2 forms during catalysis, as do the disulfide oxidoreductases, or between EH_2 and EH_4 forms. Among other indirect evidence, the inability of NADPH to reduce native enzyme to EH_4 has suggested that EH_4 forms of the enzyme (with reduced flavin and reduced cysteines at positions 135 and 140) are not on the main reaction pathway (Fox, 1983). Through thiol titrations of EH_2 forms of native enzyme, Miller et al. (1986) have recently shown that Hg(II) binds to two thiols of EH_2 in the absence of 2-mercaptoethanol and quenches the charge transfer band, but the Hg(II) is not reduced. This result, together with rapid scanning stopped flow evidence from Sahlman et al. (1984) for facile formation of an EH_2-NADPH complex when mercuric reductase is treated with only two equivalents of NADPH, strongly suggests that mercuric reductase, unlike the disulfide oxidoreductases, requires the presence of a four electron redox inventory for Hg(II) reduction. On the basis of this work, Miller et al. (1986) propose the minimal mechanistic scheme outlined in Figure 4-6.

This discussion brings us to the main mechanistic question: can any of the four mutants, each of which is limited to monodentate thiol ligation and a two electron capacity, reduce mercuric ions? Under standard assay conditions with dimercaptide Hg(II) salts, none of the mutant enzymes show any detectable activity ($< 1\ min^{-1}$). However, in the presence of 200 μM $Hg(CN)_2$, the ser_{135}, cys_{140} mutant catalyzes NADPH oxidation at a rate of 7

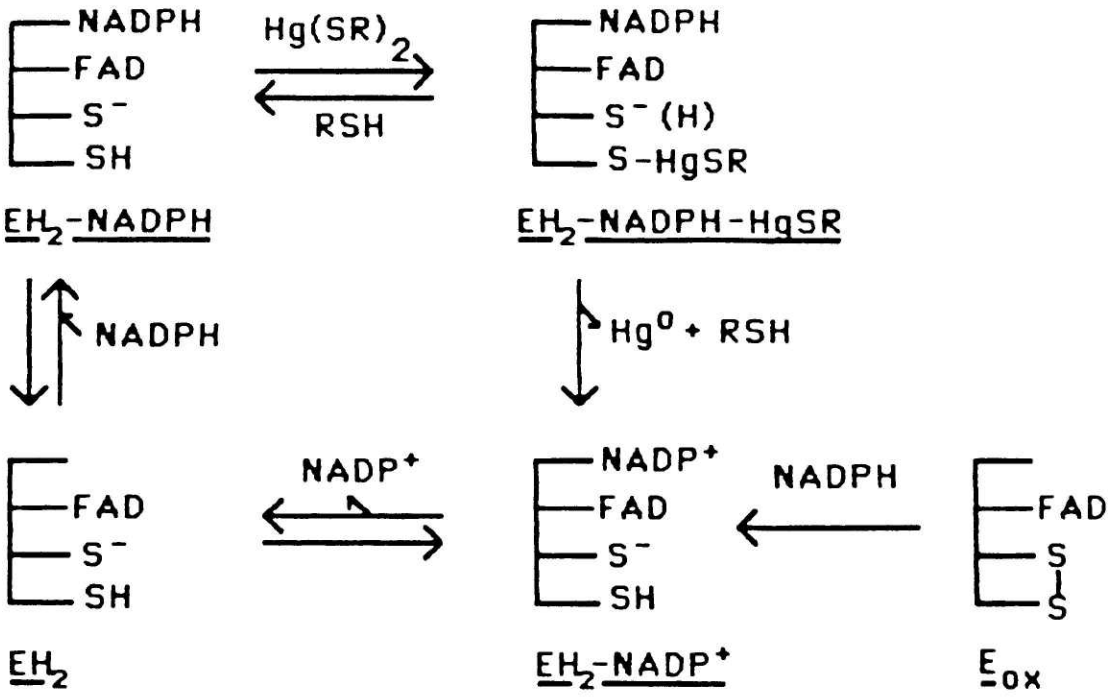

Figure 4-6. Minimal mechanistic scheme proposed for mercuric reductase (from Miller et al., 1986). $Hg(SR)_2$ is shown as binding to EH_2-NADPH for simplicity, but additional pathways for substrate binding are equally likely and are under investigation (Miller et al., 1986).

min^{-1}. This turnover, originally interpreted as NADPH-dependent reduction of $Hg(CN)_2$ to Hg(0) plus $2CN^-$ (Schultz et al., 1985) is most probably due to a mercuric cyanide-dependent increase in the O_2 reductase activity in this mutant as discussed in Results. The apparent correlation between O_2 reductase activity and bound flavin redox potential suggests that when $Hg(CN)_2$ binds to cys_{140} in the ser_{135}, cys_{140} mutant, the bound flavin redox potential may become less negative, since binding of $Hg(CN)_2$ appears to decrease the charge transfer interaction (Figure 4-2). If this is the case, then by analogy, transient binding of Hg(II) to the cys_{140} thiolate of native enzyme, for which there is some spectroscopic evidence (Miller et al., 1986; see above), may raise the bound flavin EH_2/EH_4 redox potential and thereby allow reduction of the enzyme-bound FAD to $FADH_2$ by NADPH, which does not normally occur in the absence of mercuric ion. Reduction of the bound Hg(II) by electron transfer from $FADH_2$ would then follow. As other factors, such as steric accessibility of the reduced flavin, may play a role in $Hg(CN)_2$-dependent NADPH oxidation by the ser_{135}, cys_{140} enzyme, the precise effect of $Hg(CN)_2$ is as yet unclear.

There remains the question of why electrons from $FADH_2$ in this mutant can be transferred to O_2, but apparently not to Hg(II), even in the latter case when O_2 is not present as a potential competitor for electrons. One possibility is that the binding geometry for the Hg(II) to the active site of this mutant is incorrect for catalysis to occur. Another possibility is that the reduction potential of the mercuric complex formed in the active site may be unfavorable. Rinderle et al. (1983) propose that turnover of Hg(EDTA) by native enzyme followed by inactivation suggests that free Hg(II) ion inhibits the native enzyme by binding incorrectly at the active site or elsewhere. One could envision, for example, that bidentate complexation of

Hg(II) to both cys_{135} and cys_{140} in the active site may lead to inactivation, whereas monodentate complexation, presumably to the more accessible cys_{135}, may result in turnover (see hypothetical scheme outlined in Figure 4-7). Alternatively, complexes in which Hg(II) is bound to one or both cysteines in the C-terminal region may be involved, as the C-terminal region has been proposed to function in substrate binding (Brown et al., 1983). The bidentate complexation of EH_2 by Hg(II) observed by Miller et al. (1986) clearly involves cys_{140}. An interesting question which Miller has raised (unpublished) is whether a bidentate complex might be formed between cys_{140} and a cysteine on the C-terminal arm. Fox (1983) has noted that computer modeling indicates that the C-terminal arm of one subunit may be able to reach the active site of the other subunit. It would be interesting to see, then, if either the ser_{135}, cys_{140} or ala_{135}, cys_{140} mutant enzyme forms bidentate thiol-Hg(II) complexes, since cys135 would be absent. Clearly, further studies are needed to establish the nature of Hg(II) binding in reduction and in inactivation.

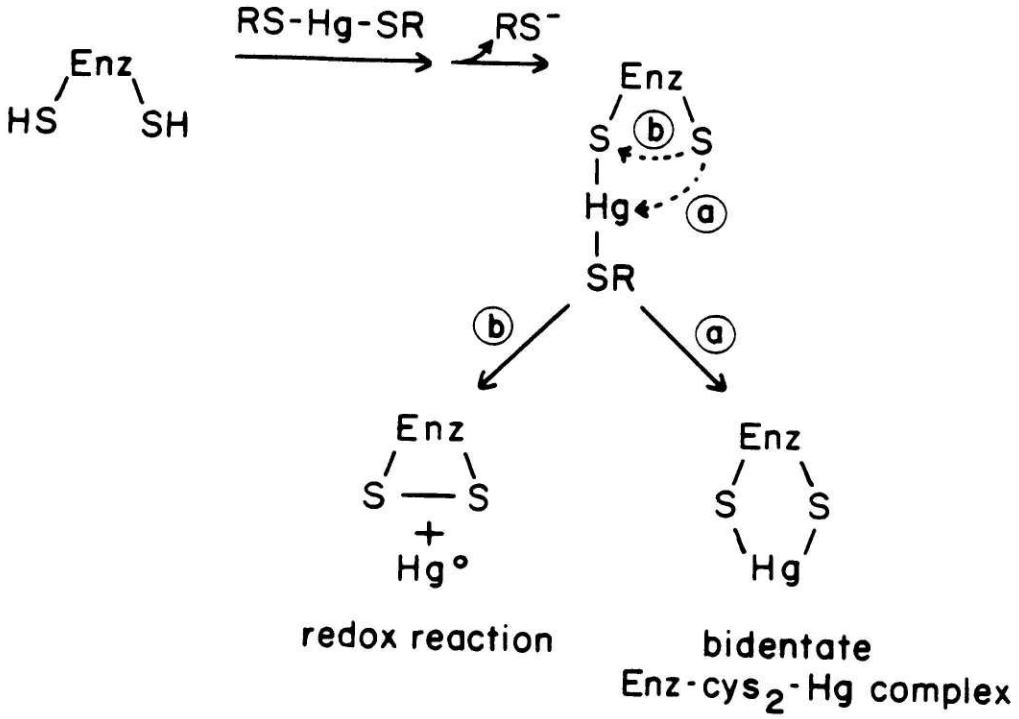

Figure 4-7. Possible mode of binding of Hg(II) in the active site of mercuric reductase during reduction and inactivation.

Conclusion

This thesis has described the construction, overproduction, physical properties, and catalytic properties of four mercuric reductase active site mutant enzymes in which cys_{135} and cys_{140} have each been altered independently to serine or alanine. In contrast to the native enzyme, the resulting mutants have only a two electron redox capacity, rather than the four electron capacity of native enzyme, and have the potential for only monodentate thiol complexation in the active site by Hg(II).

Studies of the physical and catalytic properties of these mutants have revealed distinct differences among the native and four mutant enzymes, which are discussed in Chapters 3 and 4. The UV-visible and fluorescence spectra, cys_{140} pK_a values, bound flavin redox potentials, and catalytic behavior toward O_2, thioNADP$^+$, Hg(II) complexes, and DTNB are all influenced by the nature of the residues both at position 135 and 140. Since none of the mutant enzymes reduces Hg(II), the issue of monodentate versus bidentate complexation of Hg(II) for catalysis remains unresolved. In contrast, catalytic DTNB reduction by the mutant enzymes suggests that disulfide reduction can occur by direct electron transfer from $FADH_2$ and that monodentate thiol complexation is sufficient for this activity. O_2 and thioNADP$^+$ reduction rates show some correlation with estimates of bound flavin redox potentials, as discussed in Chapter 4.

In the future, determination of the Xray crystal structure of mercuric reductase and comparison to the structure of glutathione reductase should be useful in identifying structural differences which allow mercuric reductase, but not glutathione reductase, to reduce Hg(II). Further studies of the native and active site mutant enzymes and construction of cys to ala

mutations in the C-terminal region of mercuric reductase may be useful in addressing the issue of cooperativity in mercuric reductase. Stopped flow kinetic experiments are in progress to determine the relevance of various proposed intermediate species in catalysis (Miller et al., unpublished). In addition, study of the properties of some new active site mutant enzymes may provide some new information on structure-function relationships in the active site of mercuric reductase and related enzymes.

References

Amersham (1983) M13 Cloning and Sequencing Handbook.

Arscott, L. D., Thorpe, C. & Williams, C. H. (1981) Biochemistry 20, 1513.

Begley, T. P., Walts, A. E. & Walsh, C. T. (1986a) manuscript in preparation.

Begley, T. P., Walts, A. E. & Walsh, C. T. (1986b) manuscript in preparation.

Bennett, P. M., Grinsted, J., Choi, C. L. & Richmond, M. H. (1978) Molec. Gen. Genet. 159, 101.

Brown, N. L. (1985) Trends in Biochemical Sciences 10, 400.

Brown, N. L., Ford, S. J., Pridmore, R. D. & Fritzinger, D. C. (1983) Biochemistry 22, 4089.

Brown, N. L. & Goddette, D. (1984) in Flavins and Flavoproteins (Bray, R. C., Engel, P. C., & Mayhew, S. G., Eds.) p. 165, deGruyter, New York.

Brown, N. L., Misra, T. K., Winnie, J. N., Schmidt, A., Lien, C., Seiff, M. & Silver, S. (1986) manuscript in preparation.

Carlberg, I., Altmejd, B. & Mannervik, B. (1981) Biochim. Biophys. Acta 677, 146.

Casas, J. S. & Jones, M. M. (1980) J. Inorg. Nucl. Chem. 42, 99.

Casola, L. & Massey, V. (1966) J. Biol. Chem. 241, 4985.

Clonis, Y. D. & Lowe, C. R. (1980) Biochem. J. 191, 247.

Cooper, T. G. (1977) The Tools of Biochemistry, p. 228, Wiley, New York.

Cotton, F. A. & Wilkinson, G. (1980) Advanced Inorganic Chemistry, p. 595, Wiley, New York.

Cox, E. C. (1976) Annu. Rev. Genet. 10, 135.

de Boer, H. A., Comstock, L. J. & Vasser, M. (1983) Proc. Natl. Acad. Sci. USA 80, 21.

de Boer, H. A., Comstock, L. J., Yansura, D. G. & Heynecker, H. L. (1982) in Promoters, Structure and Function (Rodriguez, R. L. & Chamberlin, M. J., Eds.) pp 462-481, Praeger, New York.

Dohet, C. Wagner, R. & Radman, M. (1985) Proc. Natl. Acad. Sci. USA 82, 503.

Dutton, P. L. (1978) Methods Enzymol. 54, 411.

Farrar, W. V. & Williams, A. R. (1977) in The Chemistry of Mercury (McAuliffe, C., Ed.) p. 37, Macmillan, Toronto.

Foster, T. J. (1983) Microbiol. Rev. 47, 361.

Foster, T. J. & Brown, N. L. (1985) J. Bacteriol. 163, 1153.

Fox, B. S. (1983) Ph.D. Thesis, Massachusetts Institute of Technology.

Fox, B. S. & Walsh, C. T. (1982) J. Biol. Chem. 257, 2498.

Fox, B. S. & Walsh, C. T. (1983) Biochemistry 22, 4082.

Furukawa, K. & Tonomura, K. (1971) Agric. Biol. Chem. 35, 604.

Hibner, U. & Alberts, B. M. (1980) Nature 285, 300.

Inouye, S. & Inouye, M. (1985) in DNA and RNA Synthesis (Narang, S., Ed.), Academic Press, New York (in press).

Itakura, K., Rossi, J. J. & Wallace, R. B. (1984) Annu. Rev. Biochem., 323.

Izaki, K. (1981) Can. J. Microbiol. 27, 192.

Izaki, K., Tashiro, Y. & Funaba, T. (1974) J. Biochem. (Tokyo) 75, 591.

Jackson, W. J. & Summers, A. O. (1982) J. Bacteriol. 151, 962.

Kramer, B., Kramer, W. & Fritz, H.-J. (1984) Cell (Cambridge, Mass.) 38, 879.

Kramer, W., Schughart, K. & H.-J. Fritz (1982) Nucl. Acids Res. 10, 6475.

Krauth-Siegel, R. L., Blatterspiel, R., Saleh, M., Schiltz, E., Schirmer, R. H. & Untucht-Grau, R. (1982) Eur. J. Biochem. 121, 259.

Kunkel, T. A. (1985) Proc. Natl. Acad. Sci. USA 82, 488.

Laemmli, U. K. (1970) Nature 227, 680.

Light, D. R. & Walsh, C. (1980) J. Biol. Chem., 255, 4264.

Lo, K.-M., Jones, S. S., Hackett, N. R. & Khorana, H. G. (1984) Proc. Natl. Acad. Sci. USA 81, 2285.

Lowry, O. H., Rosebrough, N. J., Farr, A. L. & Randall, R. J. (1951) J. Biol. Chem. 193, 265.

Lu, A.-L., Clark, S. & Modrich, P. (1983) Proc. Natl. Acad. Sci. USA 80, 4639.

Maniatis, T., Fritsch, E. F. & Sambrook, J. (1982) Molecular Cloning; a Laboratory Manual, Cold Spring Harbor Laboratory, Cold Spring Harbor, New York.

Marshall, J. L., Booth, J. E. & Williams, J. W. (1984) J. Biol. Chem. 259, 3033.

Massey, V. & Ganther, H. (1965) Biochemistry 4, 1161.

Massey, V. & Williams, C. H. (1965) J. Biol. Chem. 240, 4470.

Matthews, R. G. & Williams, C. H. (1976) J. Biol. Chem. 251, 3956.

Maxam, A. & Gilbert, W. (1979) Methods Enzymol. 65, 499.

McGary, J. D., Donkin, P. & King, H. K. (1968) Arch. Biochem. Biophys. 126, 973.

Merck (1976) Merck Index, 9th ed., (Windholz, M., Ed.) Merck, Rahway, New Jersey.

Messing, J. (1983) Methods Enzymol. 101, 20.

Miller, J. H. (1972) Experiments in Molecular Genetics, Cold Spring Harbor Laboratory, Cold Spring Harbor, New York.

Miller, S. M., Ballou, D. P., Massey, V., Williams, C. H., Jr. & Walsh, C. T. (1986) manuscript in preparation.

Misra, T. K., Brown, N. L., Haberstroh, L., Schmidt, A., Goddette, D. & Silver, S. (1985) Gene 34, 253.

Mills, D. R. & Kramer, F. R. (1979) Proc. Natl. Acad. Sci. USA 76, 2232.

New England Biolabs (1983) M13 Cloning and DNA Sequencing System Manual.

Norris, K., Norris, F., Christianson, L. & Fiil, N. (1983) Nucl. Acids Res. 11, 5103.

Ogawa, H. I., Tolle, C. L. & Summers, A. O. (1984) Gene 32, 311.

O'Halloran, T. V. & Walsh, C. T. (1986) manuscript in preparation.

Pai, E. F. & Schulz, G. E. (1983) J. Biol. Chem. 258, 1752.

Pan-Hou, H. S. K., Hosono, M. & Imura, N. (1980) Appl. Env. Microbiol. 40, 1007.

Pan-Hou, H. S. K. & Imura, N. (1981) Arch. Microbiol. 129, 49.

Pan-Hou, H. S. K., Nishimoto, M. & Imura, N. (1981) Arch. Microbiol. 130, 93.

Pharmacia (1984) Molecular Biologicals Catalog, p. 148.

Pukkila, P. J., Peterson, J., Herman, G., Modrich, P. & Meselson, M. (1983) Genetics 104, 571.

Rice, D. W., Schulz, G. E. & Guest, J. R. (1984) J. Mol. Biol. 174, 483.

Rinderle, S. J., Booth, J. E. & Williams, J. W. (1983) Biochemistry 22, 869.

Robinson, J. B. & Tuovinen, O. H. (1984) Microbiol. Rev. 48, 95.

Sahlman, L., Lambeir, A.-M., Lindskog, S. & Dunford, H. B. (1984) J. Biol. Chem. 259, 12403.

Sanger, F., Coulson, A. R., Barrell, B. G., Smith, A. J. H. & Roe, B. A. (1981) J. Mol. Biol. 143, 161.

Schottel, J. S. (1978) J. Biol. Chem. 253, 4341.

Schultz, P. G., Au, K. G. & Walsh, C. T. (1985) Biochemistry 24, 6840.

Schulz, G. E., Schirmer, R. H. & Pai, E. F. (1982) J. Mol. Biol. 160, 287.

Sillen, L. G. & Martell, A. E. (1964) Spec. Publ. Chem. Soc. 17, 637.

Stanisch, V. A., Bennett, P. M. & Richmond, M. H. (1977) J. Bacteriol. 129, 1227.

Stephens, P. E., Lewis, H. M., Darlison, M. G. & Guest, J. R. (1983) Eur. J. Biochem. 135, 519.

Summers, A. O. & Silver, S. (1978) Ann. Rev. Microbiol. 32, 637.

Tabor, S. & Richardson, C. C. (1985) Proc. Natl. Acad. Sci. USA 82, 1075.

Tan, Z. K., Ikuta, S., Huang, T., Dugaiczyk, A. & Itakura, K. (1983) Cold Spring Harbor Symp. Quant. Biol. 47, 383.

Thieme, R., Pai, E. F., Schirmer, R. H. & Schulz, G. E. (1981) J. Mol. Biol. 152, 763.

Thorpe, C. & Williams, C. H. (1981) Biochemistry 20, 1507.

Untucht-Grau, R., Schulz, G. E. & Schirmer, R. H. (1979) Febs. Lett. 105, 244.

Walsh, C., Fisher, J., Spencer, R., Graham, D. W., Ashton, W. T., Brown, J. E., Brown, R. D. & Rogers, E. F. (1978) Biochemistry 17, 1942.

Wasserman, S. A. (1983) Ph.D. Thesis, Massachusetts Institute of Technology.

Watanabe, T. (1966) N. Engl. J. Med. 275, 888.

Williams, C. H. (1976) in The Enzymes (Boyer, P. D., Ed.), 3rd ed., Vol. 13, pp 89-173.

Williams, C. H., Jr., Arscott, D. L., Matthews, R. G., Thorpe, C. & Wilkinson, K. D. (1979) Methods Enzymol. 62D, 185.

Williams, C. H., Arscott, L. D. & Schulz, G. E. (1982) Proc. Natl. Acad. Sci. U.S.A. 79, 2199.

Williams, J. W. & Silver, S. (1984) Enzyme Microb. Technol. 6, 530.

Wilson, G. S. (1978) Methods Enzymol. 54, 396.

Zoller, M. J. & Smith, M. (1983) Methods Enzymol. 100, 468.

APPENDIX

STEREOCHEMICAL STUDIES OF A FLUOROACETATE HALIDOHYDROLASE

Introduction

Fluoroacetate, a naturally occurring compound with a rare carbon-fluorine linkage, is toxic because of metabolic processing to 2-fluorocitrate (1), specifically the (-)-erythro stereoisomer having the 2R, 3R configuration (2, 3, 4), whose target has long been held to be aconitase (but see ref. 5). Microorganisms resistant to fluoroacetate have been detected. Some yeasts overproduce aconitase (6), the proposed target enzyme for fluorocitrate toxicity, while various bacteria induce haloacid halidohydrolases (dehalogenases), which detoxify 2-haloacids by conversion to 2-hydroxyacids. Goldman et al. (7) have previously noted that an impure enzyme from a pseudomonad will convert L-2-chloropropionate (2S) to D-lactate with net inversion of configuration. Very recently Motosugi et al. (8) purified a haloacid dehalogenase from a pseudomonad grown on DL-2-chloropropionate and found that the pure enzyme will convert both D- and L-2-chloropropionate to the corresponding L- and D-lactates respectively. This enzyme will also work on chloroacetate, bromoacetate, and iodoacetate, but it shows no activity toward fluoroacetate or other 2-fluoroacids, perhaps because of the low reactivity of C-F bonds to S_N2 displacements (9, 10). On the other hand, Kawasaki and colleagues (11, 12) have found pseudomonads with constitutive resistance to fluoroacetate by virtue of harboring a plasmid encoding a fluoroacetate-specific halidohydrolase, H-1, which they have purified and crystallized, making it the enzyme of choice to analyze how enzymic cleavage of the strong C-F bond by the weak nucleophile H_2O (or hydroxide ion, enzyme's pH optimum = 9) is effected in fluoroacetate detoxification. (See Scheme 1.)

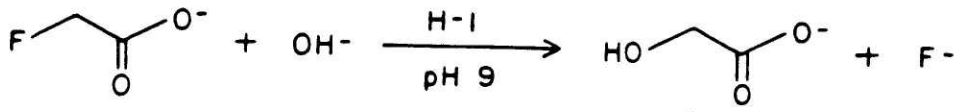

Scheme 1. Reaction catalyzed by haloacetate halidohydrolase H-1.

Kawasaki et al. have shown that the H-1 halidohydrolase is inactivated by sulfhydryl-blocking reagents, raising the possibility that an active site cysteine could be involved in covalent catalysis, e.g. by way of an S-carboxymethyl enzyme intermediate, as proposed initially by Goldman (13). This possibility was also raised by the very recent observation by Weightman et al. (14) that certain bacteria contain two halidohydrolase activities separable at a crude extract stage by gel electrophoresis. One activity converts chiral chloropropionate to lactate with inversion, the other with retention of configuration at carbon two; this latter one shows a markedly higher sensitivity to sulfhydryl-blocking reagents.

We have now investigated the stereochemical course of action of purified haloacetate halidohydrolase from Pseudomonas sp., strain A, with (R)- and (S)-2-fluoropropionate and the (S)-enantiomer of monodeuterated fluoroacetate to analyze stereochemical outcome on a 2-fluoroacid substrate for the first time.

Experimental Procedures

Abbreviation: (-)-MTPA = (S)-(-)-α-methoxy-α-(trifluoromethyl)phenylacetic acid

Methods

Haloacetate halidohydrolase activity was assayed with an Orion fluoride ion electrode by monitoring fluoride ion production from incubations carried out according to the procedure of Kawasaki et al. (11). Standards containing known amounts of fluoride ion in a background solution made up of the components of the quenched incubation mixtures (except enzyme) were used to prepare calibration curves for the fluoride electrode. D-Lactate was measured by the procedure of Gawehn and Bergmeyer (15). L-Lactate was measured by the procedure of Gutmann and Wahlefeld (16). ^{1}H-NMR spectra were recorded with a JEOL FX-90Q, Bruker WM250 or Bruker WM270 spectrometer. Chemical shifts are reported in ppm on the δ scale relative to internal standards (tetramethylsilane or sodium 2,2-dimethyl-2-silapentane-5-sulfonate). Abbreviations used to present NMR data are the following: s = singlet; d = doublet; t = triplet; q = quartet; m = multiplet; dd = doublet of doublets; dt = doublet of triplets; dq = doublet of quartets; J = coupling constant. The relaxation delay was set to 4.0 s for deuterated compounds. ^{19}F-NMR spectra were recorded with a JEOL FX-90Q spectrometer. UV measurements were made with a Perkin-Elmer 554 or Lambda 5 spectrophotometer.

Materials

Haloacetate halidohydrolase H-1 was purified from Pseudomonas sp., strain A (kindly provided by Dr. H. Kawasaki, College of Agriculture,

Univ. of Osaka) by the procedure of Kawasaki et al. (11) with the following modifications: a) a DE52 column (2.5 x 34 cm), which was run twice, was substituted for the DEAE cellulose column, using the same elution buffer as in reference 11; b) after purification on hydroxyapatite, the enzyme was concentrated by ultrafiltration (Amicon PM 10 membrane), frozen in liquid nitrogen, and stored at -70°C. The specific activity of the enzyme was 32.2 μmol $min^{-1}mg^{-1}$ at 30°C (lit. value = 38.4 U/mg for crystalline enzyme (11)).

L-Lactic dehydrogenase from rabbit muscle was purchased from Boehringer Mannheim. Hydroxyapatite (HTP) and AG50W-X8 (50-100 mesh) were from BioRad. DE52 was from Whatman. D-Lactic dehydrogenase from Lactobacillus leichmanii, L-alanine aminotransferase (glutamic pyruvic transaminase) from porcine heart, L-alanine, D-alanine, glycine-d_5, NAD, NADH, and glycolic acid were purchased from Sigma. (S)-[2-$^2H_1$]-Glycolic acid was prepared by the method of Massey et al. (17) by reduction of dimethyloxalate with Mg in D_2O to deuterated glyoxylic acid, followed by reduction of the glyoxylate with L-LDH and NADH. Hydrogen fluoride-pyridine, (-)-MTPA, and (R)-(-)-mandelic acid were from Aldrich. Analytical and preparative TLC were performed on E. Merck precoated silica gel 60F-254 plates. Flash column chromatography was carried out on E. Merck silica gel 60 (230-400 mesh ASTM). All other chemicals were of reagent grade and were used without further purification, unless otherwise noted.

Substrates

The (R)- and (S)-isomers of 2-fluoropropionic acid were prepared from D- and L-alanine respectively by the procedure of Olah et al. (18)

for the synthesis of 2-fluorobutanoic acid, except that D- or L-alanine was substituted for 2-aminobutanoic acid. The products were purified by distillation under reduced pressure. 250 MHz ^{1}H-NMR ($CDCl_3$) δ 9.9 (1 H, broad), 5.08 (1 H, dq, J_{HH} = 6.9 Hz, J_{HF} = 48 Hz), 1.64 (3 H, dd, J_{HH} = 6.9 Hz, J_{HF} = 24 Hz). The ^{19}F-NMR (D_2O) showed a doublet of quartets (J = 24 Hz, 48 Hz).

(S)-2-Chloropropionic acid was prepared from L-alanine by the method of Fu et al. (19). 250 MHz ^{1}H-NMR ($CDCl_3$) δ 10.1 (1 H, broad), 4.46 (1 H, q, J = 6.9 Hz), 1.74 (3 H, d, J = 6.8 Hz).

The concentration of the 2-halopropionic acids in aqueous solution was determined by titration with a standard solution of NaOH.

(S)-[2-$^{2}H_1$]-Fluoroacetic acid was prepared from (S)-[2-$^{2}H_1$]-glycine by the procedure of Keck (20), which was essentially analogous to the method used to prepare fluoropropionic acid, except that continuous extraction was used to extract the product from the quenched reaction mixture. 90 MHz ^{1}H-NMR ($NaOD/D_2O$) δ 4.7 (1 H, dt, J_{HD} = 2 Hz, J_{HF} = 46 Hz). The ^{19}F-NMR (D_2O) showed a doublet of triplets (J_{HF} = 46 Hz, J_{DF} = 7.3 Hz) plus a smaller signal due to dideuterated fluoroacetate (m, J_{DF} = 7.3 Hz) and a tiny signal due to nondeuterated fluoroacetate (t, J_{HF} = 48 Hz). (S)-[2-$^{2}H_1$]-Glycine was prepared from glycine-d_5 by the following procedure, based on that of Keck (20). Glycine-d_5 (1.05 g) was placed in a flask with 0.106 g of pyridoxal-5'-phosphate, and 200 ml of 10 mM KPi buffer, pH 6.5. The pellet from centrifugation of 1000 U (10 mg) of L-alanine aminotransferase was resuspended in 10 ml of the buffer and added to the reaction mixture at 37^{o}C. After incubation for 48 hours, the reaction was quenched with trichloroacetic acid and then neutralized with KOH. The resulting solution was applied to an AG50W-X8

(H^+ form) 50-100 mesh column (2.5 x 35 cm), washed with 2 l of deionized distilled water, and then eluted with 700 ml of 2 N NH_4OH. The NH_4OH eluate was concentrated to dryness under reduced pressure, and the residue was recrystallized in ethanol/water to give 0.78 g of product. ^{1}H-NMR (D_2O) analysis of the methyl ester of the product prepared by the method of Rachele (21) showed that 25-30% of the glycine was still dideuterated at C-2.

Derivatives of Substrates and Incubation Products

The esters of 2-haloacids with methyl (R)-mandelate and the esters of (-)-MTPA with deuterated and nondeuterated phenacyl glycolate were prepared by the procedure of Neises and Steglich at 0°C (22), with the amounts of reagents scaled down appropriately for the amount of haloacid or alcohol to be esterified. Typically 0.1 to 1.0 mmol of the limiting acid or alcohol was used. The products were purified by flash column chromatography on silica gel with ethyl acetate/hexane (typically 25-35% ethyl acetate) as the solvent. Diastereomeric products eluted together in this solvent system. (R)-2-fluoropropionic acid esterified with methyl (R)-mandelate, 250 MHz ^{1}H-NMR ($CDCl_3$) δ 7.48-7.39 (5 H, aromatic), 6.02 (1 H, s), 5.14 (1 H, dq, J_{HH} = 6.9 Hz, J_{HF} = 48 Hz; this signal was partially overlapped by a small dq downfield), 3.74 (3 H, s), 1.71 (2.4 H, dd, J_{HH} = 6.9 Hz, J_{HF} = 24 Hz), 1.63 (0.6 H, dd, J_{HH} = 6.8 Hz, J_{HF} = 24 Hz). (S)-2-fluoropropionic acid esterified with methyl (R)-mandelate, 250 MHz ^{1}H-NMR ($CDCl_3$) δ 7.49-7.38 (5 H, aromatic), 6.03 (1 H, s), 5.18 (1 H, dq, J_{HH} = 6.9 Hz, J_{HF} = 48 Hz; this signal was partially overlapped by a small dq upfield), 3.74 (3 H, s), 1.71 (0.48 H, dd, J_{HH} = 6.8 Hz, J_{HF} = 24 Hz), 1.63 (2.52 H, dd, J_{HH} = 6.9 Hz, J_{HF} =

23 Hz). (R)-2-chloropropionic acid esterified with methyl (R)-mandelate, 250 MHz ^{1}H-NMR ($CDCl_3$) δ 7.49-7.39 (5 H, aromatic), 5.98 (1 H, s), 4.56 (1 H, q, J = 7.0 Hz), 3.74 (3 H, s), 1.79 (3 H, d, J = 7.0 Hz). (S)-2-chloropropionic acid esterified with methyl (R)-mandelate, 250 MHz ^{1}H-NMR ($CDCl_3$) δ 7.50-7.39 (5 H, aromatic), 5.98 (1 H, s), 4.54 (1 H, q, J = 7.2 Hz), 3.74 (3 H, s), 1.78 (0.2 H, d, J = 7.2 Hz), 1.75 (2.8 H, J = 7.2 Hz). Fluoroacetic acid esterified with methyl (R)-mandelate, 270 MHz ^{1}H-NMR ($CDCl_3$) δ 7.48-7.39 (5 H, aromatic), 6.07 (1 H, s), 5.04 (1 H, dd, J_{HH} = 15.3 Hz, J_{HF} = 47 Hz), 4.95 (1 H, dd, J_{HH} = 15.3 Hz, J_{HF} = 47 Hz), 3.74 (3 H, s). (S)-[2-$^2H_1$]-fluoroacetic acid esterified with methyl (R)-mandelate, 250 MHz ^{1}H-NMR ($CDCl_3$) δ 7.45-7.39 (5 H, aromatic), 6.07 (1 H, s), 5.02 (0.7 H, dt, triplet unresolved, J_{HF} = 47 Hz), 4.96 (0.08 H, dt, triplet unresolved, J_{HF} = 47 Hz; some small unresolved peaks, presumably due to non-deuterated compound are also present), 3.75 (3 H, s). (-)-MTPA esterified with phenacyl glycolate, 250 MHz ^{1}H-NMR ($CDCl_3$) δ 7.93-7.41 (10 H, aromatic), 5.51 (1 H, d, J = 16.3 Hz), 5.43 (1 H, d, J = 16.3 Hz), 5.10 (1 H, d, J = 15.8 Hz), 4.94 (1 H, d, J = 15.7 Hz), 3.65 (3 H, broad singlet). (-)-MTPA esterified with phenacyl (S)-[2-$^2H_1$]-glycolate, 250 MHz ^{1}H-NMR ($CDCl_3$) δ 7.91-7.39 (10 H, aromatic), 5.50 (1 H, d, J = 16.2 Hz), 5.42 (1 H, d, J = 16.2 Hz), 5.07 (1 H, unresolved triplet), 3.64 (3 H, broad singlet). (-)-MTPA esterified with phenacyl [2-$^2H_1$]-glycolate derived from H-1 incubation with (S)-[2-$^2H_1$]-fluoroacetate, 250 MHz ^{1}H-NMR ($CDCl_3$) δ 7.92-7.40 (10 H, aromatic), 5.50 (1 H, d, J = 16.3 Hz), 5.43 (1 H, d, J = 16.4 Hz), 5.08 (0.09 H, unresolved triplet), 4.93 (0.63 H, unresolved triplet), 3.65 (3 H, broad singlet); three small peaks due to the nondeuterated species were observed at

5.13, 5.07, and 4.97 ppm (a fourth peak was obscured by the signal due to the monodeutero species).

The methyl ester of (R)-(-)-mandelic acid was prepared according to the procedure of Rachele (21). The product, recrystallized from petroleum ether and derivatized with (-)-MTPA by the procedure of reference 22, was shown to be enantiomerically pure by comparison of its ^{1}H-NMR spectrum ($CDCl_3$) with that of the ester of (-)-MTPA with racemic methyl mandelate.

Phenacyl esters of glycolate and fluoroacetate were prepared by the method of Clark and Miller (23), using commercially available α-bromoacetophenone, which was recrystallized from petroleum ether before use.

Results and Discussion

Stereochemical Studies with (R)- and (S)-2-Fluoropropionate

The procedure of Olah et al. (18), employing HF/pyridine and sodium nitrite, was used to convert D-alanine (2R) and L-alanine (2S) to (R)-2-fluoropropionate and (S)-2-fluoropropionate respectively. Keck and Retey (24) have reported that this reagent mix produces retention of configuration for several amino acids, although Lowe and Potter (25), in its use in the preparation of 2-fluorosuccinates, present evidence that partial racemization may occur.

In the incubation of the synthesized (S)-2-fluoropropionate sample with halidohydrolase H-1, the initial rate of fluoride ion production, assayed by fluoride ion electrode, was found to be about 9% of the V_{max} observed for fluoroacetate conversion. When the (R)-2-fluoropropionate sample was tested as a substrate, an even lower rate of fluoride ion production (about 5% of the V_{max} with fluoroacetate) was measured. We suspected that this fluoride ion formation might derive from enzymatic processing of contaminating (S)-2-fluoropropionate in the (R)-2-fluoropropionate sample generated in a stereoselective but not stereospecific synthetic route. We therefore assayed the chiral purity of the (R)- and (S)-2-fluoropropionate samples by NMR analysis of their esters with methyl (R)-(-)-mandelate. The diastereomeric composition of these derivatives as determined by 250 MHz ^{1}H-NMR suggested that the "(R)" sample contained about 20% (S)-isomer and the "(S)" sample contained about 16% (R)-isomer. Apparently the Olah procedure in the present case yielded a mixture (about 4:1 in favor of retention) of 2-fluoropropionates from D- and L-alanine.

In order to define further the stereochemical course of this

enzymatic reaction, large scale incubations of the "(R)"- and "(S)"-2-fluoropropionate samples (10 μmol each) were conducted for 30 minutes with 0.35 mg enzyme each (S.A.= 32.2 U/mg) in duplicate samples and blanks, and the amounts of D-lactate, L-lactate, and fluoride ion product were analyzed. From the "(R)"-2-fluoropropionate, 1.8 ± 0.1 μmol of D-lactate was produced, a nominal 18% conversion, while 6.9 ± 0.2 μmol of D-lactate was produced from the "(S)"-2-fluoropropionate, a 69% conversion. No significant L-lactate was detected in either sample. Similar results were obtained by fluoride ion electrode assay, since the "(R)" sample yielded 1.7 ± 0.0 μmol F^- ion, while the "(S)" sample yielded 6.6 ± 0.2 μmol F^- ion. As reported previously by Goldman (7), partially purified haloacid degrading enzyme used only the (S)-isomer of 2-chloropropionate. Incubation of (S)-2-chloropropionate (9.3 μmol) with purified enzyme (0.86 mg) for one hour did lead to conversion of 84% of the substrate (7.8 μmol) to D-lactate with no significant production of L-lactate. The enantiomeric purity of the (S)-2-chloropropionate was estimated to be at least 93% by 250 MHz ^{1}H-NMR analysis of its ester with methyl (R)-(-)-mandelate. These results indicate that the H-1 halidohydrolase processes (S)-2-fluoropropionate with inversion, and that any D-lactate produced from the "(R)"-enantiomer is explicable by the approximately 20% contamination of (S)-enantiomer present.

Chiral Fluoroacetate Processing

Because the H-1 halidohydrolase apparently recognizes only one enantiomer of 2-fluoropropionate, and even then at about 1/10 the V_{max} rate with fluoroacetate, we decided to examine the stereochemistry of processing of the preferred substrate fluoroacetate, which would be free

of these constraints. For this purpose we needed a chiral fluoroacetate sample and an assay for the chirality of the enzymic product glycolate. Keck et al. (26) have reported the preparation of chiral monodeutero-fluoroacetates by the Olah procedure. Enzymic conversion should yield chiral monodeuteroglycolate.

(S)-[2-$^{2}H_{1}$]-Glycine was prepared by enzymic exchange at the $^{2}H_{R}$ position of glycine-d_5 in H_2O with L-alanine aminotransferase. The ^{1}H-NMR of the corresponding methyl ester prepared by the method of Rachele (21) indicated that about 0.70-0.75 proton equivalents were incorporated at C-2 of glycine. Therefore, about 25% of the glycine product was still dideuterated at C-2. Olah's procedure was then used to generate (S)-[2-$^{2}H_{1}$]-fluoroacetate. The chiral purity at C-2 of the synthesized monodeuterated fluoroacetate sample was determined by 250 MHz ^{1}H-NMR of its ester with methyl (R)-(-)-mandelate. (The NMR spectrum of nondeuterated fluoroacetate esterified with methyl (R)-mandelate showed sufficient resolution of the diastereotopic C_2-protons.) As expected, about 25% of the fluoroacetate molecules were still dideuterated at C-2, 70-75% were monodeuterated, and a small amount was the diprotio species. The exact amount of diprotio species was not measurable because of insufficient resolution of its ^{1}H-NMR signal from that due to the monodeutero species. The monodeutero species (plus diprotio contributors at H_R and H_S) showed a net H_R/H_S ratio of 90/10. The presence of the dideutero species should not complicate the ^{1}H-NMR analysis of enzyme product chirality, since the dideutero species should make no contribution to the H_R and H_S signals of either the derivatized substrate or derivatized product.

The synthetic (S)-[2-$^{2}H_{1}$]-fluoroacetate sample (50 mg) was

incubated with 87 units of enzyme for 40 minutes at 30°C, and reaction progress was monitored by assay of removed aliquots for F^- production. The incubation mixture was brought to pH 1, and then continuously extracted with 25 volumes of ether for 3 days. The collected ether extract was evaporated, and the residue neutralized with 1 N LiOH. The water was then removed under reduced pressure, and the resulting [2-$^2H_1$]-glycolate was converted to its phenacyl ester and separated from the phenacyl ester of unreacted fluoroacetate by preparative TLC (silica plate, 1% methanol/chloroform). TLC of the product of phenacyl esterification of a control sample (containing no enzyme) showed that no phenacyl glycolate was produced from the control. The recovered phenacyl [2-$^2H_1$]-glycolate was recrystallized from ether/hexane, further derivatized on its hydroxyl group with (-)-MTPA, and analyzed by ^1H-NMR at 250 MHz. (See Scheme 2.)

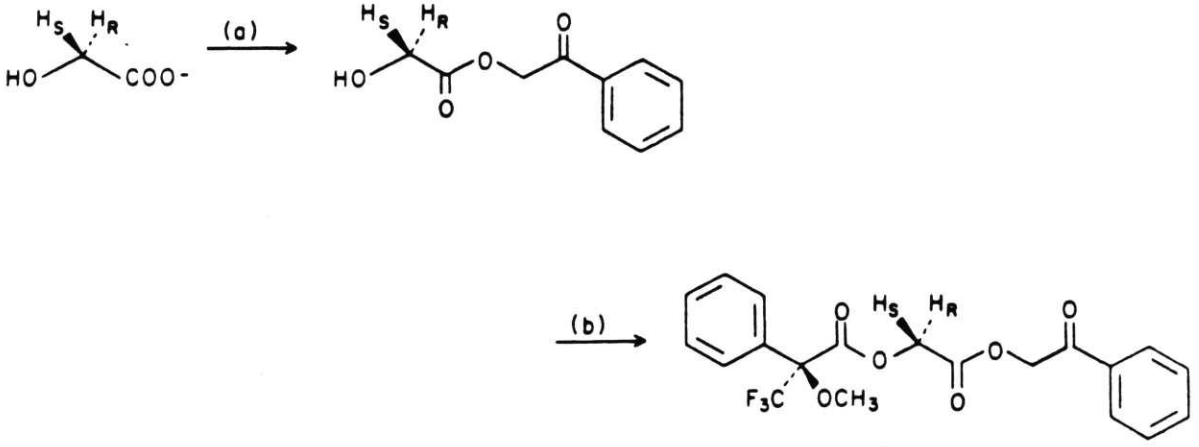

Scheme 2. Derivatization of glycolate for stereochemical analysis by NMR. (a) $PhCOCH_2Br$/KF/DMF, 25°C. (b) (S)-(-)-MTPA/DCC/4-dimethylaminopyridine/CH_2Cl_2, 0°C.

The ^{1}H-NMR spectra of two standards employed for reference and of the derivatized enzyme incubation product are shown in Figures 1a, b, and c. As shown in Figure 1a, a baseline-resolved AB quartet was observed for the now diastereotopic C-2 methylene hydrogens of (-)-MTPA esterified with nondeuterated phenacyl glycolate. Assignment of the low field and high field doublets as the H_R and H_S resonances respectively was based on the NMR spectrum of (-)-MTPA esterified with the phenacyl ester of authentic (S)-[2-$^{2}H_1$]-glycolate, prepared by reduction of [2-$^{2}H_1$]-glyoxylate with NADH and L-LDH. Integration of the corresponding C-2 methylene peaks in Figure 1c showed an 88/12 ratio of protons at the H_S position to protons at the H_R position. Therefore, the [2-$^{2}H_1$]-glycolate incubation product was predominantly the (R)-isomer. Since within experimental error the (S)-[2-$^{2}H_1$]-fluoroacetate sample (H_R/H_S = 90/10) was converted stereospecifically to predominantly (R)-[2-$^{2}H_1$]-glycolate (H_R/H_S = 12/88), the enzymatic reaction catalyzed by halidohydrolase H-1 must proceed with inversion of configuration at C-2 of fluoroacetate.

These combined stereochemical results render unlikely a double displacement mechanism, involving a covalent enzyme-substrate intermediate (unless one step goes with inversion and the other with retention) and favor the direct displacement process for this enzyme. Since this enzyme is the only one purified to homogeneity which carries out the decomposition of fluoroacetate to glycolate, it is the prime candidate for subsequent mechanistic studies on the cleavage mechanism of the strong C-F bond. Because the enzyme is encoded by a stable multicopy plasmid with constitutive expression, it is available in large quantities, and recombinant methodology for enzyme structure analysis

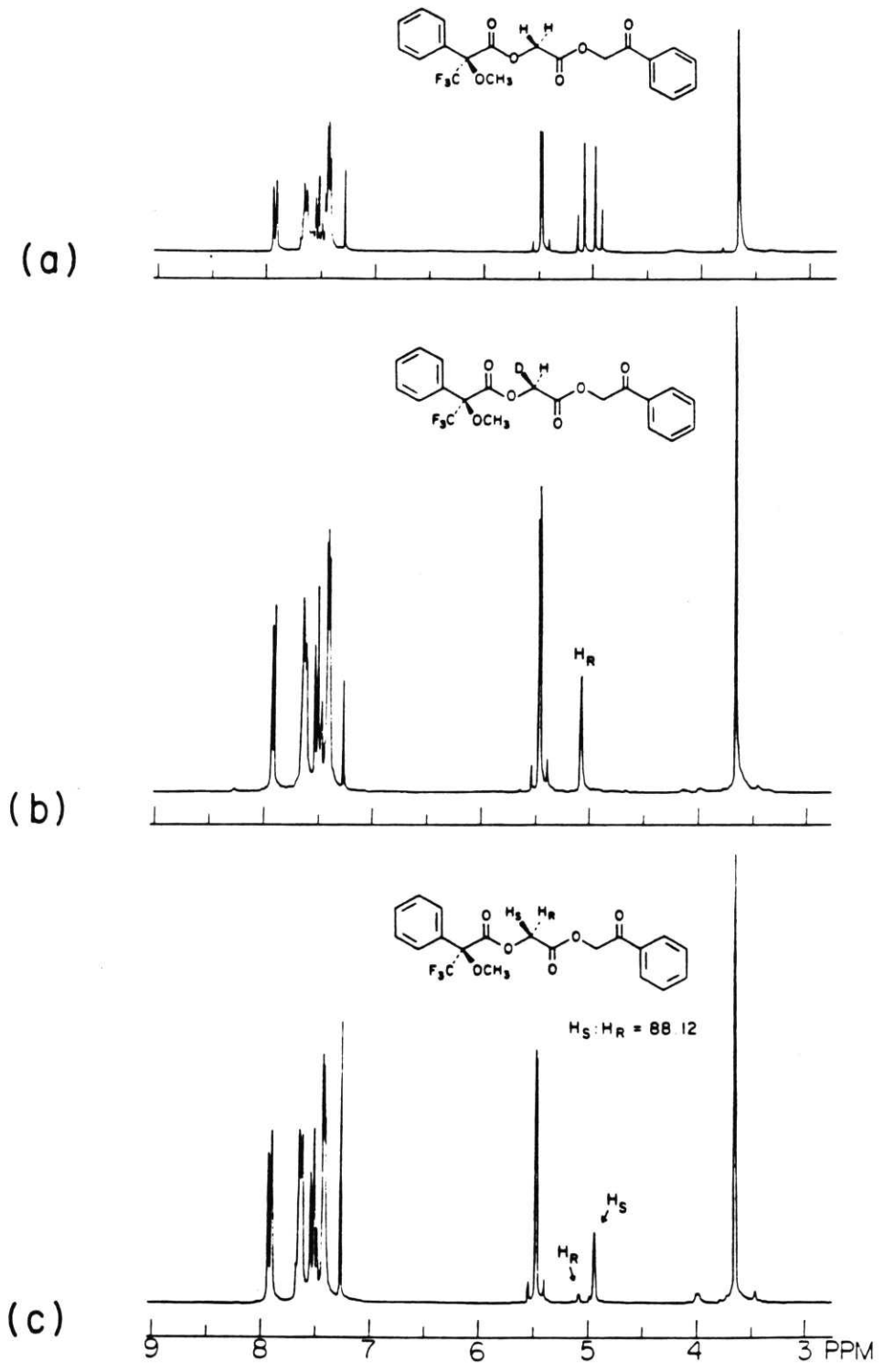

Figure 1. 250 MHz ^{1}H-NMR spectra ($CDCl_3$). (a) (S)-(-)-MTPA, phenacyl glycolate ester. (b) (S)-(-)-MTPA esterified with the phenacyl ester of authentic (S)-[2-$^2H_1$]-glycolate. (c) (S)-(-)-MTPA esterified with the phenacyl ester of the incubation product of (S)-[2-$^2H_1$]-fluoroacetate with halidohydrolase H-1.

will be possible. This will ultimately be instructive in determining how organisms carry out C-F cleavage and detoxification (Walsh, (27)) of this prototypic fluoroacid involved in the celebrated "lethal synthesis" metabolic reactions (Peters, 1972 (1)).

References

1. Peters, R. (1972) in Carbon-Fluorine Compounds, Chemistry, Biochemistry, and Biological Activities (Ciba Foundation Symposioum), p. 55, Elsevier, Amsterdam.

2. Carrell, H. L., Glusker, J. P., Villafranca, J. J., Mildvan, A. S., Dummel, R. J., Kun, E. (1970) Science, 170, 1412.

3. Stallings, W. C., Blount, J. F., Srere, P. A., Glusker, J. P. (1979) Arch. Biochem. Biophys., 193, 431.

4. Marletta, M. A., Srere, P. A., Walsh, C. (1981) Biochemistry, 20, 3719.

5. Kun, E., Kirsten, E., Sharma, M. L. (1977) Proc. Natl. Acad. Sci. U.S.A., 74, 4942.

6. Akiyama, S., Suzuki, T., Sumino, Y., Nakao, Y., Fukuda, H. (1973) Agric. Biol. Chem., 37, 879, 885.

7. Goldman, P., Milne, G. W. A., Keister, D. B. (1968) J. Biol. Chem., 243, 428.

8. Motosugi, K., Esaki, N., Soda, K. (1982) J. Bacteriol., 150, 522.

9. DuPuy, C., Shultz, A. (1974) J. Org. Chem., 39, 878.

10. Sharpe, A. (1972) in Carbon-Fluorine Compounds, Chemistry, Biochemistry, and Biological Activities (Ciba Foundation Symposium), p. 49, Elsevier, Amsterdam.

11. Kawasaki, H., Miyoshi, K., Tonomura, K. (1981) Agric. Biol. Chem., 45, 543.

12. Kawasaki, H., Hayaishi, S., Yahara, H., Minami, F., Tonomura, K. (1982) J. Ferment. Technol., 60, 5.

13. Goldman, P. (1965) J. Biol. Chem., 240, 3434.

14. Weightman, A. J., Weightman, A. L., Slater, J. H. (1982) J. General Microbiol., 128, 1755.

15. Gawehn, K., Bergmeyer, H. U. (1974) in Methods of Enzymatic Analysis (Bergmeyer, H. U., ed.), Vol. 3, 2nd ed., p. 1492, Academic Press, New York.

16. Gutmann, I., Wahlefeld, A. W. (1974) in Methods of Enzymatic Analysis (Bergmeyer, H. U., ed.), Vol. 3, 2nd ed., p. 1464, Academic Press, New York.

17. Massey, V., Ghisla, S., Kieschke, K. (1980) J. Biol. Chem., 255, 2796.

18. Olah, G. A., Welch, J. T., Vankar, Y. D., Nojima, M., Kerekes, I.,

Olah, J. A. (1979) J. Org. Chem., 44, 3872.

19. Fu, S.-C. J., Birnbaum, S. M., Greenstein, J. P. (1954) J. Am. Chem. Soc., 76, 6054.

20. Keck, R. (1980) Ph.D. Dissertation, p. 57, Universitat Karlsruhe, Karlsruhe, German Federal Republic.

21. Rachele, J. (1963) J. Org. Chem., 28, 2898. When ^{1}H-glycine was esterified by this procedure with 2,2-dimethoxypropane and DCl, no exchange of the C_2 protons with deuterium was observed in the ^{1}H-NMR of the product.

22. Neises, B., Steglich, W. (1978) Angew. Chem. Int. Ed. Engl., 17, 522.

23. Clark, J. H., Miller, J. M. (1977) Tetrahedron Lett., 599.

24. Keck, R., Retey, J. (1980) Helv. Chim. Acta, 63, 769.

25. Lowe, G., Potter, B. V. L. (1980) J. Chem. Soc., Perkin Trans. 1, 9, 2029.

26. Keck, R., Haas, H., Retey, J. (1980) FEBS Lett., 114, 287.

27. Walsh, C. T. (1983) Adv. Enzymology, 55, 137.